Genetic Analysis of Cellulose Crystallization in *Gluconacetobacter xylinus*

by

Luis Fernando Salgado

A Thesis Submitted in Partial Fulfillment
of the Requirements for the Degree of

Master of Science

in

The Faculty of Science

Applied Bioscience

University of Ontario Institute of Technology

August 2015

Abstract

In nature, polysaccharides, such as cellulose, are important biopolymers involved in numerous biological functions including prevention of cellular desiccation, energy storage, osmoregulation, and cell wall formation. Apart from having a relevant biological role, cellulose also has a great economic importance. For instance, cellulose provides the raw material for paper and textile production, and it is predicted to become a key precursor for glucose-derived ethanol. The mechanisms underlying cellulose biosynthesis are not completely understood. Elucidation of these mechanisms are essential for efficient cellulose production and industrial applications. In an effort to gain a better understanding of the cellulose biosynthesis process and its regulation, the crystallization of cellulose was investigated in *Gluconacetobacter xylinus* mutants resistant to a novel inhibitor of cellulose I formation known as pellicin. Through the use of forward genetics and site-directed mutagenesis, the mutations A449T and A449V in the *G. xylinus* BcsA protein were found to be important to confer high levels of pellicin resistance. Phenotypic analysis of the BcsA A449T and BcsA A449V mutants did not reveal other apparent phenotypic alterations when compared to the wild type. This suggests that these mutations are exclusively involved in cellulose crystallization. The localization of the A449 amino acid residue in the BcsA protein and structural analysis of both the native and the mutant BcsA proteins, by means of 3D modelling, suggest that pellicin may inhibit cellulose crystallization either by affecting the translocation process of the glucan within the BcsA protein or by allosterically altering protein-protein interactions.

Keywords: *Gluconacetobacter xylinus*, bacterial cellulose, cellulose synthase, pellicin, site-directed mutagenesis, forward genetics, protein modelling.

Acknowledgements

I would like to express my gratitude towards Dr. Dario Bonetta for his unconditional support, admirable patience, and invaluable guidance over the past three years. I also want to extend my sincere gratitude to my lab mates: Isaac Shim, and Sara Poormohammadvalibehnami. Aside from the very insightful discussions we have had in the last few years, they have made my graduate experience enjoyable. Furthermore, I am grateful to Silvia Blank who isolated the mutants that were analyzed in the present study. Additionally, I want to thank Dr. Janice Strap and Dr. Ayush Kumar for their advices and kind disposition to collaborate and assist at all times. I also want to express my gratitude towards Dr. George Stamatiou for his feedback and insightful suggestions regarding the DNA sequencing analysis and electrocompetent cell preparations and Dr. Sylvie Bardin for her assistance on the bacterial cell electroporation procedures. Finally, I would like to thank my entire family and in particular to my beloved wife Elizabeth Saldarriaga, my mother Gloria Patarroyo, my grandmother Maria Torres de Patarroyo, and my brother Ivan Camilo Salgado. Their unconditional support, immense patience, and invaluable advice have been indispensable for the completion of my graduate degree as a whole.

Table of Contents

List of Tables

List of Figures

Abbreviations

AAB	acetic acid bacteria
ATCC	American Type Culture Collection
BC	bacterial cellulose
bcs	bacterial cellulose synthase
bcsA	bacterial cellulose synthase A gene
BcsA	bacterial cellulose synthase A protein
CBDs	carbohydrate-binding domains
CBMs	carbohydrate binding molecules
CBHI	cellobiohydrolases
Cel^-	cellulose non-producing mutant
CESA	cellulose synthase catalytic subunit
CI	crystallinity index
Co-IP	complex co-immunoprecipitation
CSL	corn steep liquor
CTAB	cetyl trimethyl ammonium bromide
Cyclic-di-GMP	3', 5'-cyclic diaguanylic acid
DGC	diguanylate cyclase
DMSO	dimethyl sulfoxide
DNA	deoxyribonucleic acid
EMI/MS	electrospray ionization mass spectrophotometry
EMS	ethyl methanesulfonate
EtBr	ethidium bromide
GTs	glycosyltransferases
HPR*Gx*	high pellicin-resistant *G. xylinus*
IF	interfacial helix
ISs	insertion sequences
LMT	low melting temperature
LPR*Gx*	low pellicin-resistant *G. xylinus*
PNAG	poly-β-D-*N*-acetylglucosamine
PCR	polymerase chain reaction
PDEA	phosphodiesterase A
PDEB	phosphodiesterase B
PEG	polyethylene glycol
PR*Gx*	pellicin-resistant *G. xylinus*

SDS	sodium dodecyl sulfate
TC	terminal complex
TMH	transmembrane helix
TPR	tetratricopeptide repeats
UDP-glucose	uridine diphosphoglucose
UV	ultraviolet
WT	wild type

Chapter 1

Introduction

1.1 General introduction

Cellulose is the most abundant biopolymer on earth and has been recognized as the major component of plant biomass as well as an important microbial extracellular polymer (Ross et al., 1991). This polysaccharide is a linear polymer composed of glucose molecules linked via β-1-4 glycosidic linkages (Römling, 2002).

In nature, polysaccharides, such as cellulose, are important biopolymers involved in numerous biological functions including prevention of cellular desiccation, protection from UV light, energy storage, osmoregulation, cell wall formation, tissue growth, and stem strength (Whitney and Howell, 2013; Whitney et al., 1999; Sakurai, 1991; Nunes et al., 1984). Apart from having a relevant biological role, cellulose also has a great economic importance. For instance, cellulose provides the raw material for paper and textile production, and it is predicted to become a key precursor for glucose-derived ethanol (Keshk, 2014; Somerville, 2006).

In addition, cellulose produced by bacteria has a great impact in human health. Cellulose is the major exopolysaccharide of biofilms which functions as an adherent factor in pathogens, leading to persistence and resistance to antimicrobial treatments (Omadjela et al., 2013). In particular, *E. coli* frequently cause nosocomial infections such as sepsis, biliary tract infections, and catheter related cystitis produced by biofilm-forming isolates (Römling, 2002).

Bacterial cellulose (BC) is synthesized by different genera of which *Komagataeibacter* (previously known as *Gluconacetobacter*) strains are the best

characterized (Ross et al., 1991; Yamada et al., 2012). The structure of cellulose depends on the organism despite the fact that the pathway for its biosynthesis and mechanism of regulation are likely common in most of the BC-producing bacteria (Ross et al., 1991). The acetic acid bacteria (AAB) *Gluconacetobacter xylinus* (the scientific name used in this study) which has been reclassified and included within the genus *Komagataeibacter*, as *Komagataeibacter xylinus* (Yamada et al., 2012), is the most competent cellulose producer which has been studied as a model organism for the study of bacterial cellulose biosynthesis (Gayathry and Gopalaswamy, 2014). Different techniques have been used to improve BC production, but cost and scale of production still prevent a diverse number of applications of this material (Krystynowicz et al., 2005; Yoshinaga and Tonouchi, 1997). Although cellulose is the most abundant biopolymer on earth, the mechanisms underlying its biosynthesis are still not completely understood. Elucidation of these mechanisms are essential for efficient cellulose production and industrial applications.

1.2 Biological significance of bacterial cellulose

In addition to vascular land plants, the synthesis of cellulose also occurs in bacteria like *Gluconacetobacter* (Brown et al., 1976), *Rhizobium*, (Napoli et al., 1975), *Agrobacterium* (Matthysse et al., 1995) *Salmonella*, *Escherichia coli* (Zogaj et al., 2001), and *Cyanobacteria* (Nobles et al., 2001). Cellulose is also produced by many algal groups (Baldan et al., 2001), the mold *Dictyostelium* (Blanton et al., 2000), and tunicates (Kimura and Itoh, 1995).

In contrast to plant cellulose, which is an intrinsic component of the cell wall, the cellulose formed by bacteria is distinguished by the extracellular nature of the glucan products and formation of cell aggregates which is conferred by the high self-affinity of cellulosic material (Ross et al., 1991). Cellulose aggregation forms a dense reticulated structure due to the formation of both intra and intermolecular hydrogen bonds (Ross et al., 1991).

Although the BC is not an intrinsic component of the cell, it plays an important structural role. BC provides mechanical, chemical, or biological protection from the surrounding environment in some bacteria, and in others BC facilitates cell adhesion mechanisms required for symbiotic or infection interactions (Robledo et al., 2012; Williams and Cannon, 1989). In *G. xylinus*, BC has been suggested to serve as an

extracellular matrix that improves colonization on substrates and prevents competitors to have access to the nutrients used by the this bacterium (Ross et al., 1991). In this case, the polymer matrix contributes to the adhesion of cells onto different accessible surfaces that facilitates nutrient supply and that can also be utilized as a storage carbon source for the starving bacterial cells (Williams and Cannon, 1989).

Another phenotype that has been studied on cellulose formation in bacteria is the protection that the polymer provides to cells from UV light. In *G. xylinus*, it has been shown that about 23% of acetic acid bacteria are able to survive after 1 h treatment with UV radiation whereas removal of the protective cellulose decreases their viability to only 3% (Williams and Cannon, 1989). On the other hand, due to the viscosity and hydrophilic properties of cellulose, cells are able to retain moisture which prevents drying of substrates (Williams and Cannon, 1989).

As mentioned above, a significant synthesis of cellulose occurs in *G. xylinus* and more notably when it is grown on enriched media in laboratory settings. This gram-negative bacterium, is an obligate aerobe, rod to oval in shape. *G. xylinus* grows singly, in pairs or in chains, its reproduction occurs by binary fission, it exhibits motility by flagella, and does not produce endospores (Krystynowicz et al., 2005). Finally, this bacterium is usually found on decaying fruits, vegetables, vinegar, fruit juices, and alcoholic beverages (Williams and Cannon, 1989).

G. xylinus has emerged as a model organism for the investigation of cellulose biosynthesis and particularly for the study of structural details of biogenesis of cellulose microfibrils (Haigler, 1985). In this regard, cellulose production was first reported in 1886 by A.J Brown, who observed that the resting cells of *G. xylinus* produced cellulose in the presence of oxygen and glucose (Brown, 1886). The extracellular secretion of pure cellulose synthesized by cell-free extracts of this bacterium was also demonstrated in 1958 by Glaser (Glaser, 1958). In addition, the visualization of cellulose product obtained *in vitro* (Lin et al., 1985), the chemical elucidation of the regulatory compound cyclic-di-GMP (Ross et al., 1987), the membrane localization of the cellulose synthase (Bureau and Brown, 1987), and the first bacterial cellulose synthase gene cloned and characterized were possible to achieve using *G. xylinus*.

The strains of *G.xylinus* are susceptible to spontaneous mutations leading to cellulose non-producing bacterial cells. The presence of these strains was first analyzed by Schramm and Hestrin in 1954 (Hestrin and Schramm, 1954) who

identified three separate types of *G. xylinus* cells characterized by differences in colony morphologies and efficacy of cellulose biosynthesis. The first type of *G. xylinus* identified was the wild type cellulose producing cells, the second type was a cellulose non-producing cells capable of reverting back to cellulose producing cells, and the third was cellulose non-producing cells incapable of reverting back to cellulose producing cells.

1.3 Properties and applications of cellulose from bacteria

The increased demand for cellulose based products, which results in an increased consumption of wood, as it is the raw material for cellulose, have caused environmental problems due to deforestation (Park et al., 2003). Traditional production of polysaccharides such as cellulose obtained from plants and seaweed is inadequate to supply the required mass production of polysaccharides (Park et al., 2003). Therefore, there is an increased interest of cellulose production from a difference source such as from microbial cells.

Bacterial cellulose is an interesting biopolymer with various commercial applications. The cellulose produced by bacteria has some advantages over the cellulose produced by plants. One of the most important features of BC is its high purity which differs from plant cellulose that is generally associated with other components such as hemicelluloses and lignin which are inherently difficult to remove (Goelzer et al., 2009). Another advantage of using a bacterial system for cellulose production is that bacteria grow fast under controlled conditions and are able to produce cellulose from a diverse number of carbon sources including glucose, ethanol, sucrose, and glycerol (Goelzer et al., 2009). Finally, bacterial cellulose possesses a higher degree of crystallinity, as well as polymerization, tensile strength, and water holding capacity making it an interesting economic alternative with characteristics that originate from its ultra-fine reticulated nanostructure (Hornung et al., 2006; Goelzer et al., 2009).

The structure and properties of BC as an ingredient in food, permits to avoid flavor interactions and to increase stability of food over a wide range of pH's, temperatures, and freeze-thaw conditions (Shi et al., 2014). Potential uses of cellulose in the food industry are for thickening, gelling, stabilizing, emulsifying, and water-binding agents

(Shi et al., 2014).

Furthermore, BC is an exceptional component in papers which provides exceptional mechanical properties (Shah and Brown, 2005). The paper obtained from BC has several advantages over synthetic paper such as higher dimensional stability, greater mechanical strength, and a great capacity to hold water (Shah and Brown, 2005).

In addition, the great biocompatibility and low immunogenic potential render BC an alternative material for different biomedical applications. For example, BC has the potential to be used as a substrate for tissue engineering of cartilage due to its great tensile strength in wet conditions as well as its high moldability *in situ*, biocompatibility and relative low cost (Pircher et al., 2014). Furthermore, biofilms obtained from modified bacterial cellulose have the potential to be used as a temporary skin substitute in the treatment of skin wounds (Czaja et al., 2006).

Finally, the study of bacterial cellulose biosynthesis can be used towards potential industrial applications. As mentioned above, BC has a higher degree of crystallinity when compared to plant cellulose. This property along with the fact that the assembly of glucan chain aggregates into crystalline cellulose I occurs outside of the bacterial cell (Brown, 1992), facilitate the study of the cellulose crystallization process. Cellulose crystallinity has an important role in governing the mechanical and physical properties of the material. For better utilizing cellulose in the production of materials such as biofuels, it is quite important to collect information about the crystalline cellulose I formation. In this regard, one of the key challenges in the conversion of lignocellulosic biomass to biofuels is biomass recalcitrance, which decreases sugar release performance through enzymatic hydrolysis (Pu et al., 2013). The degree of cellulose polymerization as well as cellulose crystallinity have been considered the two major recalcitrance features that affect enzymatic hydrolysis performance (Hall et al., 2010; Pu et al., 2013). It has been generally accepted that amorphous cellulose is less resistant to enzymatic hydrolysis in the cellulose-to-glucose conversion than crystalline cellulose. At higher degrees of crystallinity, cellulose samples have been shown to be less amenable to enzymatic hydrolysis and less accessible (Hall et al., 2010). In terms of accessibility, a high crystalline cellulose sample has a tight structure with cellulose chains closely bound to each other, leaving too little space for enzymes to start the hydrolysis process within the cellulose crystal (Hall et al., 2010). Consequently, the cost-competitive production of biofuels is highly limited by the cost of

thermochemical procedures and subsequent hydrolysis treatments in biorefineries (Himmel et al., 2007). Therefore, elucidating mechanisms underlying the process of cellulose crystallization, which may be facilitated by using a bacterial system, is a critical step to work towards the improvement of hydrolytic conversion of lignocellulosic biomass to biofuels.

1.4 Important factors for optimal bacterial cellulose production

The physical and mechanical properties of cellulose are highly influenced by the culture method employed, namely static and agitated, that depends on further biopolymer commercialization (Vandamme et al., 1998). Different components in the culture medium and levels of aeration allows for the formation of microfibril aggregates with different forms (Krystynowicz et al., 2005).

The production of bacterial cellulose under static conditions is the most common process in which the crystalline BC is formed at the air/liquid interface of the culture medium forming a pellicle. Stationary cultures encounter some problems including high labour costs as well as lower productivity (Dobre et al., 2008). The production of the biopolymer only in a form of a pellicle and the considerably low productivity obtained through this method has led to the use of novel fermentation processes. Therefore, large-scale industrial production of BC by static cultivation is not desirable (Dobre et al., 2008).

Conversely, BC produced under agitated medium conditions does not produce a pellicle, but instead, irregular granules distributed throughout the entire medium. In this case, cellulose formed by *G. xylinus* may be sunk by gentle agitation which allows the formation of fresh granules, a process that can continue until the nutrients in the medium are depleted (Dudman, 1960). The multiple pellicles formed under agitated conditions are thinner than the single pellicle formed by undisturbed cultures, and under the same conditions it is possible that cellulose synthesis is stimulated by such manipulations (Dudman, 1960). Agitated cultures are more suitable for commercial cellulose production mostly because of the higher production rates than the static cultures can achieved (Yoshinaga and Tonouchi, 1997). However, BC production under agitated conditions has some disadvantages such as the appearance of cellulose non-producing mutants (Cel^{-}), which cause a

decrease in polymer synthesis (Krystynowicz et al., 2002). One of the reasons for the decrease of cellulose is the genetic instability of the producer. Insertion sequences (ISs) elements, which are known to cause genetic instability, have been detected in cellulose-producing *G. xylinus* strains (Coucheron, 1991). Finally, agitated cultures produce cellulose characterized by a highly branched, three-dimensional reticulated structure, whereas static cultures produce pellicles of cellulose with a lamellar and less significant branching structure (Keshk, 2014).

On the other hand, medium costs limit commercial use of bacterial cellulose, so low-cost substrates are being used, such as molasses from the sugar cane process which contains 50 to 60% sucrose (Yoshinaga and Tonouchi, 1997). In this regard, the production of cellulose from different carbon sources has been studied to improve cellulose production. In *G. xylinus*, cellulose yield has been shown to be high when glucose is used as substrate compared to many other substrates (Jonas and Farah, 1998). However, the two sugar alcohols arabitol and mannitol have been shown to produce up to 6.2 and 3.8 times more cellulose than glucose respectively (Oikawa et al., 1995). These two sugars are metabolized via xylulose and fructose with no gluconic acid formed during their fermentation; thus, keeping the pH of the medium stable (Oikawa et al., 1995). It is still unclear if this is in fact the main reason for the considerable difference in cellulose production between glucose and these two alcohol sugars. Moreover, addition of citrate to culture media has been demonstrated to have a modest positive effect on cellulose production (Geyer et al., 1994).

The foundation of most work on medium development is the medium formulated by Hestrin and Schramm (Hestrin and Schramm, 1954), which includes peptone and yeast extract in a concentration of 0.5% each. However, corn steep liquor (CSL) has been shown to be one of the most effective nitrogen sources used in growth media for *G. xylinus* (Vazquez et al., 2013). In regards to defined nitrogen sources, the amino acids methionine and glutamate have been cited as important amino acids for optimal cellulose production (Jonas and Farah, 1998). For instance, methionine has been shown to be essential for cell growth and cellulose production accounting for 90% of cell growth as well as cellulose production when compared to media lacking this amino acid (Matsuoka et al., 1996). In addition, the vitamins pyridoxine, nicotinic acid, p-aminobenzoic acid and biotin have been shown to positively affect cell growth and cellulose production, whereas pantothenate and riboflavin have shown to negatively impact cellulose production (Matsuoka et al., 1996).

Finally, it is widely accepted that the optimal pH range for cellulose production

in *G. xylinus* is between 4 and 7. Hestrin and Schramm (1954) proposed a pH below 7 to be optimal (Hestrin and Schramm, 1954), whereas some others considered a low pH between 4 and 4.5 as optimal for cellulose production particularly to avoid contamination (Jonas and Farah, 1998). A negative impact on cell viability and cellulose synthesis have been observed at pH below 4, whereas as at pH 2.5 both cell growth and cellulose production is completely inhibited (Çoban and Biyik, 2013). Therefore, pH is an important factor to consider for optimal cellulose production.

1.5 Structure of cellulose

The cellulose fibrils are highly insoluble and inelastic and, due to the molecular configuration, posses a tensile strength similar to steel (Yamanaka et al., 1989). Cellulose is a linear extracellular polysaccharide composed of glucose molecules that are attached via β-1,4 glycosidic linkages (Nishiyama et al., 2002). These glycosidic linkages form β-1, 4 glucan chains that interact with each other forming microfibrils that are observed in cellulose-producing organisms (Römling, 2002). The β-1, 4 glucan chain backbone found in cellulose is relatively straight and every glucose residue within it is rotated or inverted 180° with respect to the adjacent residue, indicating that the repeating unit in the backbone is in fact cellobiose and not a glucose residue (Saxena and Brown, 2005). The molecular structure of cellulose is shown in Figure 1.1.

Polymer elongation has been shown to occur at the non-reducing end by direct transfer from the nucleotide sugar donor UDP-glucose (Charnock et al., 2001). The nascent chains of cellulose aggregate and form a dense reticulated structure that is stabilized by inter and intra chain hydrogen bonds (Endler et al., 2010). Although the cellulose produced by different organisms is chemically the same, the level of polymerization, crystallinity, and physical characteristics are specific for each organism (Saxena et al., 1994). For instance, the cellulose ribbons produced by *G. xylinus* are approximately 20 to 50 nm in width, which corresponds less than one-hundredth of plant pulp cellulose (Rehm, 2009).

The crystalline structure of cellulose is dictated by specific arrangements of the glucan chains with respect to one another. The two common crystalline forms of cellulose are designated as cellulose I and cellulose II, which can be distinguished by one another by X-ray, nuclear magnetic resonance, Raman spectroscopy,and infrared analysis (Åkerholm et al., 2004; Szymańska-Chargot et al., 2011; Park et al., 2010).

In nature, the most common form of cellulose is produced as crystalline cellulose designated cellulose I, which is synthesized by the majority of plants and also by *G. xylinus* (Saxena and Brown, 1989). The arrangements of the glucan chains found in cellulose I are parallel to one another and assembled side-by-side forming the microfibrils (Saxena and Brown, 1989). Cellulose I is found in nature as two different allomorphs known as cellulose Iα (triclinic) and cellulose Iβ (monoclinic), which can be verified using solid-state ^{13}C NMR (Park et al., 2010). The two cellulose allomorphs Iα and Iβ differ from one another by their crystal packing hydrogen bond interactions and molecular conformation, which alter the physical characteristics of the polymer (Nishiyama et al., 2002). Cellulose Iα is metastable and can be converted into the Iβ allomorph by annealing (Saxena and Brown, 2005). One cellulose microfibril may contain both types of the cellulose I allomorphs, with the Iβ form being dominant in higher plants and the Iα form dominant in bacteria and algal species (Oehme et al., 2015). The physical properties depends on the ratio between these two allomorphs (Park et al., 2010).

Another type of cellulose known as cellulose II can be obtained through either industrial mercerization (alkali treatment) or regeneration (solubilization and subsequent recrystallization) (Park et al., 2010). Cellulose II is only made by few organisms including the gametophyte cells of the marine alga *Halicystis*, the gram-positive bacterium *Sarcina* as well as some mutants of *G. xylinus* (Brown, 1996). The glucan chains of cellulose II are arranged in an antiparallel conformation, and it has been proposed that this conformation results from chain folding during cellulose biosynthesis (Saxena and Brown, 2005). In cellulose II, each glucose residue has an additional hydrogen bond which makes this allomorph more thermodynamically stable conformation than cellulose I. In addition, other allomorphs known as cellulose III_I and III_{II} can be formed from cellulose I and II respectively by treatment with liquid ammonia. The treatment with ammonia results in the formation of materials with variable degrees of crystallinity which impacts the digestibility of the substrate (Mittal et al., 2011). The level of crystallinity obtained by this method depends on treatment conditions in which high temperature treatments result in a more crystalline product when compared to the product obtained at lower temperatures (Mittal et al., 2011).

The crystalline cellulose I has been studied using different methods. For example, crystalline cellulose can be isolated from various biological materials for further analysis by sedimentation using acetic-nitric reagent (Updegraff reagent)

(Updegraff, 1969). For instance, Peng and co-workers (2001) used Updegraff reagent to determine the process of cellulose biosynthesis by *in vivo* labelling of developing cotton fibres (Peng et al., 2001). The authors found that cellulose microfibrils remain insoluble after treatment with the reagent. In addition, other studies have reported that the reagent hydrolyzes noncellulosic compounds, and that the structure resistant to the reagent corresponds to straight cellulose microfibrils (Cifuentes et al., 2010). Crystalline cellulose obtained from this procedure can be quantified using an anthrone method. Crystalline cellulose can be hydrolyzed into glucose monomers using sulfuric acid. The glucose molecules on treatment with anthrone get dehydrated to form 5-hydroxymethyl furfural which gives a green colour product that can be measured at 620 nm to estimate the amount of crystalline cellulose of the original sample (Irick et al., 1988).

The size of cellulose crystallites is small, generally about 5 nm in width, and thus a wide number of potent techniques such as X-ray diffraction and neutron fibre diffraction have being required to characterize cellulose crystallinity (Nishiyama et al., 2002). Although cellulose establishes a particular crystalline structure, its fibers are not completely crystalline in nature. The degree of crystallinity is variable and it has led to the motion of the "lateral order distribution" of crystallinity which depicts a wide number of cellulose fibers in statistical terms as continuum from completely crystalline to completely amorphous, with the entire degrees of crystallinity in between (Marchessault and Howsmon, 1957). In this regard, a parameter termed as the crystallinity index (CI) has been employed using diverse type of methods to characterize the relative amount of crystalline material in cellulose (Park et al., 2010).

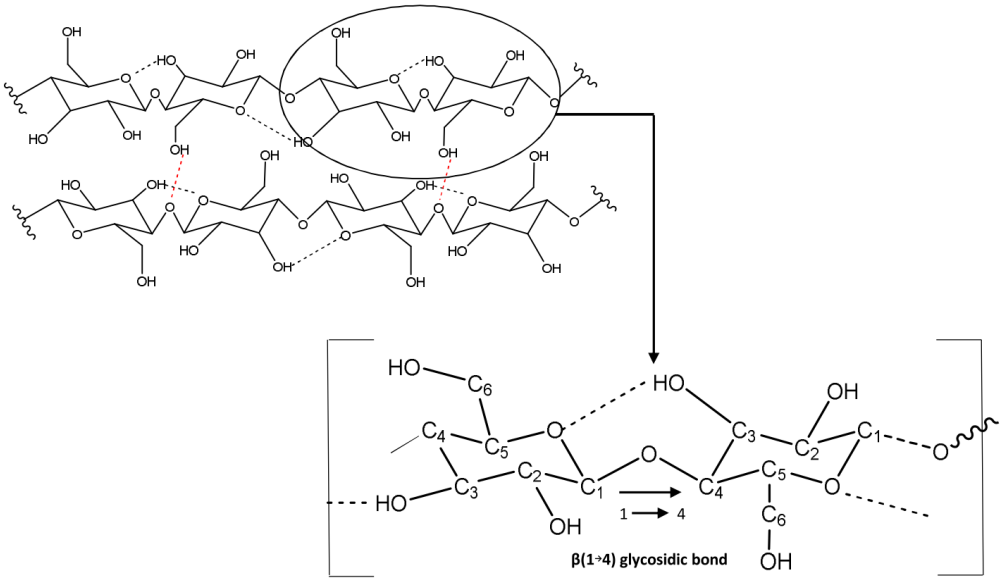

Figure 1.1: Molecular structure of a cellulose unit showing the β 1-4 glucosidic bond. The structure is stabilized by intrachain hydrogen bonding (dotted black line) and interchain hydrogen bonding (dotted red line). Note that each glucose residue found in cellulose is rotated or inverted 180°C with respect to the next residue, and thus cellobiose (bracketed) is considered the basic repeating unit. Adapted from Endler et al. (2010).

1.6 Cellulose biosynthesis

As with other extracellular polysaccharides like alginate, acetylated cellulose, and poly-β-D-N-acetylglucosamine (PNAG), cellulose is synthesized within the cell using a nucleotide-activated sugar (Whitney and Howell, 2013). More precisely, the production of cellulose takes place through a single polymerization step that uses uridine diphosphoglucose (UDP-glucose) as substrate which undergoes self-assembly at the site of biosynthesis (Saxena et al., 1994). This process is driven by membrane-integrated glycosyltransferases (GTs) that couple the elongation of the polymer with the translocation of the product outside the cell (Morgan et al., 2013). In *G. xylinus*, a single cell can polymerize up to 200,000 glucose molecules every second into the $\beta-1$, 4 glucan chains which are released into the surrounding medium (Saxena et al., 2000).

The synthesis of BC is precisely regulated by a multi-step process compromising a diverse number of enzymes and regulatory proteins. Cellulose biosynthesis in *G. xylinus* takes place between the outer membrane and cytoplasmic membrane by

cellulose synthesizing complexes or terminal complexes (TCs), which are associated with pores located in the lipopolysaccharide layer and organized in a linear row along the long axis of the bacterium. (Zaar, 1979; Cannon and Anderson, 1991; Mehta et al., 2015). It has been suggested that during the initial step of cellulose synthesis, aggregates of glucan chains, composed of 6 to 8 glucan chains, are extended from the complex. These aggregates are packed to produce microfibrils that are then assembled into ribbon bundles of microfibrils. These ribbons elongate as they remain associated with the cell envelope, even during cell division, given rise to the bacterial cellulose or pellicle (Brown, 1992; Mehta et al., 2015). A model of the cellulose biosynthesis process is shown in Figure 1.2.

The polymerization of cellulose is catalyzed by the enzyme cellulose synthase (UDPglucose: 1,4$-\beta-$D$-$glucan 4$-\beta-$D$-$glucosyltransferase) without the apparent formation of intermediates during the process (Omadjela et al., 2013). However, the formation of the crystalline structure composed of cellulose microfibrils and their interaction with intramembranous components, observed in many cellulose synthesizing organisms, indicate a greater intricate mechanism of cellulose biogenesis than just the already characterized polymerization reaction (Saxena et al., 1994).

Through the cellulose biosynthesis process, the association of organized β,-1,4-glucan chains is the result of the precise and coordinated crystallization process. If individual β-1,4- glucan chains are assembled randomly, the resulting product would be most likely a tangled mass structure of fibrils in which the chains are arranged in opposing directions or bend back themselves (Stöckmann, 1972). Since the disorganized glucan chains assembly does not usually occur in nature, nearly all cellulose fibrils isolated from plants, algae, and bacteria reveal the crystalline unit structure observed in β-1,4- glucan chains that are laterally and unidirectionally aligned (Delmer and Amor, 1995).

The nature of the crystalline structure of cellulose strongly suggest an organized arrangements in which all the atoms are fixed in separate positions with respect to one another (Lynd et al., 2002). An interesting characteristic of the crystalline array of cellulose is that the molecules of separate microfibrils are built sufficiently tight to avoid penetration of enzymes and even smaller molecules such as water (Lynd et al., 2002). On the other hand, the water-soluble nature of cellulose is necessary for organisms to live in aqueous environments. The water affinity of cellulose is related to amorphous domains, organized in the cellulose texture, where amorphous refers to the space occupied by the cellulose swollen by water or by pure water (Koizumi et al.,

2008).

On the other hand, the rate at which cellulose is produced in *G. xylinus* is approximately proportional to the cell growth and independent of the carbon source (Oikawa et al., 1995). This characteristic along with the fact that cellulose formation represents the end of glucose metabolism, provides a suitable method for deciphering metabolic pathways in *G. xylinus* in which the pattern and rate of incorporation of carbon atoms from different substrates into insoluble glucan polymers have been elucidated (Benziman, 1969; Weinhouse and Benziman, 1976, 1972). Based on these studies, the capability of any substrate to be used for cellulose formation can be understood from the operative amphibolic pathways used by *G. xylinus*: the pentose phosphate cycle which is used to oxidize carbohydrates and the citrate cycle which is involved in the oxidation of organic acids and associated compounds (Ross et al., 1991; Tonouchi et al., 2003). In *G. xylinus*, glucose metabolism is strictly aerobic due to the fact that this bacterium lacks phosphofructose kinase, which is essential for glycolysis (Gromet et al., 1957). The process of gluconeogenesis takes place from oxaloacetate in *G. xylinus* through pyruvate because of the regulation of oxaloacetate decarboxylase and pyruvate phosphate dikinase enzymes (Benziman et al., 1978; Benziman and Eizen, 1971). Cellulose is then formed in *G. xylinus* from a metabolic process of hexose phosphate that is maintained through the phosphorylation of exogenous hexoses and indirectly through the pentose and gluconeogenic pathways (Ross et al., 1991).

The biosynthesis of cellulose from glucose is catalyzed by five enzymes:

1. Glucose permease which allows glucose to be transported across the cell membrane
2. Glucokinase which is responsible for the conversion of glucose into glucose-6-phosphate by phosphorylation on C-6 of glucose
3. Phosphoglucomutase, which drives the isomerization catalysis of glucose-6-phosphate to glucose-1-phosphate.
4. Glucose-1-phosphate uridylyltransferase also known as UDP glucose pyrophosphorylase which is responsible for the synthesis of UDP-glucose from glucose-1-phosphate
5. Cellulose synthase, which make cellulose by using UDP-glucose as substrate.

In addition, it is has been suggested that UDP glucose pyrophosphorylase may play a key role in cellulose biosynthesis since an analysis of a group of cellulose non-producing cells of *G. xylinus* were found to be specifically deficient of this enzyme (Valla et al., 1989). The enzymatic pathway that leads to the formation of cellulose from glucose is shown in Figure 1.3.

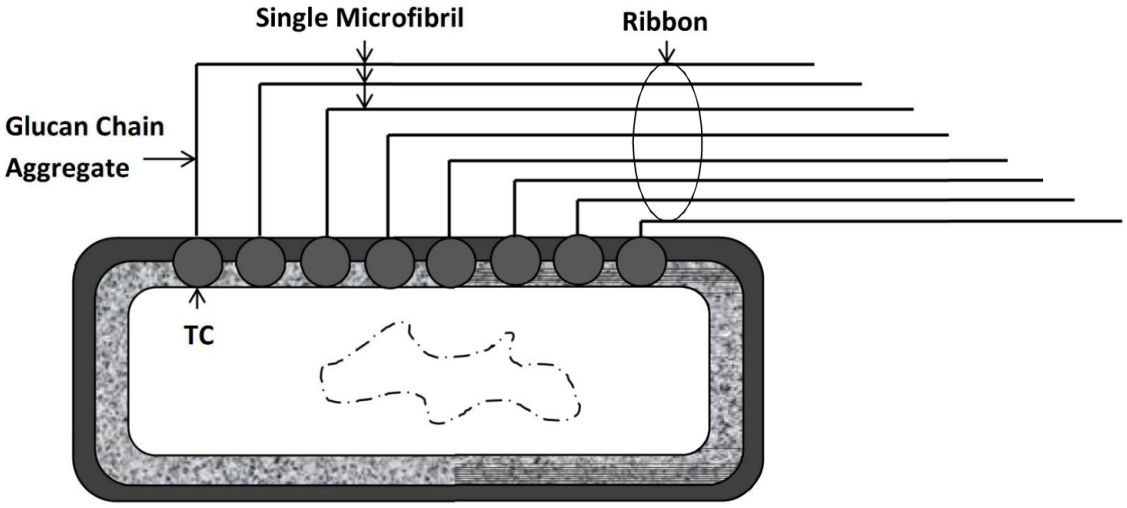

Figure 1.2: Production of bacterial cellulose. The diagram shows the linear arrangement of terminal complexes (TCs) that synthesize glucan chain aggregates that consists of approximately 6 to 8 glucan chains. Three TCs, synthesizing their corresponding glucan chain aggregates, are required for the formation of the crystalline microfibil. Microfibrils aggregate through hydrogen bonding forming the cellulose ribbon which is then secreted into the medium. Adapted from Brown (1992).

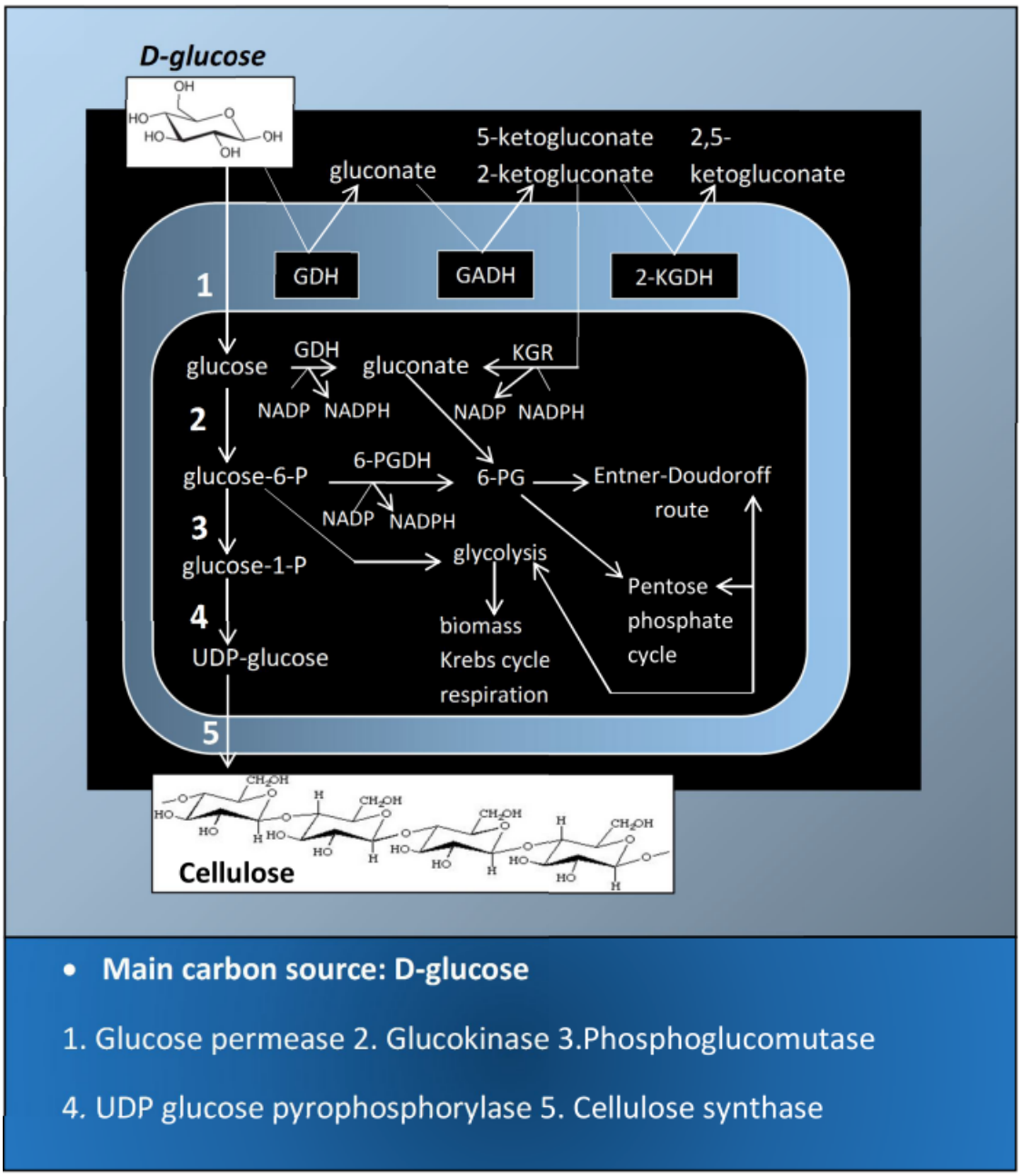

Figure 1.3: Enzymatic mediated steps for cellulose formation. This process includes the transformation of glucose to UDP-glucose via glucose-6-phosphate and glucose-1-phosphate and finally the addition of UDP-glucose at the non-reducing end of the growing polymer chain by cellulose synthase. Adapted from Klemm et al. (2001).

1.7 Regulatory genes for bacterial cellulose biosynthesis

The BC production is determined by the presence of cellulose synthesis genes arranged in operons. For example, *Enterobactericiae*, like *E. coli*, contains the operon *bcsABZC* (Zogaj et al., 2001), whereas *Agrobacterium tumefaciens* has the operon *celABC, celDE* (Matthysse et al., 1995).

G. xylinus possesses a cellulose synthase operon (*bcs* operon) that is composed by three to four genes depending on the strain or subspecies: *bcsAB* (or *bcsA* and *bcsB*), *bcsC*, and *bcsD* (Kawano et al., 2002). There are more than one cellulose biosynthesis operon in *G. xylinus*, whereby cellulose biosynthesis is mediated only by one of the synthases *in vivo* under laboratory conditions (Saxena et al., 1995).

The protein product encoded by the *bcsA* gene and the 5′ half product of the *bcsAB* gene is a glycosyltransferase (GT) enzyme containing a conserved sequence motif D,D,D,Q-X-X-R-W (Nobles and Brown, 2007; Kawano et al., 2002). This enzyme is known as cellulose synthase (1,4-β-D-glycosyltransferase), and is regarded as the most important enzyme in the cellulose biosynthesis process (Saxena et al., 1994). The activity of BcsA is stimulated by binding 3′, 5′-cyclic diguanylic acid (cyclic-di-GMP), an activator of cellulose formation, which is mediated by the PilZ domain located at the C-terminus of the protein, next to the GT domain (Amikam and Galperin, 2006; Morgan et al., 2013).

The concentration of cyclic-di-GMP inside the cell is determined by the equilibrium in activity of diguanylate cyclase (DGC), which produces cyclic-di-GMP from two molecules of GTP, and the counter activity of a Ca^{2+} sensitive phosphodiesterase A (PDEA) in combination with phosphodiesterase B, that catalyzes the degradation of cyclic-di-GMP resulting in the formation of 5′-GMP (Ross et al., 1987). The proteins DGC and PDEA1 possess similar domains that have a haem-based oxygen domain or a flavin-bound redox sensor domain located in the N-terminus followed by GGDEF or EAL motifs respectively (Ausmees et al., 2001). Therefore, the GGDEF and EAL protein domains may function as a cyclase and phophodiesterase respectively (Simm et al., 2004). These two motifs are found in a large number of domains encoded by bacterial genomes, implying that cyclic-di-GMP regulation is common in bacteria (Galperin, 2005). The chemical structure of cyclic-di-GMP is shown in Figure 1.4.

On the other hand, the product of the *bcsB* gene is a predominantly a β-stranded periplasmic protein, with a single transmembrane anchor that interacts with BcsA (Morgan et al., 2014). The BcsB protein exhibits four domains: two jellyroll domains, which show high similarity to carbohydrate binding molecules (CBMs), and two flavodoxin-like folds (Morgan et al., 2013). Although the BcsB unit is essential for catalysis, only the interactions of the C-terminal TM anchor and a proceeding amphipathic helix of the protein with BcsA seem to be necessary to stabilize the TM region of BcsA for catalysis (Morgan et al., 2014). In addition, BcsB may be required to guide cellulose across the periplasm toward the outer membrane via two carbohydrate-binding domains (CBDs)(Morgan et al., 2013).

The functions of both *bcsC* and *bcsD* have not been precisely determined, but it has been proposed that the polypeptide produced by *bcsC* forms the major channel through which cellulose is secreted (Keiski et al., 2010). The BcsC protein is predicted to form a β-barrel porin located within the outer membrane, preceded by a relatively extensive periplasmic domain carrying tetratricopeptide repeats which may be involved in complex assembly (Keiski et al., 2010; Oglesby et al., 2008). The polypeptide produced by *bcsD*, for which the crystal structure has been elucidated, is believed to bind two other gene products on the channel or the outer surface of the membrane thereby influencing the crystallinity of cellulose (Yao et al., 2008).

Recent studies have shown that the BcsD protein is actually located in the periplasm and that it could be potentially function as a channel through the periplasm for the nascent cellulose strand (Iyer et al., 2011). The crystal structure of BcsD provides a model of how this protein would potentially function as a channel (Yao et al., 2008). Isolation of *G. xylinus bcsD* mutants have been shown to form smooth colonies and produce reduced amounts of cellulose in culture; therefore, suggesting that the *bcsD* gene is involved in cellulose biosynthesis (Saxena et al., 1994). The structural map of the *bcs* operon and identified regulatory genes in *G. xylinus* ATCC53582 used in this study are shown in Figure 1.4.

In addition to the cellulose synthesis operon genes, other genes have been implicated in the synthesis of cellulose. One gene called *cmcax*, located upstream of the cellulose synthase operon, encodes an endo-β-1,4-glucanase (CMCax) which possesses a cellulose hydrolyzing activity essential for bacterial cellulose production (Kawano et al., 2008). Interestingly, while CMCax hydrolyzes cellulose, it has been shown that CMCax promotes cellulose production; thus, suggesting that this protein is involved in cellulose biosynthesis (Kawano et al., 2008). Another gene

called *ccpax*, located in the upstream region of the operon, encodes a cellulose complementing protein known as CCPax. The function of CCPax is not well understood, but it has been suggested to be important for cellulose crystallization (Nakai et al., 2002). It has been reported that mutations in the *ccpax* gene results in a significant decreased of cellulose production (Deng et al., 2013). The downstream region of the operon has one or more genes involved in the production of β-glucosidase (BglAx) (Tonouchi et al., 1997). BglAx has been shown to to have an exo-1,4-β glucosidase activity towards cellotriose or larger cello-oligosaccharides, but a slight activity on cellobiose (Tonouchi et al., 1997). Although alterations in the *bglAx* gene have been shown to significantly decrease cellulose production, the role of BglAx, if any, in cellulose biosynthesis is still unknown (Deng et al., 2013).

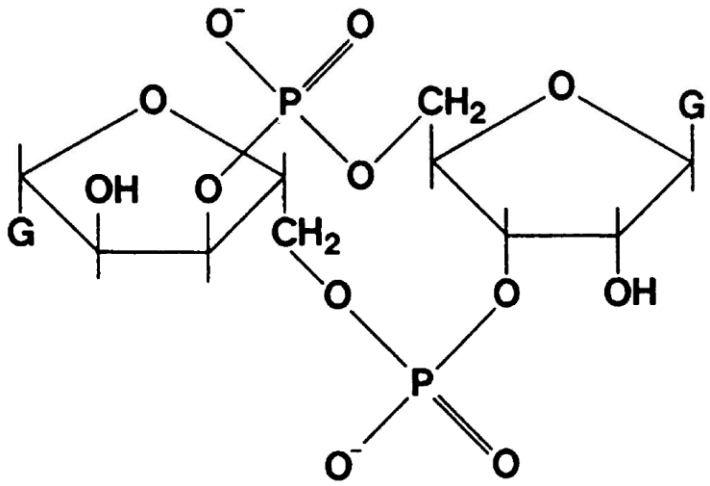

Figure 1.4: Chemical structure of the intracellular second messenger cyclic-di-GMP. Adapted from Ross et al. (1991).

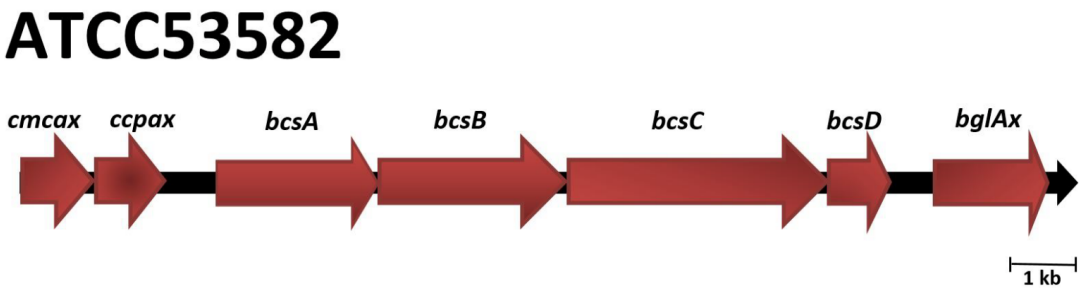

Figure 1.5: Structural map of the *bcs* operon and identified regulatory genes in *G. xylinus* ATCC53582. The location of the *cmcax, ccpax, bcsA, bcsB, bcsC, bcsD* and *bglAx* genes are shown. Modified from Kawano et al. (2002).

1.8 Cellulose synthase

Cellulose synthase has been classified within the type 2 family of glycosyltransferases (GTs) (Charnock et al., 2001). GTs are enzymes that drive catalysis transfer reactions of sugar residues from a donor substrate to an acceptor molecule (Saxena et al., 1995). The donor substrate is usually a nucleotide diphospho sugar, but in some cases it can also be a sugar phosphate or disaccharide (Saxena et al., 1995). On the other hand, the acceptor molecule is often a growing carbohydrate chain, a lipid carrier, or other molecules including steroids, bilirubin, and proteins that are modified by glycosylation (Hundle et al., 1992). The cellulose synthase as well as the chitin synthase are processive enzymes which are able to transfer multiple sugar residues to the acceptor. In these GTs, the catalysis reaction is considered as an inversion mechanism in which the substrates are α-linked nucleotide diphospho sugars from which the sugar is transferred to the acceptor molecules creating a β-linked product (Saxena et al., 1995; Charnock et al., 2001). Therefore, the cellulose synthase catalyses the formation of β-linkages by inversion, using α-linked UDP-sugar substrates. Only one nucleophilic substitution at the anomeric centre is sufficient to generate the β-configuration (Saxena et al., 1995). Most inverting GTs requires an essential divalent cation for catalysis. The cation is coordinated by the conserved Asp-X-Asp (DXD) motif at the active site to stabilize the nucleotide diphosphate leaving group during glycosyl transfer (Morgan et al., 2013). The putative mechanism for an inverting nucleotide-sugar glycosyltransferase is show in Figure 1.6. In addition to the DXD motif, cellulose synthase sequences also share the highly conserved catalytic region QXXRW, a motif characteristic of processive β-glycosyltransferases (Nobles and Brown, 2007).

Cellulose synthase, as well hyaluronan synthase and chitin synthase, are integral membrane proteins that contain multiple transmembrane domains. The BcsA protein possesses four N-terminal and four C-terminal transmembrane helices separated by an extended intracellular loop between helices 4 and 5 that forms the GT domain (Morgan et al., 2013). The GT domain of BcsA contains seven β-strands surrounded by seven α-helices (Morgan et al., 2013). The narrow channel for translocation of cellulose is formed by the transmembrane helices 3 to 8 and appears to accommodate 10 glucose residues of the translocating glucan (Morgan et al., 2013). The allosteric regulator cyclic-di-GMP has been shown to interact with a number of conserved residues in the PilZ domain of BcsA (Morgan et al., 2014). Binding of the cyclic-di-

GMP molecule to BcsA causes a conformational change in the PilZ domain disrupting a particular Arg-Glu salt bridge, which results in the displacement of a "gating loop" that allows UDP-glucose to bind (Morgan et al., 2014).

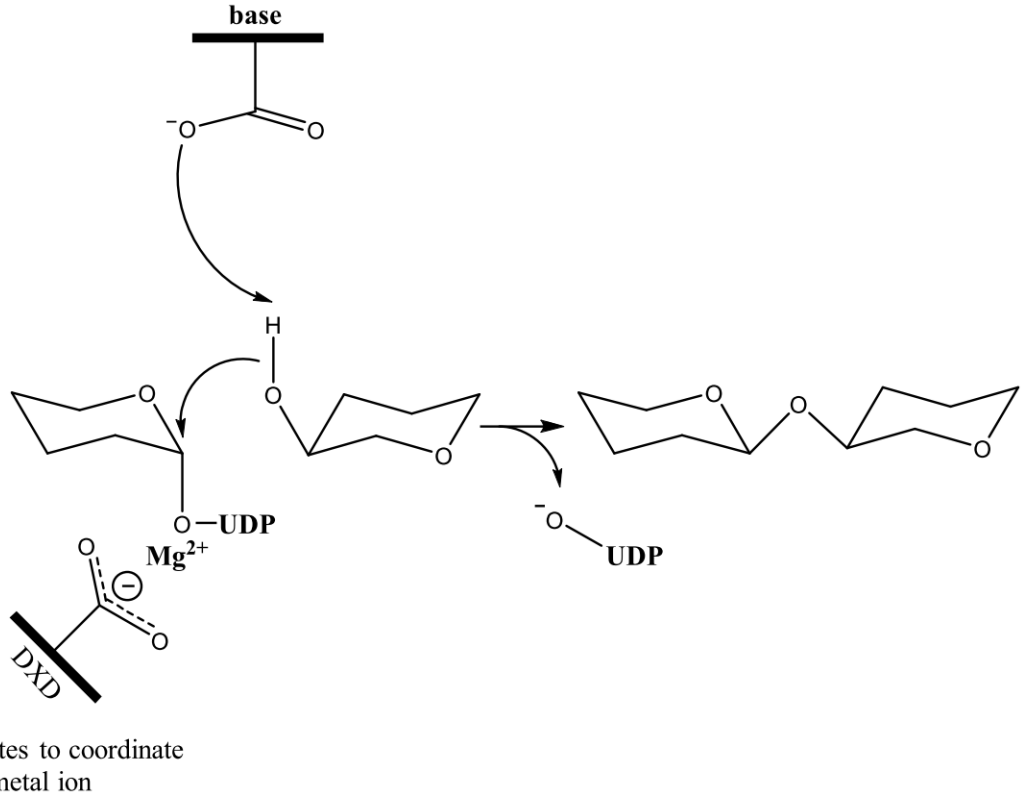

Figure 1.6: Putative mechanism for an inverting nucleotide-sugar glycosyltransferase. This mechanism involves the use of two catalytic carboxylates. The first carboxylate serves as a base to activate the acceptor species, and the second coordinates a divalent metal ion associated with the UDP-sugar. In most cases the metal ion coordination includes two carboxylates found in the conserved DXD motif. Modified from (Charnock et al., 2001).

1.9 Pellicin: a tool for cellulose biosynthesis investigation

Recent studies, using chemical genetic approaches, have identified a potent inhibitor of cellulose pellicle formation known as pellicin (Strap et al., 2011). This molecule was identified by conducting a high throughput perturbation study of cellulose biosynthesis using a library of small organic molecules. One the most important

properties of pellicin is that it can inhibit cellulose crystallization without disrupting cell growth (Strap et al., 2011).

It has been shown that a complete pellicle inhibition occurs at a concentration of 5 µM of pellicin while increasing the growth rate up to 1.5 times in *G. xylinus* cultures (Strap et al., 2011). On the other hand, *G. xylinus* cultures grow dispersed and their morphology is affected in the presence of pellicin. On solid medium, colonies of *G. xylinus* have been showed to be larger, raised, undulated and smoothed when pellicin is added as opposed to the cells growing under untreated conditions which normally show rough and convex morphologies (Strap et al., 2011). Moreover, characteristic filiform projections are visible in *G. xylinus* colonies under control conditions that are not present in pellicin treated colonies (Strap et al., 2011).

Finally, pellicin has not been shown to inhibit cellulose synthase activity. Crude membrane preparations from *G. xylinus* cells grown in pellicin containing media have shown to increase cellulose synthesis eightfold when compared to untreated membrane preparations, suggesting that cellulose synthase activity is not directly inhibited by pellicin (Strap et al., 2011). Electron microscopy (SEM) analysis, performed on pellicin treated cultures of *G. xylinus*has shown that the long fibrils observed in crystalline cellulose I are not produced in the presence of pellicin but an amorphous polysaccharide is produced instead (Strap et al., 2011). This effect of pellicin suggests that this chemical allows normal cellulose II biosynthesis assembly but inhibits the assembly of cellulose I from β-1,4-glucan chains. The chemical structure of pellicin is shown in Figure 1.7.

The strategy in this study was to analyze pellicin-resistant *G. xylinus* mutants in order to identify targets for pellicin that would help to uncover the mechanism by which aggregates of glucan chains are assembled to form the crystalline cellulose I.

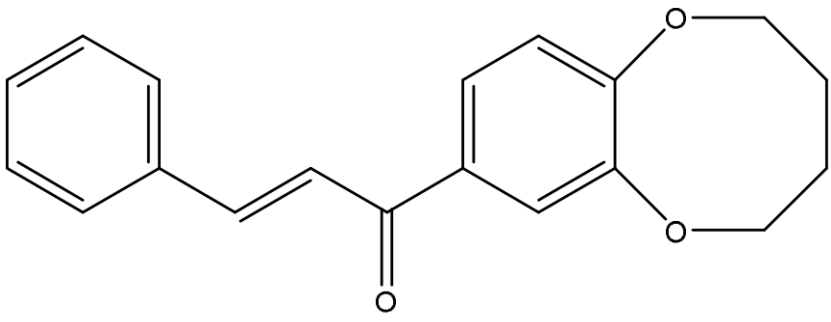

Figure 1.7: Chemical structure of pellicin ([2E]-3-phenyl-1-[2,3,4,5-tetrahydro-1,6-benzodioxocin-8-yl]prop-2-en-1-one)

1.10 Objectives and thesis rationale

Apart from being ubiquitous in nature and playing relevant biological roles, cellulose also has a great economic importance as it is the key component of products such as paper and textiles. In addition, cellulose produced from bacteria is of a great interest in fields such as biomedicine mostly because of its unique properties. As such, elucidation of cellulose biosynthesis mechanisms is essential for efficient cellulose production as well as for various industrial applications. In particular, although many of the key genes involved in cellulose biosynthesis have been identified, the mechanisms and regulation of β-1,4-glucan chain assembly during cellulose crystallization process is still unknown. For instance, the protein products encoded by the genes *bcsD*, and *ccpAx* have been suggested to influence cellulose crystallinity (Deng et al., 2013; Iyer et al., 2011), however the specific role of these proteins in this process is still unknown. The discovery of new proteins yet involved in this process would enhance our understanding of cellulose biosynthesis process, which in turn would help us to modify this process and generate cellulose-based products with desirable properties.

Since pellicin has been shown to inhibit cellulose crystallinity while maintaining other physiological functions in *G. xylinus*, it is hypothesized that investigation of high pellicin-resistant *G. xylinus* (HPR*Gx*) mutants would lead to a path that facilitates the understanding of unknown mechanisms involved in cellulose crystallization. Expanding on this idea, the main long-term objective of this project is to gain a better insight into the process of cellulose crystallization by genetically analyzing *G. xylinus* mutants resistant to the chemical pellicin. To meet this objective, HPR*Gx* mutants will be first characterized at the phenotypic level to reveal their pellicin resistance levels, crystalline cellulose production, colony morphologies, and cell growth. Secondly, mutations in the *bcs* operon genes of these mutants will be identified by PCR amplification and DNA sequencing analysis. Thirdly, the mutation found from the previous analysis will be reproduced from the wild type by site-directed mutagenesis in order to confirm the effect of the mutation. Finally, 3D modelling analysis, of both native and mutant proteins, will be performed in order to reveal potential mode of actions of pellicin and to uncover novel gene(s) likely involved in cellulose crystallization.

Therefore, the thesis herein will focus on the identification of mutations that confer resistance to pellicin in *G. xylinus*. Identification of these mutations will provide insight into the mechanisms and proteins involved in the extracellular assembly of

glucan chain aggregates into the crystalline cellulose I form.

Chapter 2

Materials and Methods

A forward genetic approach was used in this study in order to identify genes involved in the process of cellulose crystallization in *G. xylinus*. In this chapter, the materials and methods involved in the phenotypic and genotypic characterization of high pellicin-resistant *G. xylinus* (HPR*Gx*) mutants are described. High resistant mutants of a particular inhibitor correlate to specific mutations on key proteins involved in the biological function under study. Therefore, HPR*Gx* mutants were first isolated from previously generated *G. xylinus* mutants. The level of resistance to pellicin was first determined in order to isolate mutants highly resistant to the inhibitor. In order to identify other morphological alterations produced by the mutations in the HPR*Gx* mutants, these mutants were characterized at the phenotypic level. The phenotypic analysis consisted of: 1)quantification/comparison of the cellulose content present in pellicles formed by HPR*Gx* mutants and by wild type using anthrone assay; 2)observation of colony morphologies, both in the presence and in the absence of pellicin, using light microscopy; and 3)analysis of cell growth rates in the presence and in the absence of pellicin by means of spectrophotometry. Further genetic analysis of the HPR*Gx* mutants was conducted in order to identify and characterize genes involved in pellicin resistance and cellulose crystallization. DNA sequencing analysis of the *bcs* operon was used to identify mutations in this region of the genome. This analysis was followed by the recreation of the mutation observed in the *bcs* operon of the HPR*Gx* mutants from the wild type by means of site-directed mutagenesis in order to confirm that the mutation was sufficient to confer the pellicin resistant phenotype. Finally, a protein modelling analysis was performed using the sequences of native and mutated BcsA proteins. Since protein structure modelling is a useful tool for the study of potential

mode of actions of chemical inhibitors and resistance mechanisms, it was used in this study to investigate potential mode of actions of pellicin and cellulose crystallization mechanisms. A summary of the experimental design used in this study is depicted in Figure 2.1.

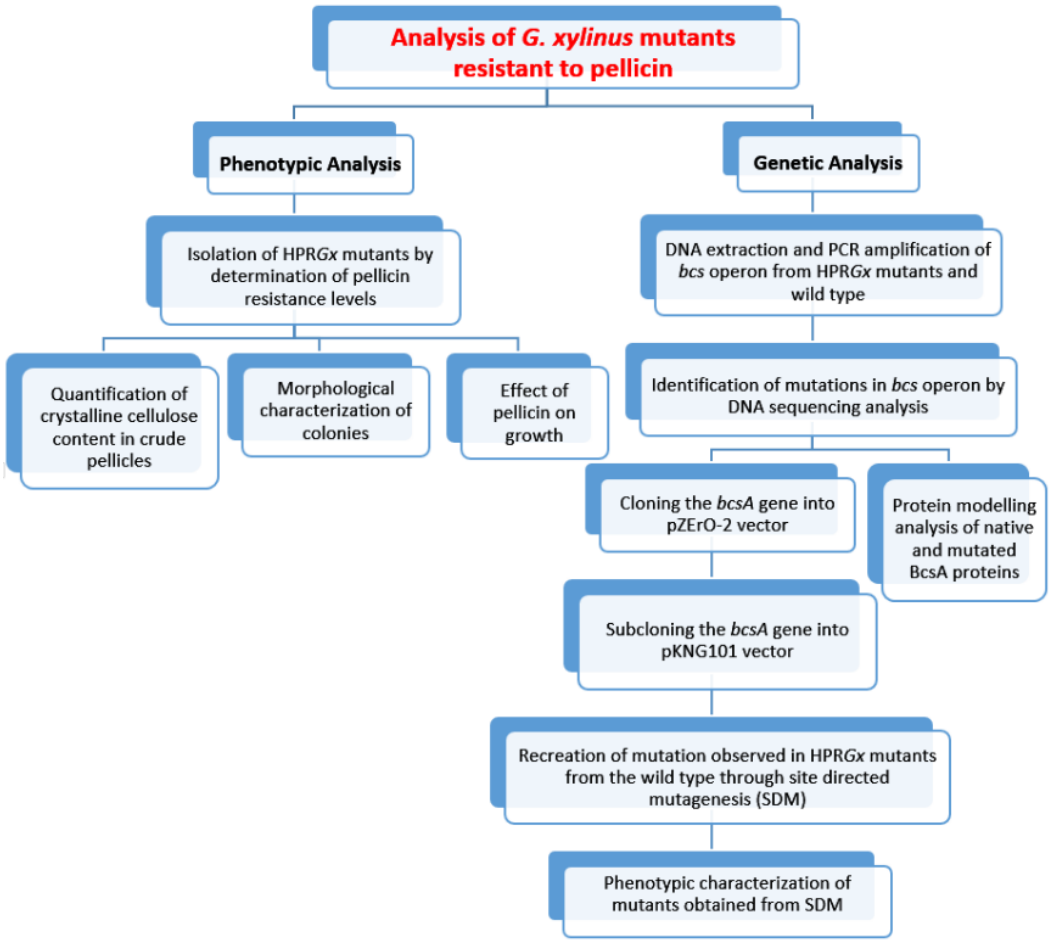

Figure 2.1: Experimental design used to identify and characterize genes involved in pellicin resistance and cellulose crystallization in HPRGx mutants.

2.1 Bacteria, medium and growth conditions

Gluconacetobacter xylinus ATCC 53582 and 15 pellicin-resistant *G. xylinus* (PRGx) mutants, obtained from the same strain, were cultured on solid Schramm-Hestrin (SH)/agar medium at 30°C for 7 days. The 15 PRGx mutants were previously isolated by Silvia Blank who used ethyl methanesulfonate (EMS) mutagenesis for this purpose.

The SH medium was prepared with 20g of glucose, 5g of peptone, 5g of yeast extract, 2.7g Na_2HPO_4, and 1.5 g of citric acid mixed in 1000 mL of MilliQ water. The SH medium was autoclaved for fifty minutes prior to use. Individual colonies were grown in SH medium under static conditions or on a rotatory shaker (150 rpm) at 30°C. For preparation of *G. xylinus* cells, cellulase from *Trichoderma reesei* ATCC 26921 (Sigma-Aldrich) was added to the culture medium 24 h before harvesting to digest the cellulose and obtain a uniform suspension. *E. coli* strains used in this study (DH5α, and 5-alpha F' I^q, and MaH_1 $pir116^+$), were grown in Luria Broth (LB) medium at 37^{o}C under static conditions or on a rotatory shaker (250 rpm). For selection of resistant markers, antibiotics were used at the following concentrations: kanamycin, 50 µg/mL; ampicillin, 100 µg/mL; and streptomycin, 50 µg/mL. The *E.coli* strain MaH1 $pir116^+$ was kindly provided by Dr. Ayush Kumar, whereas DH5α, 5-alpha F' I^q, and dam^-/dcm^- strains were purchased from New England Biolabs (Mississauga, Ontario, Canada).

2.2 Preparation of *G. xylinus* cultures to identify level of pellicin resistance

The pellicle formation of PR*Gx* mutants was analyzed under different concentrations of pellicin. *G. xylinus* cells were first cultivated in SH liquid medium on a rotary shaker at 30°C for 7 days. A cellulose-free uniform suspension of *G. xylinus* cells was obtained by adding cellulase to the growth medium to a final concentration of 0.3% (v/v). The initial inoculum was prepared as described in section 2.5. Cellulose pellicles were allowed to form for seven days under static conditions at 30°C in 96-well microtitre plates. Each well was loaded with a total volume of 200 µL bacterial culture containing either dimethylsulfoxide (DMSO) or pellicin dissolved in DMSO at different pellicin concentrations (5 to 200 µM). Due to the hydrophobic nature of pellicin, this molecule is insoluble in water. For this reason, pellicin was dissolved in the organic solvent DMSO. Nine technical replicates obtained from three biological replicates were used for this analysis. Biological replicates in this context are parallel measurements of biologically distinct samples whereas technical replicates are repeated measurements of the same biological sample. The procedure used to identify the level of pellicin resistance in PR*Gx* mutants is depicted in Figure 2.2

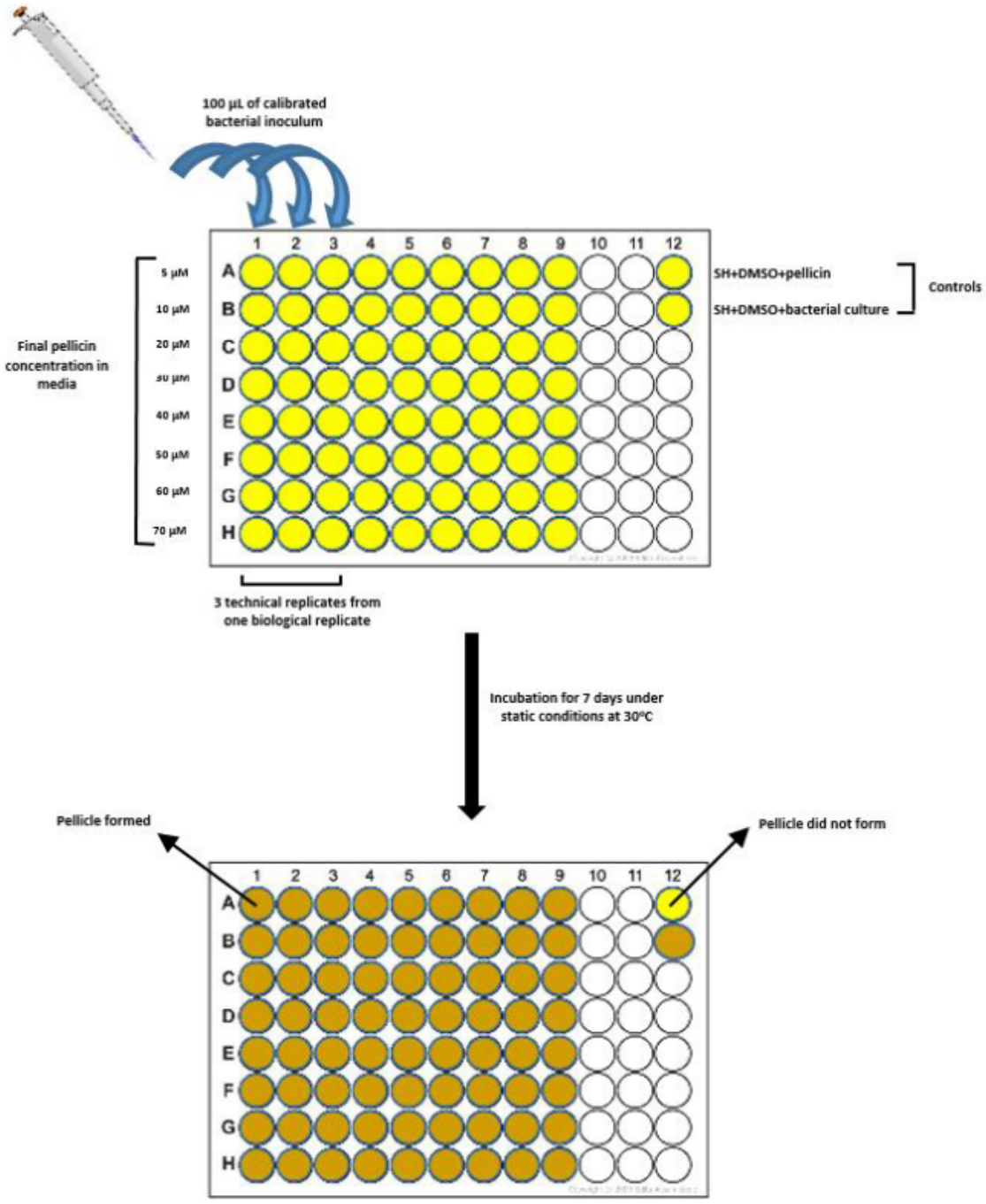

Figure 2.2: Procedure used to identify the level of pellicin resistance of PR*Gx* mutants. The level of pellicin resistance was determined by the formation of pellicles in *G. xylinus* cultures at different concentrations of pellicin in 96-well microtitre plates after incubation for 7 days under static conditions at 30°C. Cultures were tested in pellicin concentrations of up to 200 µM in additional 96-well microtitre plates. Nine technical replicates obtained from three biological replicates were used for this analysis.

2.3 Determination of crystalline cellulose content in pellicles formed by *G. xylinus* wild type and HPR*Gx* mutants

Acetic acid/nitric acid (Updegraff) reagent followed by the anthrone assay was used to estimate the crystalline cellulose content in each pellicle formed by the HPR*Gx* mutants and wild type (Updegraff, 1969). Pellicles formed by HPR*Gx* mutants and wild type were first hydrolyzed in Updegraff reagent. Initial inocula from the HPR*Gx* mutants and wild type were prepared as described in section 2.5. Cellulose from each culture was allowed to form in 6-well plates with a total volume of 5 mL of bacterial culture per well, containing either DMSO or pellicin dissolved in DMSO. Three biological replicates were used for statistical analysis. The culture samples were incubated at 30°C under static conditions for 7 days until pellicle of cellulose was formed in the wells. The pellicles produced were harvested and washed with acetone five times and air dried at room temperature for 10 days until all water in the pellicles was removed. The dried pellicles were weighed and 15 mg of each pellicle was carefully weighted and transferred to a glass test tube for further cellulose quantification. Each pellicle fraction was soaked in 3 mL of acetic/nitric acid reagent that was prepared by mixing 225 mL of 80% acetic acid and 22.5 mL concentrated nitric acid. For *G. xylinus* wild type cultures supplemented with pellicin, cells were centrifuged, the liquid was removed by aspiration, and the pellet was treated with the acetic/nitric reagent. The acetic/nitric acid reagent containing the pellicle fractions were incubated in a boiling water bath for 45 minutes. Screw caps were placed on top of each tube to minimize evaporation and allow refluxing action. The pellicles were transferred to pre-weighted Whatman 3MM glass fibre filter papers and they were washed several times with 70% ethanol by vacuum filtration using a multiple vacuum filtration system. The remaining insoluble cellulose fractions were then allowed to dry overnight at room temperature.

The total crystalline cellulose content in each pellicle fraction was estimated as glucose equivalents by anthrone test. The anthrone reagent was prepared by dissolving 0.2 g of anthrone in 100 mL concentrated sulphuric acid. The anthrone reagent was prepared fresh and it was chilled 2 hours prior to use. The pellicle fractions with the glass fibre filter papers were placed in 6-well plates and 5 mL of 67% sulfuric acid was added to each well. The pellicle fractions were allowed to dissolve for 1 hour by shaking

the 6-well plates on a rotatory shaker at room temperature. A volume of 50 µL of each sample was loaded onto a 96-well microtiter plate and 100 µL of cold anthrone reagent was added and mixed to each sample using a multichannel pipette. The 96-well microtiter plates were then incubated at 100°C on a heat blocked for 5 minutes. The samples were allowed to cool in a refrigerator at 4°C for 30 minutes. The absorbance for all the samples was measured at a wavelength of 620 nm (OD_{620}) against a reagent blank using a Bio-Rad xMark™ Microplate Absorbance Spectrophotometer (Bio-Rad Laboratories Ltd., Mississauga, ON). The total crystalline cellulose content from each pellicle was determined using glucose as standard.

2.4 Light microscopy

Light microscope images of *G. xylinus* colonies were taken using an Amscope dissecting microscope adapted with an Amscope MD900E camera (Irvine, CA). The total magnification used was 100X.

2.5 Growth curves

In order to determine the effect of pellicin on growth on both the *G. xylinus* wild type and the HPR*Gx* mutants, they were examined under non-pellicin and pellicin conditions. Growth curve data was collected in 96-well microtitre plates inoculated with a total volume of 200 µL SH medium containing 0.3% cellulase and either DMSO or pellicin dissolved in DMSO. The inoculum was prepared by harvesting 5-day old, *G. xylinus* cellulase-digested cultures by centrifugation at 17,000 x *g* for 5 minutes at room temperature followed by three washes with SH medium. The starting inoculum was adjusted to an optical density of 0.02 in SH broth at 600 nm (OD_{600}). The bacterial culture plates were incubated at 30°C with shaking at 150 rpm. The optical density was measured using Bio-Rad xMark™ Microplate Absorbance Spectrophotometer (Bio-Rad Laboratories Ltd., Mississauga, ON). The bacterial growth was followed for 154 hours. The data from eight technical replicates obtained from two biological replicates were averaged and used for statistical analysis.

2.6 Isolation of bacterial genomic DNA using CTAB extraction

Colonies of *G. xylinus* wild type and (PR*Gx*) mutants were inoculated and grown in 50 mL of SH medium under agitated conditions at 30°C for 3 days. In order to obtain a uniform suspension of cellulose-free *G. xylinus* cells, cellulase from *Trichoderma reesei* was filtered sterilized and added to the medium to a final concentration of 0.3% (v/v). A total volume of 10 mL of the bacterial culture was concentrated in a 1.5 mL Eppendorf tube by centrifugation at 17,000 x *g* (13,000 rpm) at room temperature followed by three washes with SH medium. The genomic DNA from *G. xylinus* was isolated by a modified procedure from Murray and Thompson (1980). A 2X CTAB extraction buffer was prepared by mixing 2% (w/v) cetyl trimethyl ammonium bromide (CTAB), 1.4 M NaCl, 100 mM Tris HCl pH 8.0, and 20 mM EDTA. The *G. xylinus* cells from the concentrated sample were precipitated by centrifugation and all the medium was removed by aspiration, leaving the bacterial pellet as dry as possible. The cells were mixed with 500 mL of 2X CTAB buffer and vortexed thoroughly until complete cell suspension was observed. The solution was incubated with 1 µL of RNaseA (50 µg/mL) at 65°C for 30 minutes and allowed to cold at room temperature. An equal volume of chloroform was added and the contents were mixed by inverting the tube several times. The solution was then centrifuged for 10 minutes at 17,000 x *g* to separate the aqueous and organic phases. The upper aqueous phase was transferred to a fresh tube and mixed with an equal volume of 2-propanol to precipitate the nucleic acids. The solution was then centrifuged for 20 minutes at 7,000 x *g* to pellet the DNA and the supernatant was removed. The pellet was then washed with 70% ethanol and centrifuged at 7,000 x *g* for 5 minutes. The ethanol layer was carefully removed and the pellet was air dried for 15 minutes. Finally, the pellet was re-suspended in 100 µL of TE buffer made of 10 mM Tris HCl pH 8.0, and 1 mM EDTA. The samples were cleaned by phenol/chloroform extraction followed by ethanol precipitation as described in section 2.7. The genomic DNA collected was confirmed by gel electrophoresis as described in section 2.13.

2.7 DNA clean-up

Phenol/Chloroform extraction: An equal volume of buffer-saturated phenol:chloroform (pH 8.0) was added to DNA samples suspended in Tris buffer.

The solution was mixed by inverting the tubes several times followed by centrifugation for 5 minutes. The aqueous layer was carefully removed and transferred to a new clean Eppendorf tube. Three successive chloroform extractions were performed to remove all traces of phenol. The aqueous layer was transferred to a clean tube and the DNA was collected by ethanol precipitation.

Ethanol precipitation: Nucleic acids were precipitated from solution by adding two volumes of ice cold absolute ethanol. The solution was mixed and allowed to stand for 15 minutes at room temperature. The mixture was then centrifuged at 7,000 x *g* for 30 minutes and the supernatant was discarded. The pellet was washed with 70% ethanol, air dried, and dissolved in 50 µL of 2.0 mM Tris-HCl buffer pH 8.0. The DNA was stored at -20°C.

2.8 Amplification of the cellulose synthase operon of *G. xylinus* by polymerase chain reaction (PCR)

The cellulose synthase operon containing the genes *bcsA, bcsB, bcsC, and bcsD* from *G. xylinus* wild type and PR*Gx* mutants were amplified by touchdown PCR using oligonucleotide primers designed according to the published cellulose synthase operon sequence of *G. xylinus* ATCC 53582 (GenBank accession number X54676.1). In order to amplified all the genes in one reaction, the *bcsC* gene was amplified in two fragments with 478 bp overlapped as this gene is very large when compared to the other genes. The quality of the primers was virtually examined for possible dimerization and specificity using Amplify 3X software. All primers were obtained from IDT (Integrated DNA technologies). Separate PCR reactions were prepared for each set of primers by mixing the following components: 17.5 µL MilliQ H_2O, 1.5 µL template DNA (10-100ng), 2.5 µL 10x Ex taq buffer (20 mM Mg^{2+} plus), 0.5 µL forward Primer (10 µM), 0.5 µL reverse primer (10 µM), 2 µL dNTPs (2.5 mM each), and 0.5 µL Takara Ex Taq™ DNA polymerase.

For the touchdown PCR the initial denaturation condition was 98°C for 2 minutes, followed by 10 cycles of 98°C for 30s, 60°C(decreasing by 1°C/cycle) for 30s, and 72°C for 3 minutes. This was followed by 30 cycles of 98°C for 10s, 56°C for 30s, and 72°C for 3 minutes with a final extension at 70°C for 5 minutes, followed by a 16°C hold.

The quality of the PCR products were confirmed by gel electrophoresis as described in section 2.13. The PCR products were amplified with the primers listed in Table 2.1 and sent for DNA sequencing as described in section 2.9. The primers used to sequence the cellulose synthase operon are shown in Table 2.2.

Table 2.1: Cellulose synthase operon primers. The primers were designed to amplify the genes *bcsA*, *bcsB*, *bcsC*, and *bcsD* in *G. xylinus* for further DNA sequencing analysis.

Primer Name	5′ -Sequence-3′	Tm(°C)	Length
*bcsA*Fwrd	AACGAAGAAGAATCCTAAGGC	52	21
*bcsA*Rev	GACGGGTTGTTCGTATCGT	55	19
*bcsB*Fwrd	CAGCCTCATGGACATGGTTCT	58	21
*bcsB*Rev	GGACGAAGCATATCGTTTATGG	54	22
*bcsC*Fwrd1	CGGACTGGTATATGCACAACAGA	57	23
*bcsC*Rev1	GGCGCAAGATGGTCATACG	57	19
*bcsC*Fwrd2	GACTGTCGCCGGATGACTA	57	19
*bcsC*Rev2	ATCGAAACCACCAACAAGGCTA	57	22
*bcsD*Fwrd	GTGTATCAGGCCCTTGCGAA	58	20
*bcsD*Rev	ATCCAGGCAAGCGATCGTATT	57	21

Table 2.2: Cellulose synthase operon sequencing primers. The primers were used to sequence the *bcsA, bcsB, bcsC,* and *bcsD* genes in *G. xylinus*.

Primer Name	5′ -Sequence-3′	Tm(°C)	Length
bcsA Seq Fwrd1	AACGAAGAAGAATCCTAAGGC	52	21
bcsA Seq Fwrd2	TTGGGACAATGCTTCTGGT	54	19
bcsA Seq Fwrd3	TACCGCACTCAAGATGCAG	55	19
bcsA Seq Fwrd4	AACTGTCTTTCGGCCATCTC	55	20
bcsA Seq Rev1	ACCAGAAGCATTGTCCCAA	54	19
bcsA Seq Rev2	CTGCATCTTGAGTGCGGTA	55	19
bcsA Seq Rev3	GAGATGGCCGAAAGACAGTT	55	20
bcsA Seq Rev4	GACGGGTTGTTCGTATCGT	55	19
bcsB Seq Fwrd1	AGCCTCATGGACATGGTTC	55	19
bcsB Seq Fwrd2	CTGAACGAGCAGTATATCGG	53	20
bcsB Seq Fwrd3	ACCGTGATGAGGTCATTACC	54	20
bcsB Seq Fwrd4	GCAAACAATGCGTTCCATCT	54	20
bcsB Seq Fwrd5	ACCTCCTTCAGATGTTGGG	54	19

bcsB Seq Rev1	CCGATATACTGCTCGTTCAG	53	20
bcsB Seq Rev2	GGTAATGACCTCATCACGGT	54	20
bcsB Seq Rev3	AGATGGAACGCATTGTTTGC	54	20
bcsB Seq Rev4	CCCAACATCTGAAGGAGGT	54	19
bcsB Seq Rev5	GGACGAAGCATATCGTTTATGG	54	22
bcsC Seq Fwrd1	GGACTGGTATATGCACAACAGA	55	22
bcsC Seq Fwrd2	AGCACCTGTTCAACGGTT	55	18
bcsC Seq Fwrd3	GCATCGTTACCTCGAAGATG	53	20
bcsC Seq Fwrd4	GATTCAGCGCAGAAGGTC	54	18
bcsC Seq Fwrd5	CTGTCGCCGGATGACTATT	55	19
bcsC Seq Fwrd6	ATAATCCGCAGGACCTTGAT	53	20
bcsC Seq Fwrd7	CCTGCAGAACCAGAACAAC	54	19
bcsC Seq Rev1	GAACCGTTGAACAGGTGC	55	18
bcsC Seq Rev2	CATCTTCGAGGTAACGATGC	53	20
bcsC Seq Rev3	CGCATTGGCAAGGTTGAT	54	18
bcsC Seq Rev4	GCGCAAGATGGTCATACG	54	18
bcsC Seq Rev5	GTTGTCCTTGCCGTCATT	53	18
bcsC Seq Rev6	CGGTATTGATGCGATGTTCC	54	20
bcsC Seq Rev7	GAAACCACCAACAAGGCTA	53	19
bcsD Seq Fwrd1	GTATCAGGCCCTTGCGAA	55	18
bcsD Seq Fwrd2	AGATCGAACTGAACGCG	54	17
bcsD Seq Rev1	CGACATAATCACCAAACGCA	53	20
bcsD Seq Rev2	ATCCAGGCAAGCGATCGTATT	57	21

2.9 DNA sequencing analysis

PCR products containing regions of interest were amplified using Taq polymerase. About 7 µL of 50 ng PCR product was added to PCR tubes containing 0.7 µL of 50 pmols of either forward or reverse primers. The samples were sent to Sanger Sequencing Facility in Toronto, Canada for further PCR sequencing. Chromatograph sequences were analyzed using CLC Main Workbench version 6.9.

2.10 Isolation of plasmid DNA

Plasmid DNA was isolated from small-scale bacterial cultures by treatment with alkali and sodium dodecyl sulfate (SDS) using a modified procedure from Sambrook and Russell (2001). Three alkaline lysis solutions (I, II, and III) were prepared for this procedure. The alkaline lysis solution I was prepared using the following components: 50 mM glucose, 25 mM Tris-HCl (pH 8.0), and 10 mM EDTA (pH 8.0). The alkaline lysis solution II was prepared using the following components: 0.2 N NaOH (freshly prepared from 10 N stock), and 1% (w/v) SDS. The alkaline lysis solution III was prepared using the following components: 5 M KCH_3CO_2 60 mL, glacial acetic acid 11.5 mL, and H_2O 28.5 mL. Approximately 100 mL of alkaline lysis solution I was prepared, autoclaved for 15 minutes on liquid cycle and stored at 4°C. Alkaline solution II was prepared fresh and it was used at room temperature. The alkaline lysis solution III was stored at 4°C and transferred to ice just before use. Approximately 3 mL of LB medium supplemented with the appropriate selection antibiotics were inoculated with a single bacterial colony and grown overnight with vigorous shaking (250 rpm) at 37°C. A volume of 1.5 mL of the bacterial culture was transferred to an Eppendorf tube and centrifuged at maximum speed for 10 minutes at room temperature. The medium was removed by aspiration leaving the pellet as dry as possible. The pellet was re-suspended in 100 µL of ice-cold alkaline solution I and mixed thoroughly by vortexing. A volume of 200 µL of freshly prepared alkaline lysis solution II was added to the bacterial suspension and the contents were mixed by inverting the tubes several times. A volume of 150 µL of ice-cold alkaline solution III was then added and dispersed through the viscous bacterial lysate by gently shaking the tubes. The solution was stored on ice for 5 minutes. The bacterial lysate was then centrifuged at maximum speed for 5 minutes at room temperature and the supernatant was transferred to a new microfuge tube. In order to digest the RNA present in the solution, 1 µL of RNaseA (50 mg/mL) was added followed by incubation at 57°C for 10 minutes. An equal volume of phenol:chloroform was added to the solution and mixed by inverting the tubes several times. The emulsion was centrifuged at maximum speed for 10 minutes at room temperature and the aqueous upper later was transferred to a fresh tube. One chloroform extraction was performed to remove all traces of phenol. Nucleic acids were precipitated from the supernatant by ethanol precipitation as described in section 2.7 and dissolved in 50 µL of 2.0 mM Tris-HCl buffer pH 8.0. The quality of the plasmid DNA was confirmed by gel electrophoresis as described in section 2.13.

2.11 Preparation of *G. xylinus* electrocompetent cells

Wild type *G. xylinus* cells were grown overnight in 2 mL SH medium. The cultures were diluted into 250 mL of SH medium containing 0.3% (v/v) cellulase from *Trichoderma reesei* and incubated with aeration (150 rpm shaking) at 30°C until the cells reached early log phase with an optical density of 0.5 to 0.8 at 550 nm using a Spectronic™ GENESYS™ 20 spectrophotometer (Thermo Electron Corporation).

The total volume of the bacterial cultures were then transferred to centrifuge tubes followed by incubation on ice for 20 minutes. The cells were kept on ice through the rest of the procedure. The cells were pelleted by centrifugation at 2,700 X *g* for 10 minutes at 4°C and subsequently washed with 100 mL of cold 1 mM HEPES (pH 7.0). The centrifugation and washing procedure was repeated twice. The cells were then re-suspended in 50 mL of cold 12.5% glycerol and precipitated again by centrifugation. This procedure was repeated twice. Finally the cells were re-suspended in 5 mL of cold 10% glycerol and aliquots of 100 µL were prepared and frozen at -80°C.

2.12 DNA manipulations

2.12.1 PCR amplification of the *bcsA* gene with additional restriction sites to the termini of the amplified DNA

The *bcsA* gene was PCR-amplified with high fidelity Phusion polymerase purchased from New England Biolabs (Mississauga, Ontario, Canada). The high fidelity Phusion polymerase enzyme possesses a 3′-5′ exonuclease proof reading activity that decreases the number of errors in nucleotide incorporation during PCR amplification and hence it was used to clone the *bcsA* gene into the pZErO-2 cloning vector. Specific PCR primers were designed to amplify the region of interest including desired recognition sequences for restriction enzymes at the 5′ end of each primer. A *BamHI* (GGATCC) restriction site was added at the 5′ end of the forward primer, and a *SpeI* restriction site (TGATCA) was added at the 5′ end of the reverse primer. In order to increase digestion efficiency, additional nucleotides were included besides the restriction enzyme sequences. The designed primers are

shown below with the restriction sites in bold and underlined. The enzymes were purchased from New England Biolabs (Mississauga, Ontario, Canada) and the primers were synthesized by IDT (Integrated DNA technologies). After PCR amplification the quality of the plasmid DNA was confirmed by gel electrophoresis as described in section 2.13.

BcsA_BamHI Frwd: 5′-**TAC<u>GGATCC</u>**AACGAAGAAGAATCCTAAGGC-3′
BcsA_SpeI Rev: 5′-**ATC<u>ACTAGT</u>**GACGGGTTGTTCGTATCGT-3′

The PCR reaction to amplified the *bcsA* gene with the additional restriction sites was carried out by mixing the following components: 14.25 µL MilliQ H_2O, 1.5 µL template DNA (10-100ng), 5 µL 5x Phusion HF buffer, 0.5 µL MgCl2 solution (50 mM), 1 µL forward Primer (10 µM), 1 µL reverse primer (10 µM), 2 µL dNTPs (2.5 mM each), and 0.25 µL Phusion High-Fidelity DNA Polymerase.

For the touchdown PCR used to amplify the *bcsA* gene with additional restriction sites to the termini of the amplified DNA, the initial denaturation condition was 98°C for 2 minutes, followed by 10 cycles of 98°C for 30s, 60°C(decreasing by 1°C/cycle) for 45s, and 72°C for 2 minutes and 30s. This was followed by 30 cycles of 98°C for 10s, 56°C for 45s, and 72°C for 2 minutes and 30s with a final extension at 70°C for 5 minutes, followed by a 16°C hold.

The quality of the PCR products were confirmed by gel electrophoresis as described in section 2.13.

2.12.2 Blunt-end cloning of PCR products

The pZErO-2 plasmid was cut with *EcoRV* to produce a blunt-ended linearized plasmid. Enzymatic reaction was incubated for 3 hours and carried out using the following components: 15 µL MilliQ H_2O, 2 µL 10x NEBuffer, 2 µL plasmid DNA, and 1 µL restriction enzyme

The linearized pZErO-2 plasmid and *bcsA* PCR product were run at 100 V for 70 minutes on 1% agarose gels containing 5 µL of ethidium bromide (EtBr) dye to facilitate further visualization. The DNA bands of interest were visualized using a Dark Reader DR89X Transilluminator (Integrated Scientific Solutions Inc.) and cut from the gel with a sharp scalpel. The gel pieces were collected in Eppendorf tubes and the DNA was isolated by using a gel extraction kit from Qiagen as per manufacturer's instructions. The quality of purified DNA samples was confirmed by gel electrophoresis as described in section 2.13.

The purified *bcsA* PCR fragment was blunt-end ligated into the linearized pZErO-2 plasmid vector using T4 DNA ligase. Approximately 150 ng of linearized vector was used in the ligation reaction. Reactions with vector:insert molar ratios between 1:1 and 1:10 were tested and 1:6 was found to be the best. Polyethylene glycol (PEG) was used in the reaction as it can induce macromolecular crowding of solutes in aqueous solutions which increase the rate of ligation of blunt-ended DNA by one to three orders of magnitude (Sambrook and Russell, 2001). The following components were mixed for the ligation reaction: $\sim$ 150 ng linearized plasmid DNA, 1 µL 6x amplified insert, 1 µL 10x ligation buffer, 1 µL T4 DNA ligase, 1 µL PEG 8000 50% (v/v), and MilliQ H_2O to 10 µL.

The reaction mixture was incubated at 16°C overnight in a thermocycler. The complete volume of the ligated mixture was used for transformation into competent *E. coli* cells as described in section 2.12.4 and colony PCR was performed for screening purposes as described in section 2.12.5. The resulting plasmid was named pZErO-2_*bcsA*. All the enzymes used were purchased from New England Biolabs (Mississauga, Ontario, Canada).

2.12.3 Sticky-end cloning

The suicide plasmid vector pKNG101 was used in the present study in an attempt to generate *G. xylinus* mutants altered in the *bcsA* gene. The *bcsA* fragment was inserted between the *BamHI* and *SpeI* sites of pKNG101 cloning vector. The construct pZErO-2_*bcsA* was first double digested with *BamHI* and *SpeI* endonucleases to obtain a *bcsA* fragment with sticky ends. The pKNG101 cloning vector was also double digested with *BamHI* and *SpeI* enzymes to yield a linearized plasmid with compatible cohesive sticky ends.

A protocol of DNA purification using low melting point agarose gel modified from (Sambrook and Russell, 2001) was performed. The digested fragments were first separated on a 0.8% low melting temperature agarose gel prepared using 1X TAE buffer. The electrophoresis was carried out at 50 V for 3 hours. The gels were prepared with 5 µL of EtBr dye to facilitate visualization of DNA. The DNA bands of interest were visualized using a Dark Reader DR89X Transilluminator (Integrated Scientific Solutions Inc.) and cut from the gel with a sharp scalpel. The gel pieces were collected in pre-weighted Eppendorf tubes. Approximately 5 volumes of low melting temperature (LMT) elution buffer (20 mM Tris-Cl (pH 8.0)

and 1 mM EDTA (pH 8.0)) was added to the slice of agarose and the gel fractions were melt by incubation for 10 minutes at 65°C. The solution was let to cool at room temperature, and an equal volume of equilibrated phenol (pH 8.0) was added. The solution was mixed by inverting the tube several times, and the aqueous phase was recovered by centrifugation at maximum for 10 minutes at room temperature. The aqueous phase was extracted once with an equal volume of phenol:chloroform and once with an equal volume of chloroform. The aqueous phase was transferred to a fresh Eppendorf tube and the nucleic acids were precipitated from the supernatant by ethanol precipitation as described in section 2.7 and concentrated in 25 µL 2.0 mM Tris-HCl buffer pH 8.0. Sticky-end ligation reactions were performed using various vector to insert molar ratios with overnight incubation at 16°C in a total volume of 10 µL as described in section 2.12.2. The ligation reactions were used to transform *E. coli* DH5α competent cells and colony PCR was used to select for colonies carrying the plasmid of interest as described in section 2.12.5. The resulting plasmid was named pKNG101_*bcsA*_ColE1 ori. All the enzymes used were purchased from New England Biolabs (Mississauga, Ontario, Canada).

2.12.4 Transformation of plasmid DNA into competent *E. coli* cells

Transformation of ligation products into *E.coli* cells was achieved using a heat shock method. Frozen *E.coli* competent cells (DH5α, 5-alpha F' I^q or dam$^-$/dcm$^-$) were thawed on ice for 7 minutes. A total volume of 50 µL of competent cell suspension was used per transformation and mixed with 10 µL of ligation product in an Eppendorf tube. Each transformation mixture was incubated on ice for 30 minutes and then heat shocked for exactly 30 seconds at 42°C. The mixtures were then incubated on ice for 5 minutes. Cells were allowed to recover by adding 950 µL of SOC outgrowth medium to each mixture followed by incubation with vigorous shaking (250 rpm) at 37°C for 1 hour. Selection LB/agar plates were prepared and warmed to 37°C. The cells from each reaction were mixed and 200 µL of solution were spread onto a selection plate followed by incubation at 37°C overnight.

2.12.5 Colony PCR

Plasmids transformed into cells may not carry the desired gene of interest. Therefore, for screening purposes, colonies from transformed *E. coli* cells carrying the plasmid of interest were selected using colony PCR. Single bacterial colonies were inoculated with sterilize pipette tips from selection plates into each well of 96-well plates containing 200 µL LB with appropriate selection antibiotics. The cells were cultures overnight at 37°C. For colony PCR reactions One Taq DNA polymerase with 5X Standard Buffer purchased New England Biolabs (Mississauga, Ontario, Canada) were used. A master mix for 40 PCR reactions was prepared with the following components: 640 µL MilliQ H_2O, 200 µL 5X One Taq standard buffer, 20 µL forward primer (10 µM), 20 µL reverse primer (10 µM), 80 µL dNTPs (2.5 mM each), and 5 µL One Taq DNA polymerase.

Aliquots of 23 µL of this master mix solution was added into individual PCR tubes. A total volume of 2 µL of each bacterial culture from the 96-well plate, were added to the PCR tubes containing the master mix. The PCR reaction was performed with the same parameters used to amplify the cellulose synthase operon with Ex Taq™ DNA polymerase.

A total volume of 2 µL of each PCR reaction was loaded onto a 1% agarose gel, alongside the molecular marker Lambda DNA/*HindIII* Plus, and visualized under UV light. Bacterial colonies that produced PCR products with an equivalent size than the insert of interest were inoculated in selective LB medium and incubated overnight at 37°C on a rotatory shaker at 250 rpm. The plasmids were isolated as described on section 2.10 and the presence of the insert was verified by single and double enzymatic restriction digestions using *BamHI* and *SpeI*. The digested samples were loaded onto a 1% agarose gel, alongside an appropriate DNA ladder, and the resulted fragments were visualized under UV light. In addition, the insert was verified by PCR using the same primers that employed to amplify the *bcsA* gene from the genome. Finally, in order to confirm the integrity of the *bcsA* gene, plasmid samples were sent for sequencing as described in section 2.9 using the universal M13 primers.

2.12.6 Site-directed mutagenesis using polymerase chain reaction (PCR)

Site-directed mutagenesis allows to design selected changes in DNA in order to study the functions of particular genes. In this study, site directed mutagenesis of the *bcsA* gene was performed wherein ACG, which encodes for alanine, was substituted by ACA, which encodes for threonine. This substitution was performed at position 1345 of the nucleotide sequence of the *bcsA* gene which corresponds to the mutation observed in HPR*Gx* mutants (see section 1.2 of Results). The 22 (forward) and 18 (reverse) primer oligonucleotides shown below were designed to substitute the G nucleotide into the A nucleotide in the ACG codon. These primers were then used for the mutagenesis using PCR. The primers are:

BcsA_Ala1345Thr Fwrd: 5′-CATGTTCCACACCGTCGGCACG-3′

BcsA_Ala1345Thr Rev: 5′-TGCGGGATGGCATAGGCC-3′

The PCR reaction for site-directed mutagenesis was performed using a site-directed mutagenesis kit purchased from New England Biolabs (Mississauga, Ontario, Canada). The following components were used for the reaction: 9 µL MilliQ H_2O, 1µL template DNA (pKNG101_*bcsA*_ColE1 ori) 20ng/µL, 1.25 µL 10 mM forward primer, 1.25 µL 10 mM reverse primer, and 12.5 µL Q5 Hot Start High Fidelity 2X master mix.

For the PCR used in site-directed mutagenesis the initial denaturation condition was 98°C for 2 minutes, followed by 25 cycles of 98°C for 30s, 60°C for 45s, and 72°C for 2 minutes and 30s. This was followed by a final extension at 70°C for 5 minutes, followed by a 16°C hold. The quality of the PCR products were confirmed by gel electrophoresis as described in section 2.13.

The 10X Kinase-Ligase-DpnI Mix (10X KLD) was then used for phosphorylation, intramolecular circularization of the PCR product, and removal of the template. The KDL reaction was performed using the following components: 3 µL MilliQ H_2O, 1 µL PCR product, 5 µL 2X KLD reaction buffer, and 1 µL 10X KLD Enzyme Mix. The KLD reaction mixture was incubated for 15 minutes at room temperature which was then used for transformation using high-efficiency DH5α competent *E.coli* cells as described in section 2.12.4. The presence of the mutation was confirmed by DNA sequencing as described in section 2.9.

2.12.7 Electroporation of *G. xylinus* competent cells

Electrocompetent *G. xylinus* wild type cells were electroporated with both methylated and unmethylated pKNG101_*bcsA*_ColE1 ori plasmid. Some bacteria possess efficient restriction systems that are able to degrade DNA with foreign methylation pattern; thus, it was decided to transform *G. xylinus* wild type cells with both methylated and unmethylated plasmids.

Frozen electrocompetent *G. xylinus* cells were thawed on ice for 7 minutes. A total volume of 100 µL thawed competent *G. xylinus* cells were mixed with pKNG101_*bcsA*_ColE1 ori plasmid DNA (0.3 to 0.7 µg/mL) containing the corresponding point mutations on the *bcsA* gene on a pre-chilled Eppendorf tube. The cell-plasmid DNA mixture was immediately transferred to a cold 0.2-cm-diameter cuvette.

Electroporation of *G. xylinus* cells was performed using ECM 399 Electroporator system (BTX Harvard Apparatus, 45-0000). One pulse was set at 2.5 kV and the cells were immediately diluted with 950 µL of SH medium containing 0.3% (v/v) cellulose from *Trichoderma reesei*. The cells and incubated with shaking (150 rpm) at 30°C for four hours. Thereafter, the cells were plated on SH solid selective medium and incubated at 30°C for 72 hours until colonies formed on the plates. Controls were transformed with water instead of plasmid DNA.

2.12.8 Positive selection of double homologous recombination in *G. xylinus*

A total of 30 independent streptomycin-resistant transformants obtained from electroporation of *G. xylinus* wild type cells with the pKNG101_*bcsA*_ColE1 ori construct were grown in SH rich medium deprived of antibiotic with shaking (150 rpm) at 30°C overnight. A volume of 150 µL of diluted cultures obtained from these streptomycin-resistant transformants were plated on SH medium supplemented with 5% sucrose. A total of 400 sucrose-tolerant colonies were grown in 200 µL SH medium containing 30 µM pellicin. The genomic DNA from the colonies in where pellicle was produced as well as from some colonies that did not produce pellicle, was extracted by CTAB method as described in section 2.6. The presence of the mutation in the *bcsA* gene was confirmed by DNA sequencing as described in section 2.9.

Transformation of *G. xylinus* with pKNG101_*bcsA*_ColE1 ori resulted in the appearance of streptomycin-resistant transformants (Sm^R) from the first homologous recombination. A total of 30 independent Sm^R transformants were grown in SH rich medium deprived of antibiotic with shaking (150 rpm) at 30°C overnight. A volume of 150 µL of diluted cultures obtained from these Sm^R transformants were plated on SH medium supplemented with 5% sucrose. A total of 400 sucrose-tolerant colonies were grown in 200 µL SH medium containing 30 µM pellicin. The genomic DNA from the colonies in where pellicle was produced as well as from some colonies that did not produce pellicle, was extracted by CTAB method as described in section 2.9. The presence of the mutation in the *bcsA* gene was confirmed by DNA sequencing as described in section 2.9.

2.13 Gel electrophoresis

Agarose gel electrophoresis was performed to estimate the size and purity of DNA. The electrophoresis was conducted using 0.8-1% agarose gel prepared with 1X TAE buffer and containing approximately 0.5 µg per mL of ethidium bromide. The gels were run for 35 to 50 minutes at 100 constant volts and they were analysed by photographing the gels exposed to UV light using a UV transilluminator. For electrophoresis using low melting agarose gel please refer to section 2.12.2.

2.14 Statistical analysis

All statistics were performed using SigmaPlot 12.5 software. A student's t-test or a one-way ANOVA test were performed for statistical analysis, and values were determined to be significant at a P value of < 0.05. A Saphiro-Wilk test was run in parallel to the one-way ANOVA test with P values for normality and equal variance set up at 0.050 in order to determine homogeneity of variance.

2.15 Protein modelling

Structural analysis of native and mutant BcsA proteins was performed using Phyre2 Protein Fold Recognition Server (Kelley et al., 2015) and a SWISS-MODEL tool to

predict regions of the proteins with no detectable homologies and to model a cellulose translocation intermediate of cellulose synthase subunit A. The templates of native and mutated proteins were built in Phyre2 using the the amino acid sequences of the proteins. The pdb files created from these models were opened simultaneously in Swiss-PdbViewer 4.1.0 to superimposed the models using the magic fit option. The structure of the BcsA-BcsB cellulose translocation intermediate model was built using the pdb structure 4HG6.

Chapter 3

Results

In this chapter experimental results obtained from the analysis of high pellicin-resistant *G. xylinus* (HPR*Gx*) mutants are presented. The first step of this analysis was the phenotypic characterization of these HPR*Gx* mutants. The determination of pellicin resistance levels allowed to isolate HPR*Gx* mutants which were then used for further research. Additional morphological characterization of the HPR*Gx* mutants was conducted in the presence and absence of pellicin including the quantification of crystalline cellulose content in crude pellicles, the morphological characterization of colonies, and the effect of pellicin on growth. This analysis allowed to establish morphological and physiological alterations of these mutants when compared to the wild type. Following the phenotypic analysis of the mutants, a genetic analysis was set up. The goal of this part of the research was to provide evidence of novel genes likely involved in cellulose crystallization. A single point mutation corresponding to an A449T substitution in the cellulose synthase gene (*bcsA*) was found in the HPR*Gx* mutants. Reproduction of this mutation by site-directed mutagenesis and further phenotypic characterization of mutants obtained from this procedure are described in this chapter. In addition, a protein structural analysis, by means of 3D modelling, of the BcsA protein containing A449T substitution is also presented in this chapter.

3.1 Characterization of pellicin resistance levels in *G. xylinus* mutants

Cellulose crystallinity of pellicles formed by *G. xylinus* is greatly reduced in the presence of pellicin. In an effort to investigate cellulose biosynthesis at the crystallization level, PR*Gx* mutants previously created through ethyl methanesulfonate (EMS) mutagenesis were investigated. EMS is a monofunctional ethylating agent that has been found to be mutagenic in different genetic test systems. Genetic data obtained from microorganisms suggest that EMS may induce GC to AT and AT to GC transition mutations as well as base-pair insertions or deletions (Sega, 1984).

The survival rate of *G. xylinus* in EMS solution was first determined to produce PR*Gx* mutants. In this case, a kill curve of *G. xylinus* in a 0.1 % (v/v) EMS solution was obtained after varying incubation times. The optimal survival rate of 50% that compromises between a high mutation rate and a moderate amount of viable cells was found after 7 min of incubation in EMS. An approximate number of 4 million mutagenized cells obtained by EMS mutagenesis were tested in a high throughput screen in media containing 10 µM pellicin using 96-well microtiter plates. A total of 18 pellicin-resistant mutants were recovered from the screening.

In the present study 15 PR*Gx* mutants obtained by EMS mutagenesis were first analyzed based on the level of pellicin resistance. The resistance levels to pellicin in the *G. xylinus* mutants was assessed to confirm the resistance of these mutants and to determine which ones were the most representative candidates for further research. The cell cultures of *G. xylinus* mutants and the wild type were grown in SH medium containing either dimethyl sulfoxide (DMSO) or pellicin dissolved in DMSO at different concentrations. Two different type of mutants were found based on their level of resistance to pellicin: high pellicin-resistant *G. xylinus* (HPR*Gx*) mutants and low pellicin-resistant *G. xylinus* (LPR*Gx*) mutants. Among the 15 mutants analysed, 3 of them were HPR*Gx* mutants, being able to produce a thick pellicle of cellulose at pellicin concentrations above 140 µM (Figure 3.1). These mutants were named M13, M14, and M15. The remaining mutants were considered LPR*Gx* mutants as they were only able to produce very thin pellicles at a concentration of pellicin of 5 µM, except for one that was able to produce pellicle at a concentration of 10 µM (Figure 3.1). The formation of the pellicle was inhibited in the *G. xylinus* wild type at a pellicin concentration of 5 µM. The resistance levels observed on the LPR*Gx*

mutants was unexpected as they were initially screened in media containing 10 µM pellicin, but most of them did not show resistance at this concentration of pellicin when they were retested.

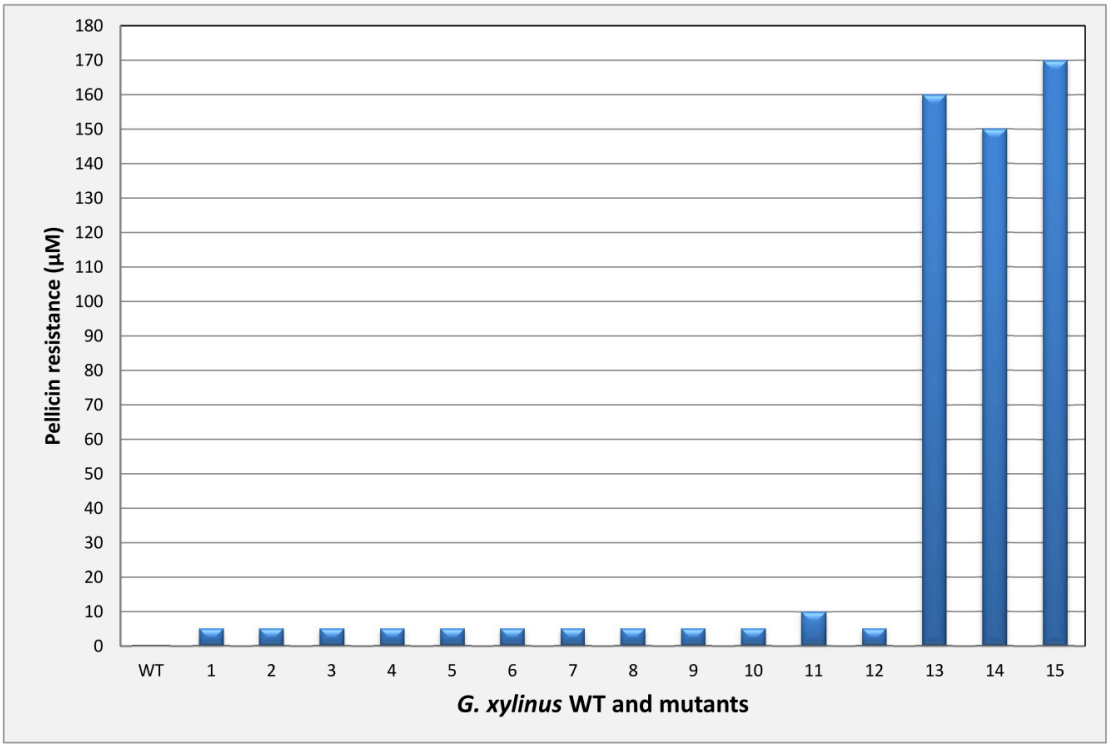

Figure 3.1: Pellicle formation of *G. xylinus* mutants under different concentrations of pellicin. Each bar represents the maximum concentration of pellicin at which pellicle was formed in 15 *G. xylinus* mutants. Pellicle was inhibited in the wild type at a concentration of 5 µM of pellicin. Measurements were taken from cultures starting with an OD_{600} = 0.05 using nine technical replicates obtained from three biological replicates.

3.2 Crystalline cellulose content of pellicles produced by HPR*Gx* mutants and by wild type in the presence of pellicin

Some mutants of *G. xylinus* have shown to produce lower amounts of crystalline cellulose I while generating more cellulose II which is rarely produced in nature (Nakai et al., 2013). In this regard, mutations leading to alterations in the production of cellulose I may be used to understand the process of cellulose

crystallization. Therefore, in order to determine if the crystalline cellulose production was altered in the HPR*Gx* mutants when compared to the wild type, the amount of crystalline cellulose produced by them was quantified and compared.

The cellulose content of crude pellicles obtained from the HPR*Gx* mutants and the *G. xylinus* wild type in the presence and absence of pellicin were estimated by cellulose assay using acetic-nitric (Updegraff) reagent treatment followed by anthrone method (Updegraff, 1969). Pellicles from HPR*Gx* mutants and the *G. xylinus* wild type, obtained after seven days of growth under static conditions, were used for crystalline cellulose quantification. The cellulose pellicles produced by the HPR*Gx* mutants displayed similar amounts of crystalline cellulose as compared to the *G. xylinus* wild type when cells were grown in SH medium lacking pellicin (Figure 3.2). On the other hand, the cellulose pellicles produced by all the HPR*Gx* mutants from bacterial cultures containing pellicin displayed significant reduced amounts of crystalline cellulose (approximately 23 % less) as compared to the pellicles produced in bacterial cultures lacking pellicin (Figure 3.3). Cellulose pellicles did not form in *G. xylinus* wild type cultures when pellicin was added to the medium. There was not significant differences in the amount of crystalline cellulose present in pellicles formed by HPR*Gx* mutants in the presence of pellicin.

Although this analysis does not provide an accurate structural information about the crystalline cellulose formed by the HPR*Gx* mutants, these results suggest that the mutations in these mutants do not affect the assembly of the glucans into the crystalline cellulose I. In addition, the reduced amounts of crystalline cellulose produced by the HPR*Gx* mutants in the presence of pellicin suggests that a mutation in these mutants make them highly resistant to pellicin but not entirely resistant.

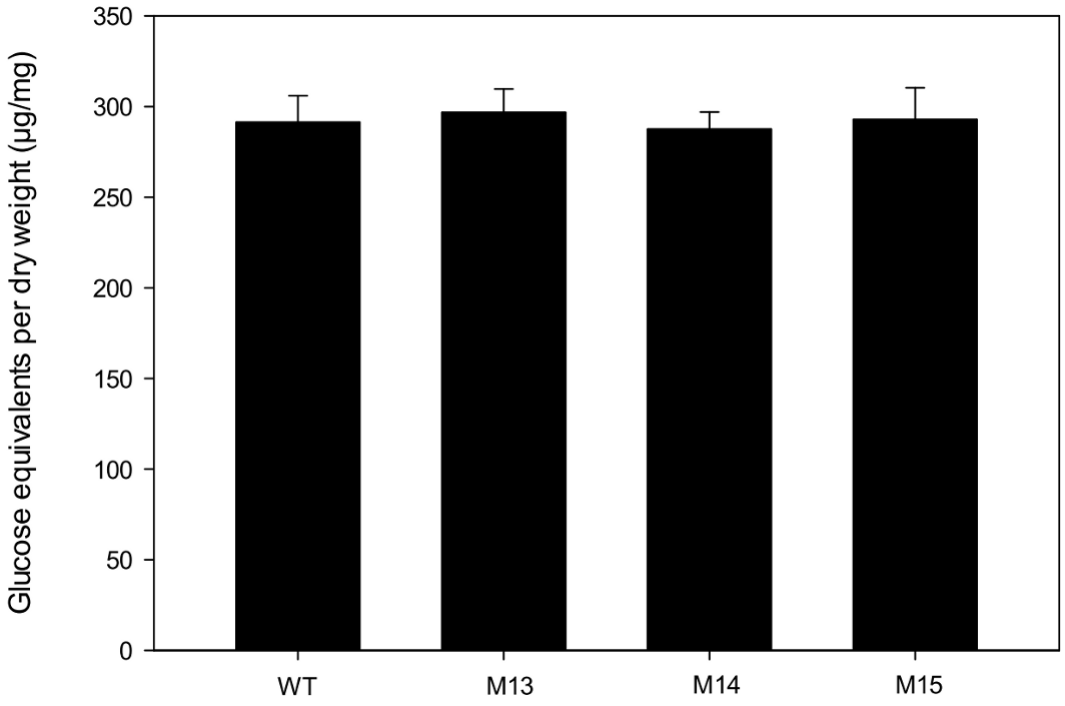

Figure 3.2: The *G. xylinus* wild type and HPR*Gx* mutants produce comparable amounts of crystalline cellulose in media lacking pellicin. The crystalline cellulose content in the pellicles formed by the wild type (WT) and the HPR*Gx* mutants (M13, M14, and M15) was determined by anthrone test. The crystalline cellulose is expressed as glucose equivalents per dry weight (µg/mg). The data shows the mean ± SE of three biological replicates.

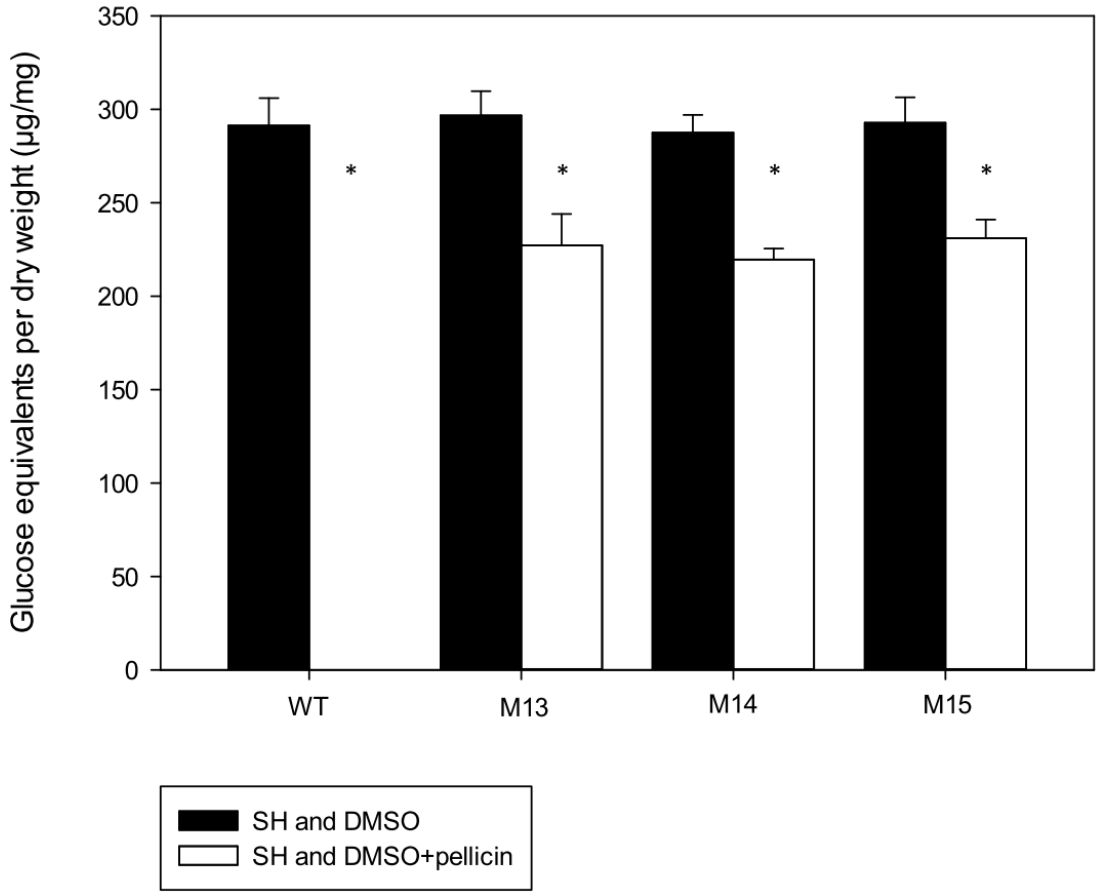

Figure 3.3: Crystalline cellulose formed by *G. xylinus* wild type and HPR*Gx* mutants in media containing pellicin. The crystalline cellulose content in the pellicles formed by the wild type (WT), and HPR*Gx* mutants (M13, M14, and M15) in SH+DMSO (blue bar) and SH+DMSO+pellicin (red bar) was determined by anthrone test. The crystalline cellulose is expressed as glucose equivalents per dry weight (µg/mg). The data shows the mean ± SE of three biological replicates. Asterisks indicate statistically significant differences between pellicin treated and pellicin untreated cultures according to one-way ANOVA ($p<0.05$).

3.3 Morphological characterization of cellulose production in colonies formed by HPR*Gx* mutants

In order to determine if mutations in the HPR*Gx* mutants affect colony morphology, a comparative colony morphology analysis with *G. xylinus* wild type was performed. This analysis also allowed to determine the effects of pellicin on colonies formed by

both HPR*Gx* mutants and the wild type.

Diluted cultures from HPR*Gx* mutants and wild type were spread on SH solid medium containing either DMSO or pellicin dissolved in DMSO. Colonies were formed after 72 hours of incubation at 30°C. The *G. xylinus* wild type formed rough colonies surrounded by an external web of cellulose microfibrils in the absence of pellicin (Figure 3.4. The same type of colony morphology was observed from HPR*Gx* mutants regardless of the presence of the inhibitor. In contrast, *G. xylinus* wild type colonies exhibited a flat and shiny colony morphology without an external web of cellulose microfibrils in the presence of pellicin (Figure 3.4).

These results suggest that mutations of HPR*Gx* mutants do not affect colony morphology. In addition, the presence of pellicin alter colony morphology and inhibit surrounded cellulose microfibril formation only of the *G. xylinus* wild type, but not of the HPR*Gx* mutants.

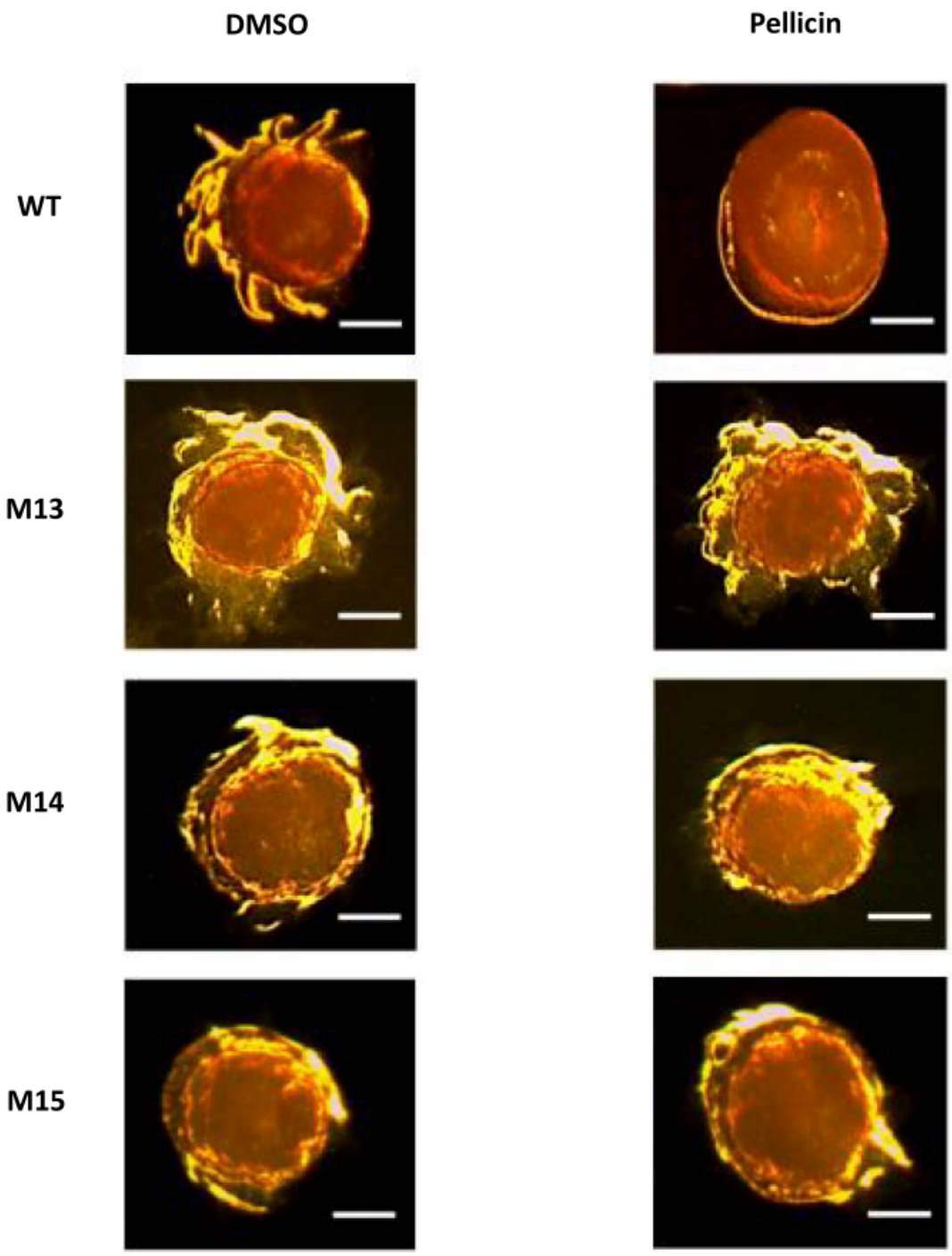

Figure 3.4: Effects of pellicin on colony morphology of *G. xylinus* wild type and HPR*Gx* mutants in solid medium. Colonies of *G. xylinus* wild type and HPR*Gx* mutants were grown at 30°C in SH agar plates supplemented with DMSO or 30 µM pellicin. The images were taken with illumination from below. Rough colonies with an external web of cellulose microfibrils were formed in the pellicin-untreated wild type as well as in HPR*Gx* mutants regardless the presence of pellicin. Smooth colonies without an external web of cellulose microfibrils were formed in the pellicin-treated wild type. Scale bars are 0.3 mm.

3.4 Pellicin does not affect the growth of HPR*Gx* mutants, but affects the growth of the wild type

In order to further characterized the HPR*Gx* mutants at the phenotypic level, differences on growth between HPR*Gx* mutants and wild type in the presence and in the absence of pellicin were examined. The growth of the HPR*Gx* mutants and the wild type was examined in the presence and absence of pellicin to determine if mutations in the HPR*Gx* mutants alter the growth in *G. xylinus* under these conditions.

The growth of the HPR*Gx* mutants was not significantly affected in media containing pellicin and it was comparable to the growth of the wild type in media lacking pellicin (Figure 3.5). However, the final cell density of *G. xylinus* wild type was significantly higher (OD_{600}=1.004 ±0.06) in media containing pellicin when compared to the final cell density in media lacking pellicin (OD_{600}=1.242 ±0.06) (Figure 3.5). Although the growth of the M13 mutant was initially lower when compared to the growth of the other mutants, all the mutants including the M13 mutant reached a similar final cell density (Figure 3.5). Based on the present results, it seems apparent that mutations on HPR*Gx* mutants do not affect growth in *G. xylinus*, and also the higher final cell density observed only in the pellicin-treated wild type suggests a possible connection between growth and cellulose biosynthesis in *G. xylinus*.

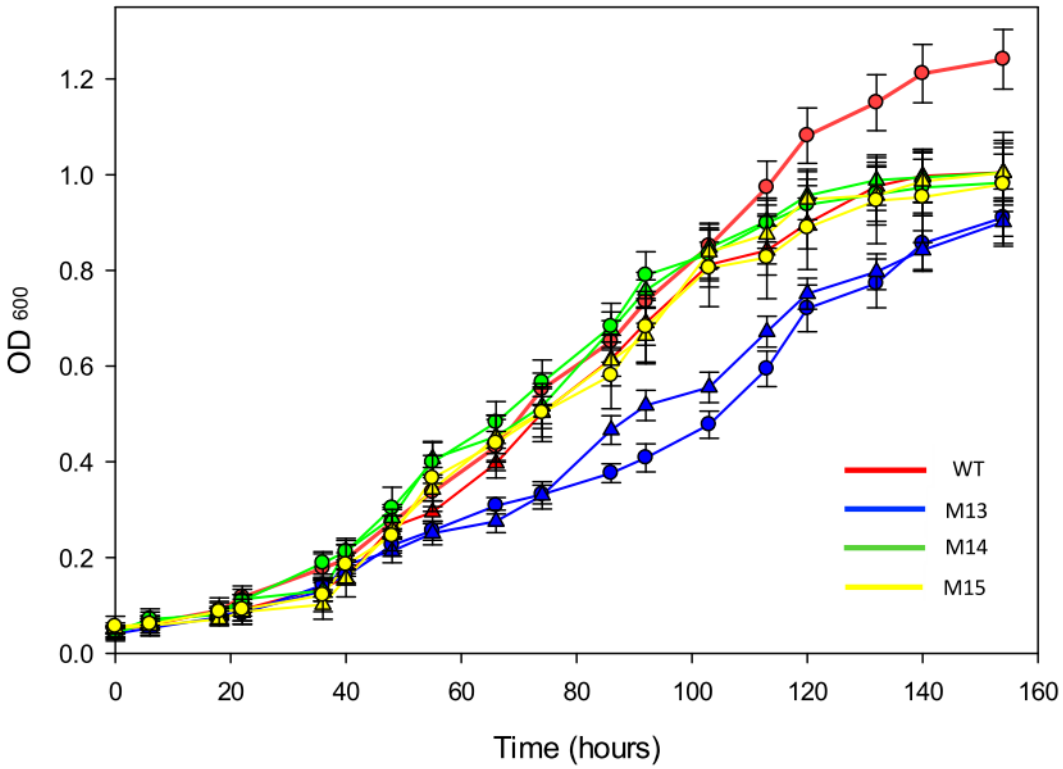

Figure 3.5: Effects of pellicin on growth of *G. xylinus* wild type and HPR*Gx* mutants. The viability of *G. xylinus* wild type (WT) and HPR*Gx* mutants (M13, M14, and M15) was not affected by pellicin, but it increases the growth of the wild type. *G. xylinus* was grown under shaking condition at 30°C in SH broth media containing 0.3% cellulase and either 30 µM pellicin (O) or DMSO (Δ) as a control. Data show the mean ± SE of eight technical replicates.

3.5 HPR*Gx* mutants display a single point mutation in the catalytic cellulose synthase gene *bcsA*

Identification of mutations from mutants resistant to a chemical inhibitor may suggest which gene(s) are important for the particular biological function inhibited. Based on this, the identification of mutations that confer resistance to the HPR*Gx* mutants would help to detect possible targets of pellicin and gene(s) that may be involved in cellulose crystallization.

In order to identify mutations in the HPR*Gx* mutants, the genomic DNA from both the HPR*Gx* mutants and wild type was first isolated by cetyl trimethyl

ammonium bromide (CTAB) extraction method and the quality of the DNA extraction products was checked by electrophoresis (Figure 3.6). The cellulose synthase operon genes, from both the HPR*Gx* mutants and wild type, were PCR amplified from the genomic DNA and the quality of the PCR products were confirmed by electrophoresis (Figure 3.7).

Comparison of the DNA sequences of the *bcs* operon genes of both the HPR*Gx* mutants and the wild type, revealed a single point mutation in the catalytic cellulose synthase gene *bcsA* in the all HPR*Gx* mutants Figure 3.8. There were no other mutations detected in the remaining region of the operon of HPR*Gx* mutants. The mutation found in the HPR*Gx* mutants corresponds to a substitution of guanine nucleotide at position 1345 of the *bcsA* gene nucleotide sequence by an adenine nucleotide. This base mutation has the effect of changing a non-polar alanine residue (A) to a polar threonine residue (T) at position 449 of the amino acid sequence. According to the nomenclature, this mutation is referred as "A449T."

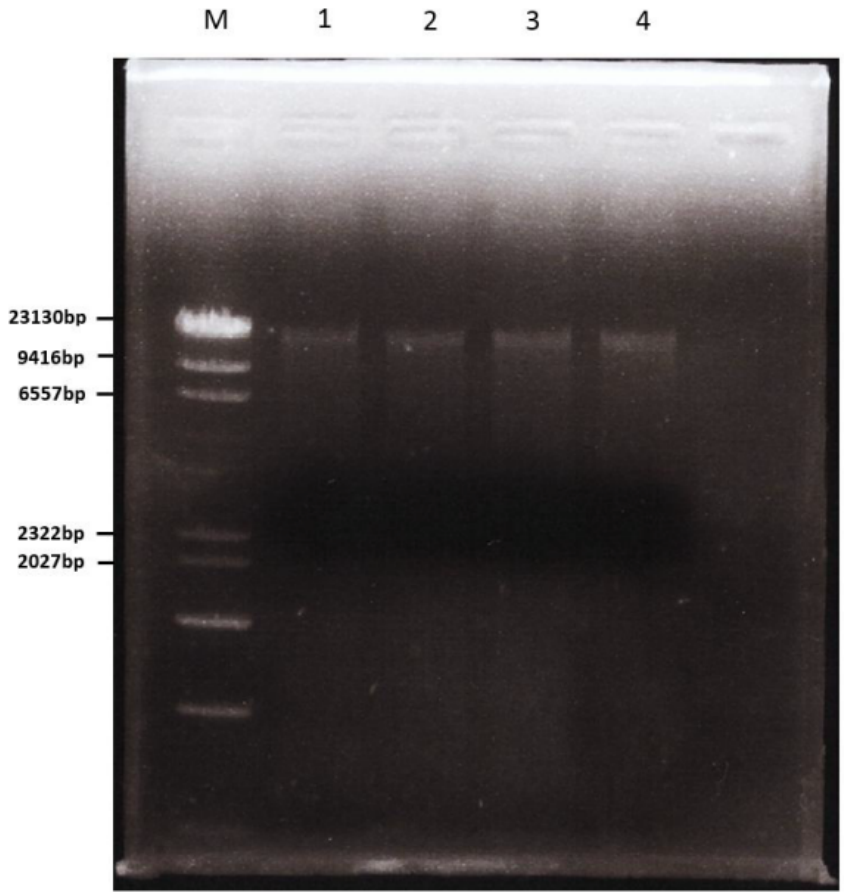

Figure 3.6: Agarose gel electrophoresis of genomic DNA from *G. xylinus*. The DNA products were subjected to electrophoresis using 1% (wt/vol) agarose gel. Lane M is the molecular marker (Lambda DNA/*HindIII* Plus). Lanes 1, 2, 3, and 4 show the genomic DNA products obtained from the DNA extraction.

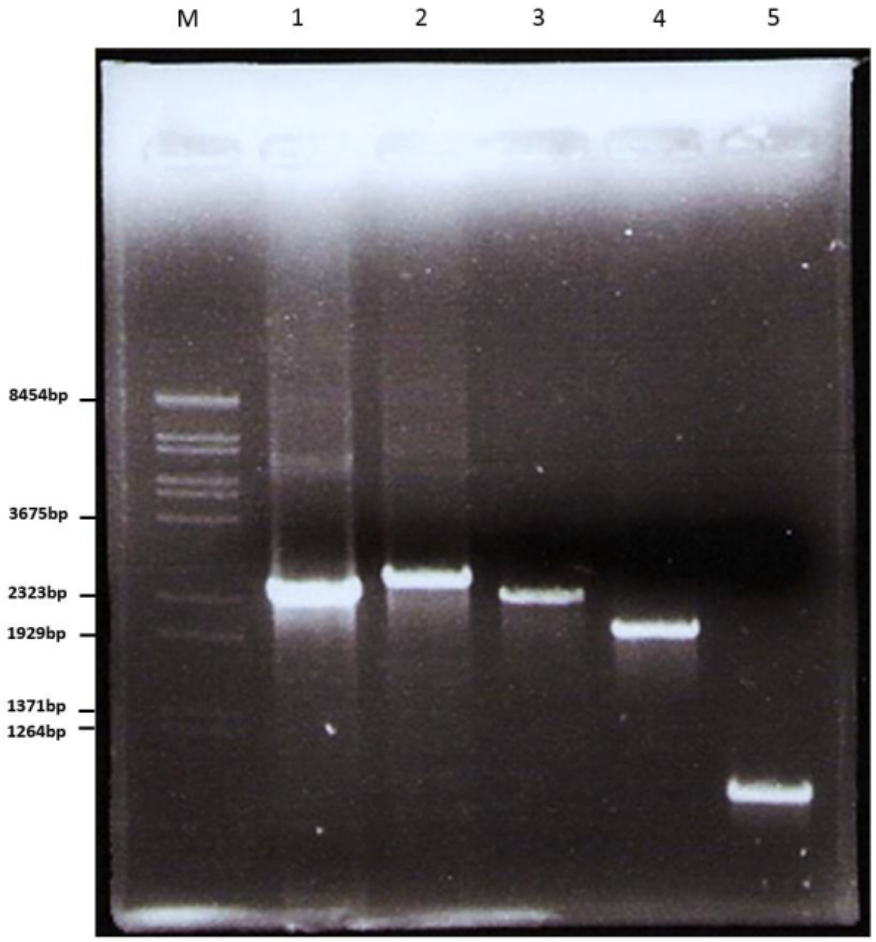

Figure 3.7: PCR amplification of the *bcs* operon of *G. xylinus*. PCR products of the *bcs* operon were subjected to gel electrophoresis using 1% (wt/vol) agarose gel. Lane M is the molecular marker (Lamda DNA-*BstEII* Digest). Lane 1 corresponds to the PCR amplified *bcsA* gene product (2415 bp). Lane 2 corresponds to the PCR amplified *bcsB* gene product (2613 bp). Lane 3 and 4 corresponds to *bcsC* gene which was amplified into two separate PCR products (2365 bp and 2174 bp respectively). Lane 5 corresponds to the PCR amplified *bcsD* gene product (1020 bp).

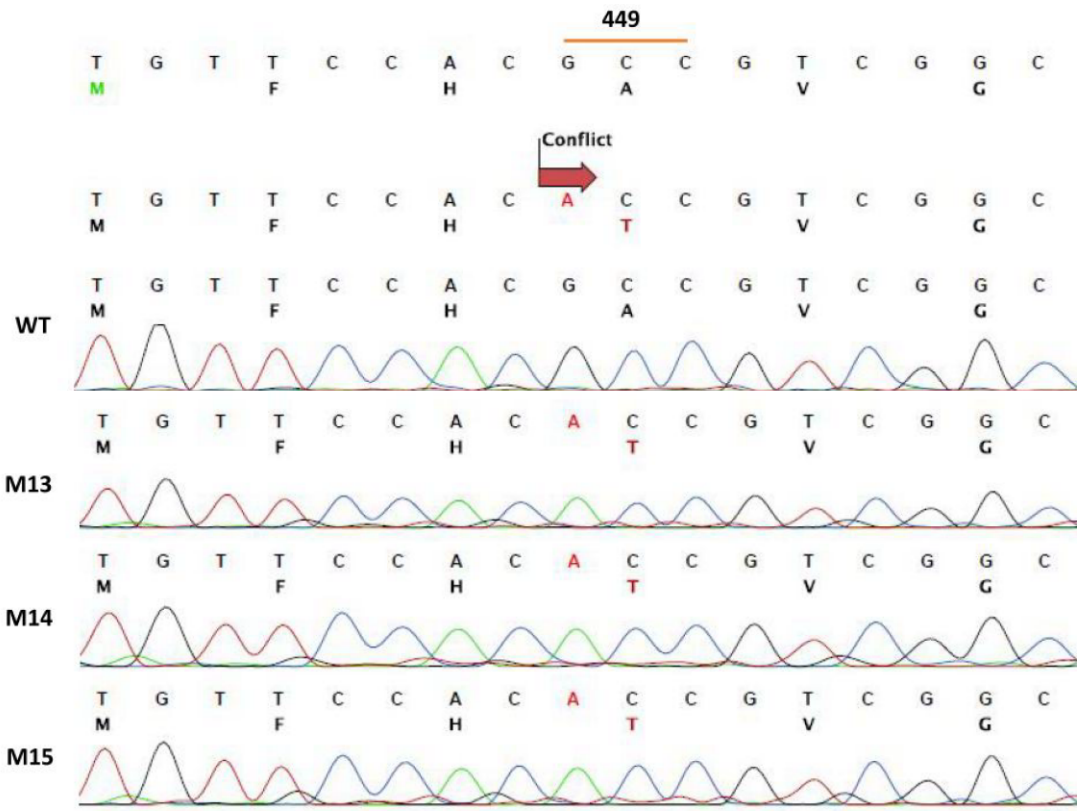

Figure 3.8: DNA chromatograph of *G. xylinus* wild type (WT) and HPR*Gx* mutants. The nucleotide G is substituted to A in the HPR*Gx* mutants at position 1345 of the nucleotide sequence of the *bcsA* gene. This mutation corresponds to a substitution of an alanine residue by a threonine residue. The number at the top indicates the amino acid position in the protein.

3.6 Cloning of the cellulose synthase gene *bcsA* into pZErO-2 vector

In order to confirm that the A449T mutation in BcsA of *G. xylinus* was actually the cause of the pellicin resistance observed in the HPR*Gx* mutants, the mutation was reproduced in the wild type by site-directed mutagenesis.

In order to manipulate the *bcsA* gene from *G. xylinus*, the gene was first PCR amplified with additional restriction sites to the termini of amplified DNA and blunt-end cloned into the pZErO-2 vector at the *EcoRV* restriction site. Many restriction enzymes fail to cleave recognition sequences located close to the ends of DNA fragments, in particular those generated by PCR (Sambrook and Russell,

2001). Based on this, the addition of complementary sticky ends at the termini of the *bcsA* gene was facilitated by blunt-end cloning the gene into the pZErO-2 vector. The complementary sticky ends then allowed sticky-end subcloning of the *bcsA* gene into the destination vector.

A total of 50 individual kanamycin-resistant transformants were analyzed by colony PCR and four of them were found to contain the insert of interest. The integrity of the insert was confirmed by DNA sequencing and the construct map is shown in Figure 3.9. The resulting plasmid construct was named pZErO-2_*bcsA*.

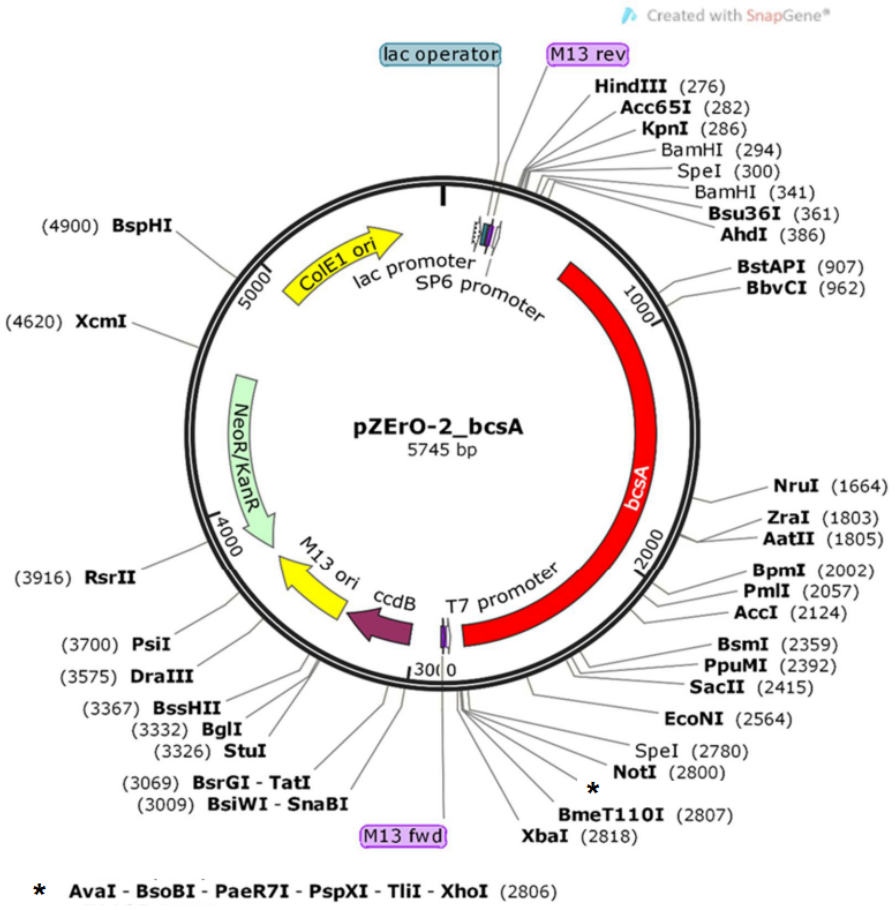

Figure 3.9: Plasmid construct map of pZErO-2_*bcsA*.

3.7 Subcloning of *bcsA* gene into the suicide plasmid vector pKNG101

Homologous recombination of a mutated version of the *bcsA* in *G. xylinus* wild type was achieved using the wide host range vector pKNG101. The pKNG101 vector allows gene replacement by homologous recombination in gram-negative bacteria; therefore, this vector was used to replace the wild type *bcsA* gene by the mutated version of the gene.

The *bcsA* gene was subcloned from the pZErO-2_*bcsA* construct into the pKNG101 vector using the *BamHI* and *SpeI* restriction sites that were previously added to the PCR amplified gene. A total of 30 individual streptomycin-resistant transformants were analyzed by colony PCR and 7 colonies were found to contain the insert of interest. Interestingly, when the integrity of the *bcsA* gene was confirmed by DNA sequencing, it was found that a DNA fragment corresponding to ColE1 origin of replication from the pZErO-2 vector was introduced in the construct. Attempts to remove this fragment was not possible, suggesting that the ColE1 origin of replication was essential to replicate and maintain the construct in *E. coli* DH5α cells. In this regard, it is possible that this fragment was introduced by plasmid recombination between the final construct and the pZErO-2_*bcsA* plasmid. Some traces of undigested pZErO-2_*bcsA* plasmid could be introduced in the ligation reaction for subcloning the *bcsA* gene into the pKNG101 vector. Both the final construct and the pZErO-2_*bcsA* plasmid could then co-transform into *E. coli* which resulted in the formation of a hybrid plasmid.

The final construct was named pKNG101_*bcsA*_ColE1 ori and the construct map is shown in Figure 3.10.

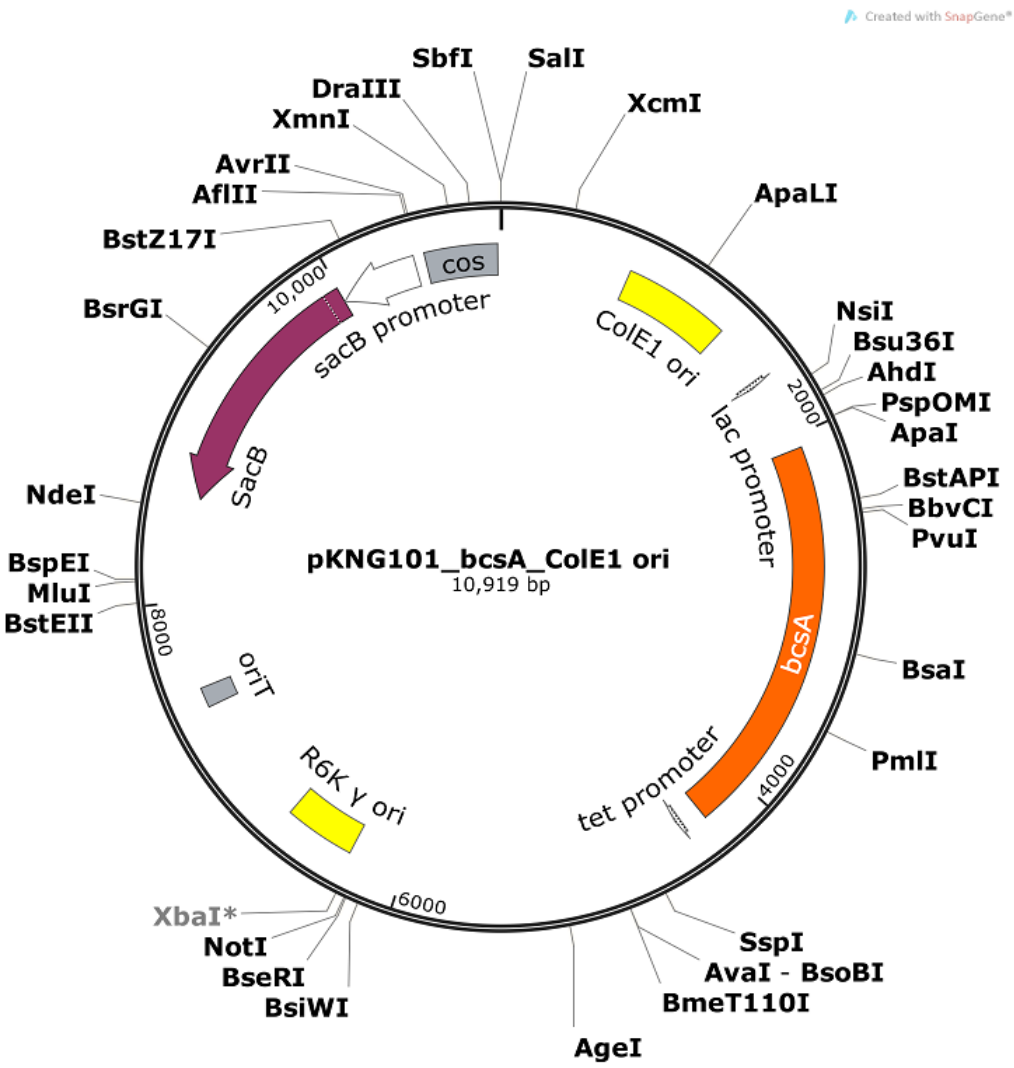

Figure 3.10: Plasmid construct map of pKNG101_*bcsA*_ColE1 ori.

3.8 Positive selection of double recombinants containing the BcsA A449T mutation

In order to reproduce the mutation observed in the HPR*Gx* mutants, site-directed mutagenesis was performed using the pKNG101_*bcsA*_ColE1 ori construct.

The construct obtained from site-directed mutagenesis was transformed into *G. xylinus* wild type cells by electroporation. Both methylated and unmethylated plasmids were used for transformation and transformants were obtained in both cases. The pKNG101 plasmid has the advantage of having a streptomycin-resistant gene as a selectable marker for the cointegration event as well as the *Bacillus subtilis sacB* gene as a counterselectable marker to improve a second crossover event (Kaniga et al., 1991). The gene *sacB* encodes a levansucrase enzyme which in several genera of gram-negative bacteria has been shown to be lethal in the presence of 5% sucrose (Kaniga et al., 1991). This property of the pKNG101 plasmid facilitated the selection for the integration of the mutated *bcsA* gene into the chromosome and for the excision of the vector. After the selection of the second recombination event (refer to section 2.12.8) 400 sucrose-resistant colonies were allowed to grow in SH medium supplemented with 30 µM pellicin. Out of the 400 colonies, 8 were able to produce pellicle of cellulose in the presence of pellicin. The DNA sequencing results from three of these colonies revealed a substitution of nucleotide G to A at position 1345 of the nucleotide sequence of the *bcsA* gene (Figure 3.11). This base mutation corresponds to the one observed in the HPR*Gx* mutants. The mutant displaying this substitution created through site-directed mutagenesis was called BcsA A449T mutant. On the other hand, the DNA sequencing analysis of the other five colonies revealed a substitution of nucleotide C to T at position 1346 of the nucleotide sequence of the *bcsA* gene (Figure 3.12). This base mutation has the effect of changing an alanine residue (A) to a valine residue (V) at position 449 of the amino acid sequence. According to the nomenclature, this mutation is referred as "A449V." The mutant displaying this substitution was called BcsA A449V mutant. The DNA sequencing results from 10 colonies that were unable to produce pellicle in the presence of pellicin revealed no nucleotide changes in the *bcsA* gene.

The pellicin-resistant phenotype observed on both BcsA A449T and BcsA A449V mutants, suggest that the A449 residue is important for pellicin sensitivity in *G. xylinus* and likely for cellulose crystallization.

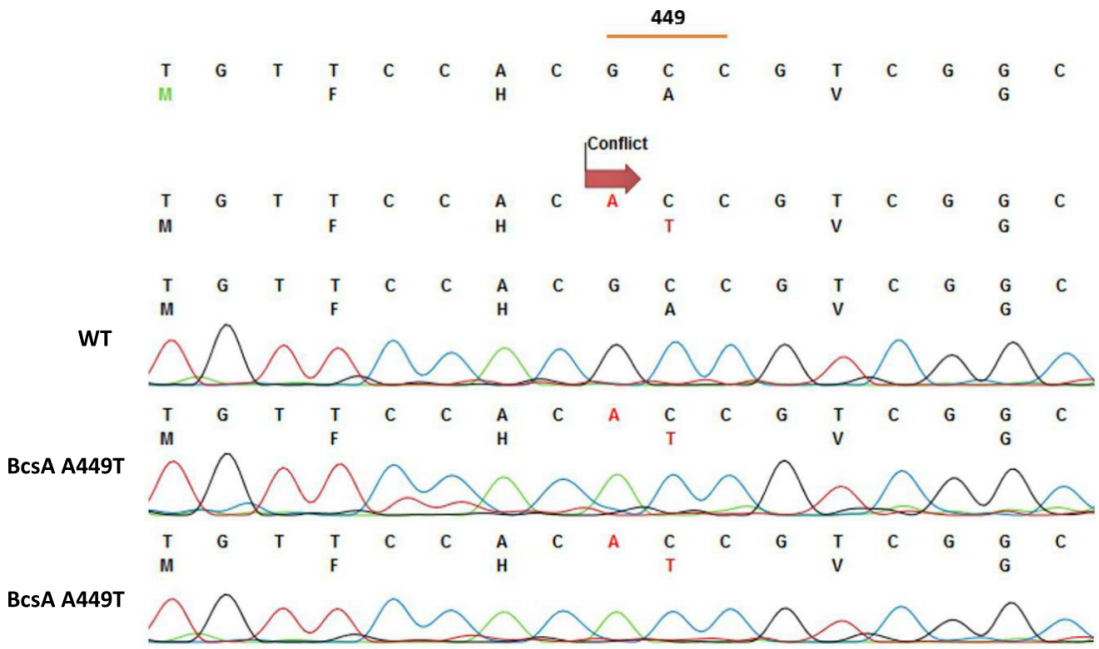

Figure 3.11: DNA chromatograph of *G. xylinus* wild type (WT) and the BcsA A449T mutant. The nucleotide G was substituted to A at position 1345 of the nucleotide sequence of the *bcsA* gene. This mutation corresponds to a substitution of an alanine residue by a threonine residue. The number at the top indicates the amino acid position in the protein.

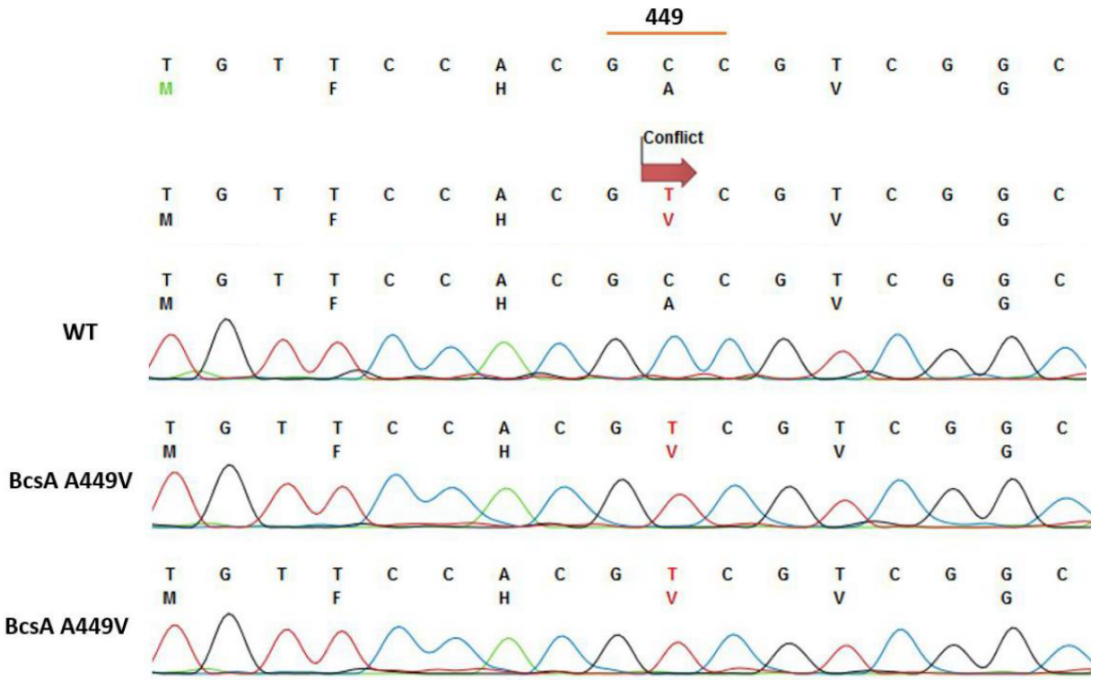

Figure 3.12: DNA chromatograph of *G. xylinus* wild type (WT) and the BcsA A449V mutant. The nucleotide C was substituted to T at position 1346 of the nucleotide sequence of the *bcsA* gene. This mutation corresponds to a substitution of an alanine residue by a valine residue. The number at the top indicates the amino acid position in the protein.

3.9 *G. xylinus* mutants created through site-directed mutagenesis exhibited similar morphological characteristics to the HPR*Gx* mutants

In order to further validate the pellicin-resistant phenotype observed on both BcsA A449T and BcsA A449V mutants, a comparison of these mutants with the original HPR*Gx* mutants and the wild type at the morphological level was performed.

First of all, both BcsA A449T and BcsA A449V mutants were grown in SH medium containing pellicin concentrations from 100 to 200 µM. These mutants were found to be highly resistant to pellicin as they were able to produce pellicles in media containing pellicin of up to 170 µM. In addition, both BcsA A449T and BcsA A449V mutants formed rough colonies with an external web of cellulose microfibrils

in solid media in the presence and the absence of pellicin (Figure 3.13). Furthermore, the BcsA A449T and BcsA A449V mutants displayed similar amounts of crystalline cellulose as compared to the *G. xylinus* wild type and the M15 mutant when cells were grown in SH medium lacking pellicin (Figure 3.14). Finally, the BcsA A449T, BcsA A449V, and M15 mutants produced less yet significant amounts of crystalline cellulose (approximately 25% less) in the presence of pellicin (Figure 3.15).

The mutations A449T and A449V in the BcsA protein of *G. xylinus* conferred resistance to pellicin, resembling the resistance profile observed in the original HPR*Gx* mutants.

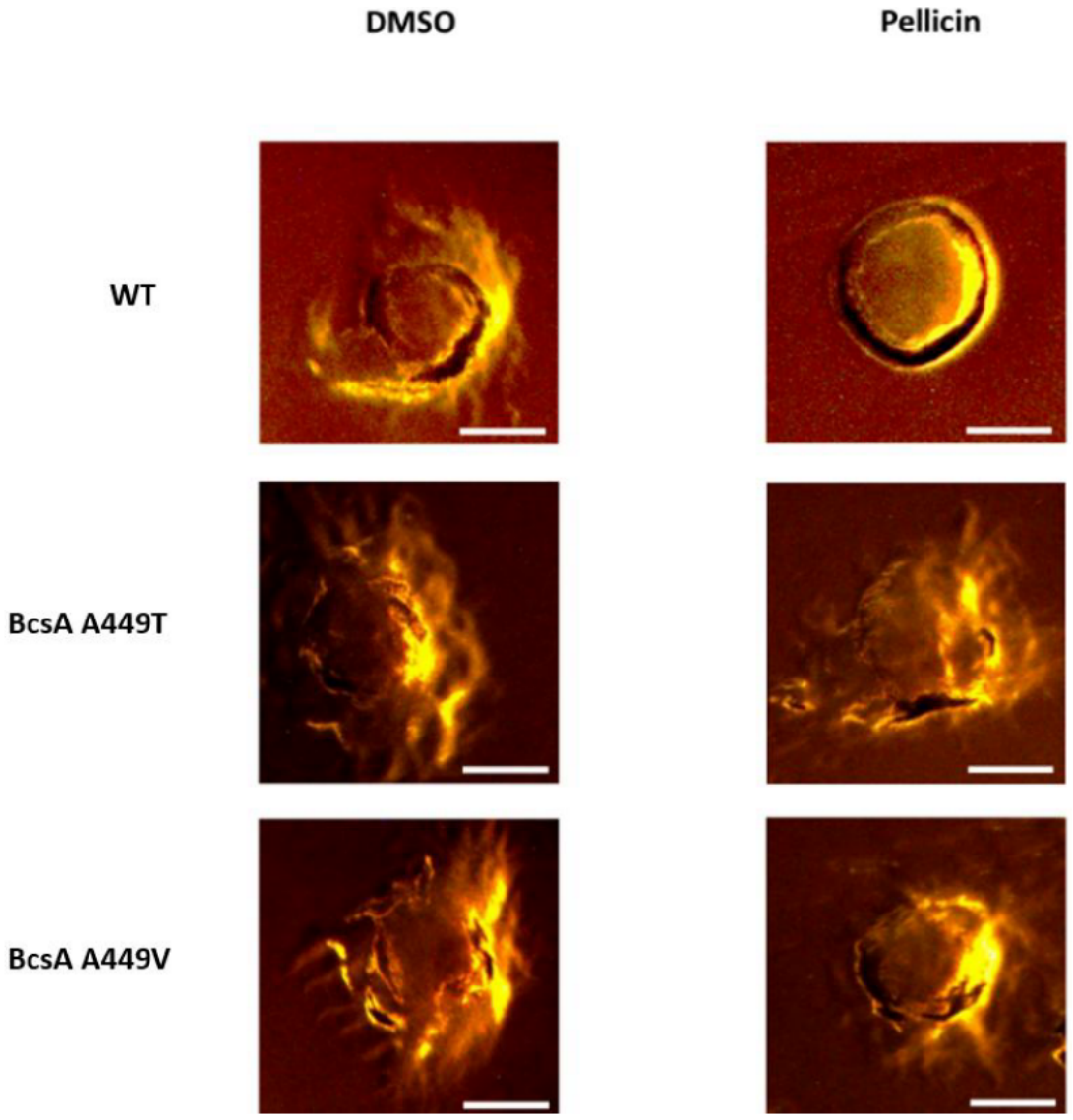

Figure 3.13: Effects of pellicin on colony morphology of *G. xylinus* wild type and on both BcsA A449T and BcsA A449V mutants in solid medium. *G. xylinus* cells were grown at 30°C in SH agar plates supplemented with DMSO or 30 µM pellicin. The images were taken with illumination from below. Rough colonies with an external web of cellulose microfibrils were formed in the pellicin-untreated wild type as well as in BcsA A449T and BcsA A449V mutants regardless the presence of pellicin. Smooth colonies without an external web of cellulose microfibrils were formed in the pellicin-treated wild type. Scale bars are 0.5 mm.

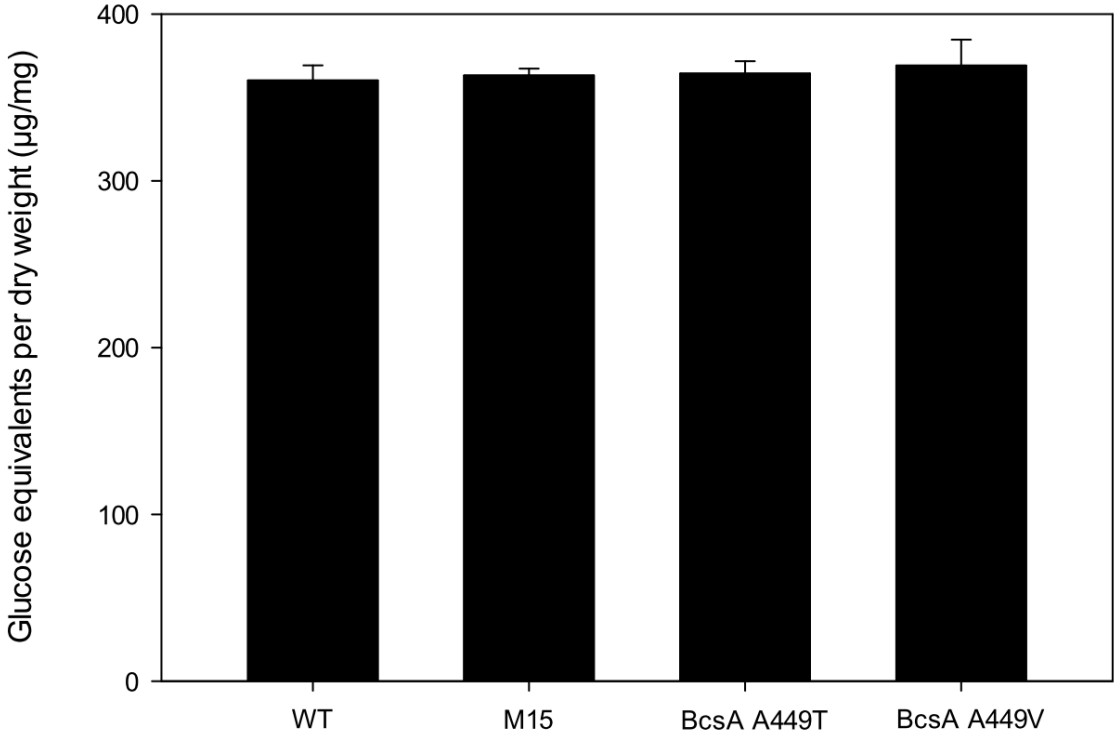

Figure 3.14: The BcsA A449T and BcsA A449V mutants produce comparable amounts of crystalline cellulose to the wild type and M15 mutant in media lacking pellicin. The crystalline cellulose content in the pellicles formed by the *G. xylinus* wild type (WT), M15 mutant, and both BcsA A449T and BcsA A449V mutants was determined by anthrone test. The crystalline cellulose is expressed as glucose equivalents per dry weight (µg/mg). The data shows the mean ± SE of three biological replicates.

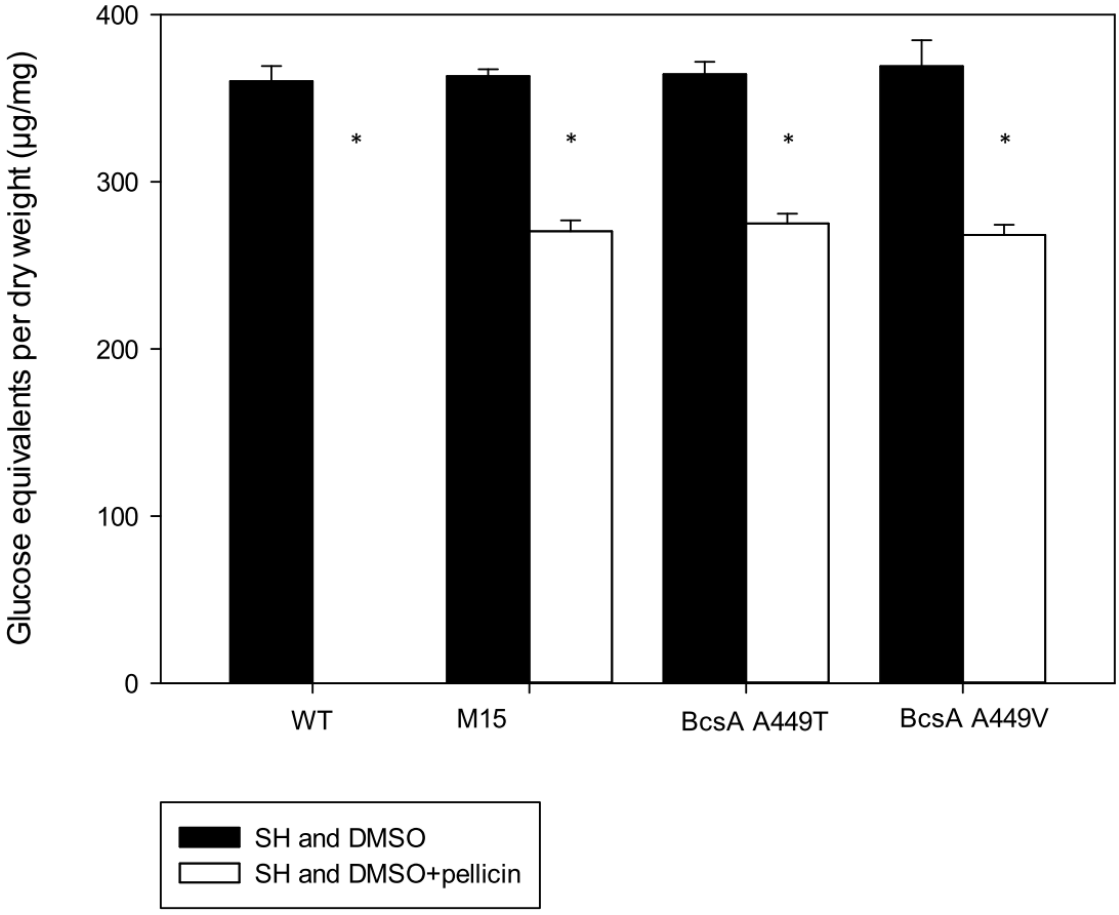

Figure 3.15: Crystalline cellulose formed by *G. xylinus* wild type, M15, BcsA A449T, and BcsA A449V mutants in media containing pellicin. The crystalline cellulose content in the pellicles formed by *G. xylinus* wild type (WT), M15, BcsA A449T, and BcsA A449V mutants in SH+DMSO (blue bar) and SH+DMSO+pellicin (red bar) was determined by anthrone test. The crystalline cellulose is expressed as glucose equivalents per dry weight (µg/mg). The data shows the mean ± SE of three biological replicates. Asterisks indicate statistically significant differences between pellicin treated and pellicin untreated cultures according to one-way ANOVA ($p<0.05$).

3.10 Structural characteristics of BcsA A449T and BcsA A449V proteins

In order to predict differences in protein structure of BcsA containing the A449T mutation and BcsA containing the A449V mutation with respect to the wild type, 3D models of the proteins were built and compared. According to the 3D model of BcsA, the substituted alanine of the mutants at position 449 of the amino acid

sequence, is predicted to be in the transmembrane helix number 6 of the protein (Figures 3.16 and 3.17 (Part 1 on page 69)). The structural superposition models allowed for the identification of differences in protein structure between the wild type BcsA protein and the mutated BcsA proteins. Structural superpositions, revealed a loop connecting two small alpha helical structures in the wild type BcsA protein at the N-terminus region (amino acids 12-27) of the protein which is not present in any of the mutated BcsA proteins (Figures 3.17 (Parts 1 and 2 on pages 69 and 70, respectively)) and 3.18 (Parts 1 and 2 on pages 72 and 73, respectively)). In addition, the wild type BcsA protein revealed an alpha helical structure at the C-terminus region (acids 709-715) of the protein that appears to have been replaced by a loop structure in both mutated BcsA proteins (Figures 3.17 (Part 3 on page 71) and 3.18 (Part 3 on page 74)). Furthermore, the wild type BcsA protein exhibits a loop structure in the C-terminal cytosolic region (amino acids 619-621) which is replaced by a small helical structure in both mutated BcsA proteins (Figures 3.17 (Part 3 on page 71) and 3.18 (Part 3 on page 74)). Finally, the wild type BcsA protein displays an alpha helical structure in the cytosolic region (amino acids 664 to 666) which is replaced by a loop in both mutated BcsA proteins (Figures 3.17 (Part 3 on page 71) and 3.18 (Part 3 on page 74)).

The predicted site of the mutated alanine residue at position 449 observed in the HPRGx mutants with respect to the translocated glucan chain in a BcsA-BcsB cellulose translocation intermediate is shown in Figure 3.19. According to the model, the alanine residue at position 449 is predicted to be in close proximity to the translocated glucan as it is part of the narrow channel formed to translocate the polysaccharide.

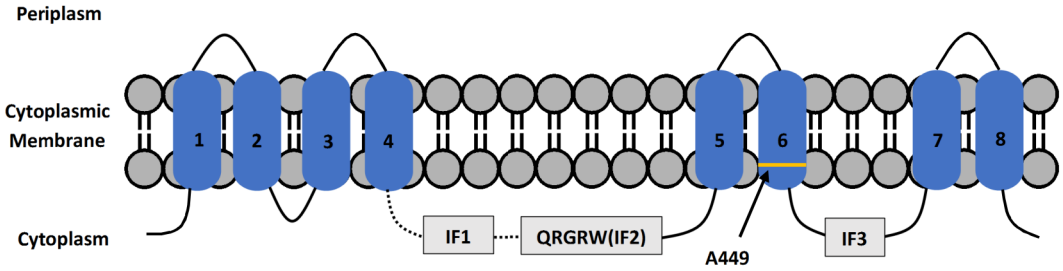

Figure 3.16: Protein schematic of the putative transmembrane helices of BcsA. The BcsA protein exhibits four N-terminal and four C-terminal helices separated by an extended intracellular glycosyltransferase loop. (IF) represents the amphipathic interphase helices of BcsA. The mutation of the alanine residue at position 449, indicated by the arrow and coloured yellow, in the BcsA is predicted to be in the transmembrane helix 6. Adapted from (Slabaugh et al., 2014).

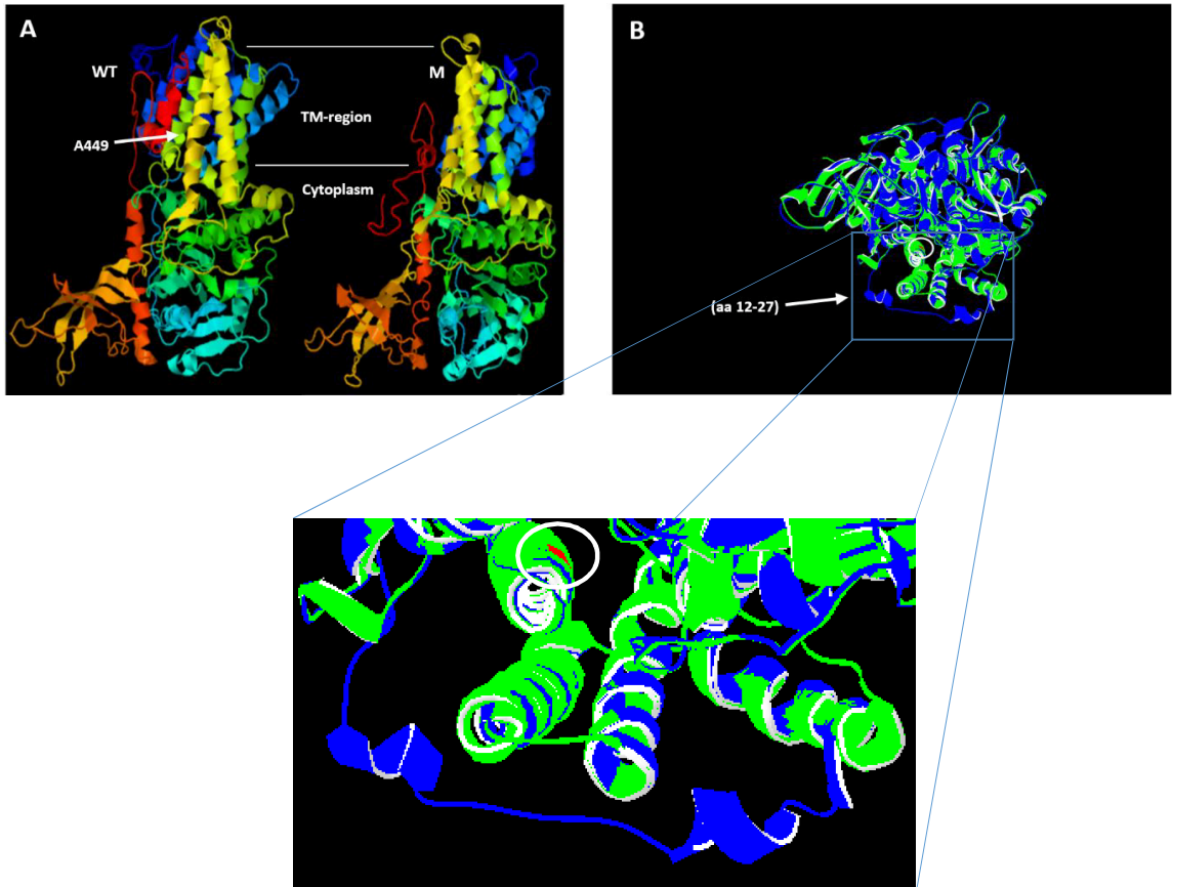

Figure 3.17: (Part 1) Architecture and superimposed models of the wild type BcsA and the mutated BcsA A449T proteins. A) 3D models of the wild type BcsA protein (WT) and mutated BcsA A449T protein (M). The location of the alanine amino acid residue at position 449 is indicated by the arrow. The models are coloured based on rainbow colouring scheme with N-terminal coloured blue and C-terminal coloured red. B) Superimposed model of the mutated BcsA A449T protein (green) on wild type BcsA protein (blue). A mismatched structure in the region of amino acids 12 to 27 is indicated by the arrow and the circle indicates the alanine residue at position 449.

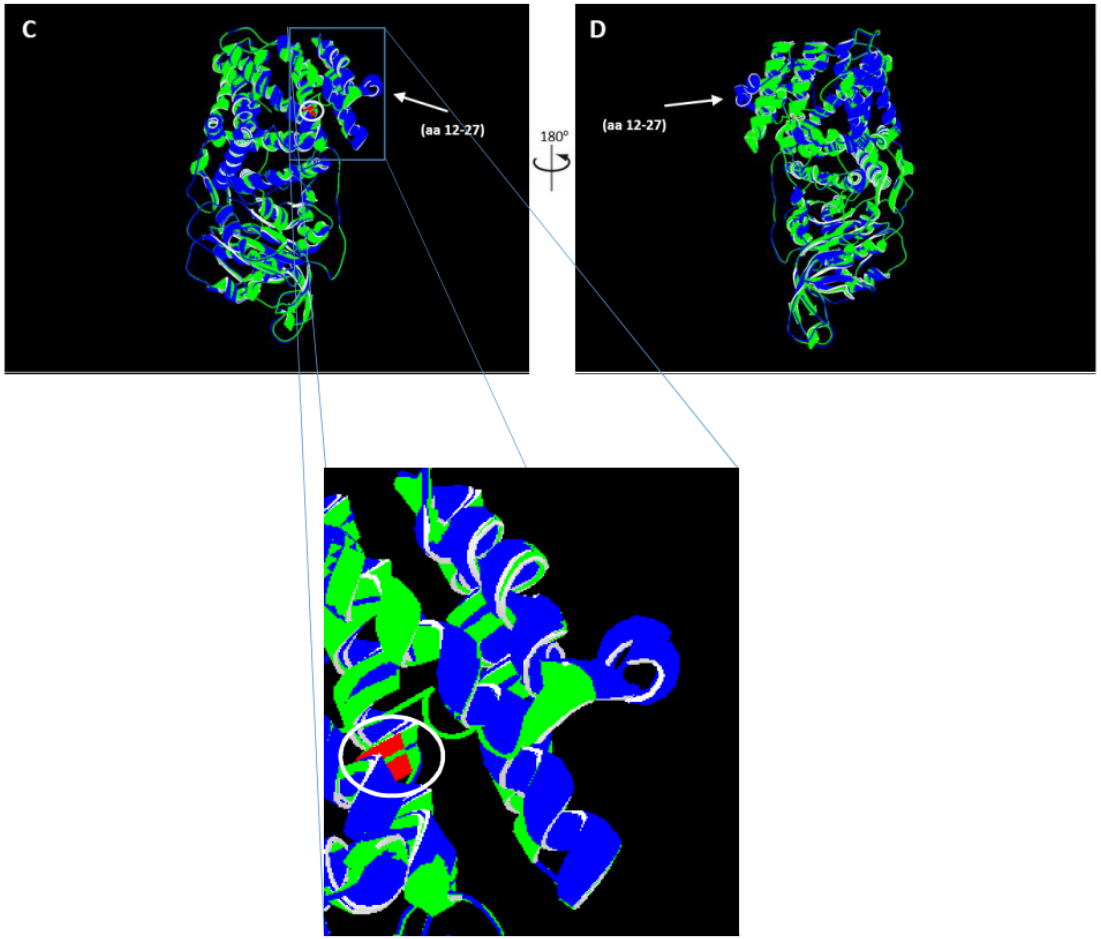

Figure 3.17: (Part 2) Architecture and superimposed models of the wild type BcsA and the mutated BcsA A449T proteins. C-D) Superimposed models of the mutated BcsA A449T protein (green) on wild type BcsA protein (blue). The superimposed structures are given with 180° rotations. A mismatched structure in the region of amino acids 12 to 27 is indicated by the arrow and the circle indicates the alanine residue at position 449.

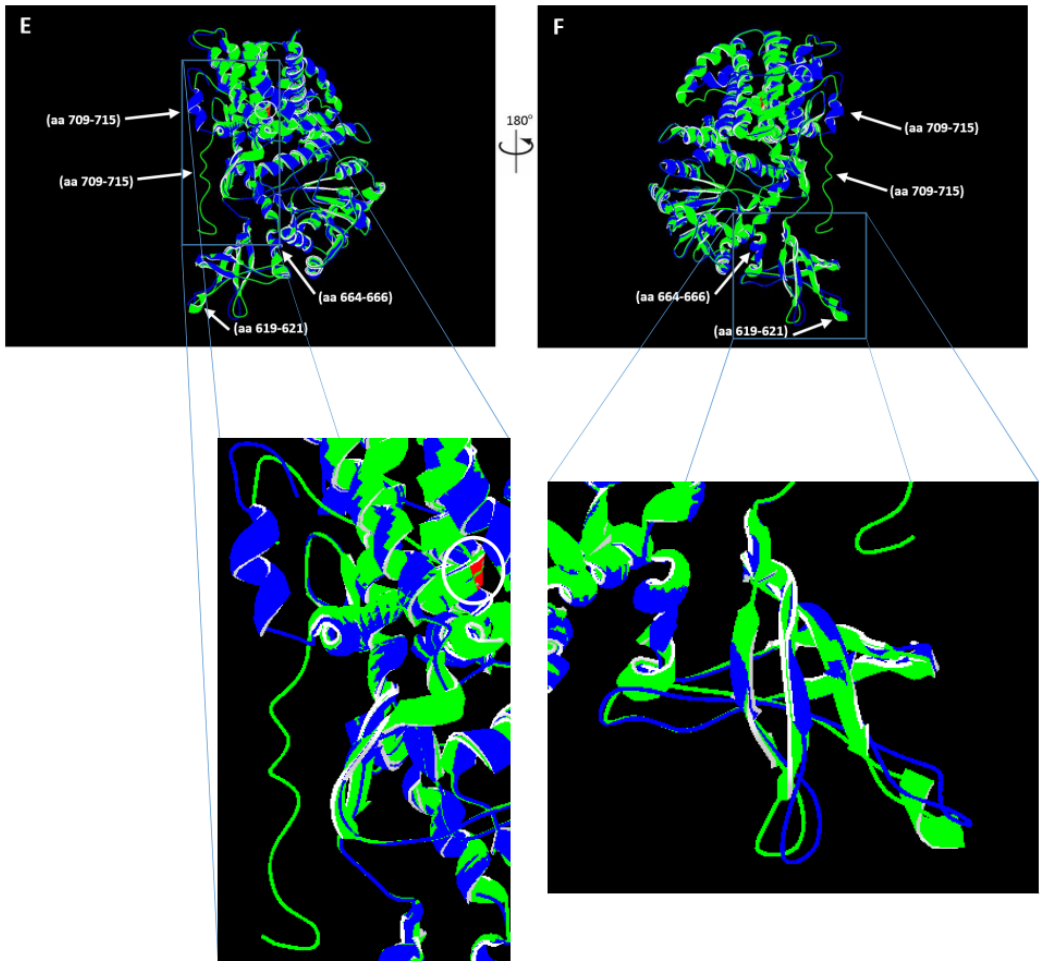

Figure 3.17: (Part 3) Architecture and superimposed models of the wild type BcsA and the mutated BcsA A449T proteins. E-F) Superimposed models of the mutated BcsA A449T protein (green) on wild type BcsA protein (blue). The superimposed structures are given with 180° rotations. Mismatched structures in the region of amino acids 619-621, 664-666, and 709-715 are indicated by the arrows and the circle indicates the alanine residue at position 449.

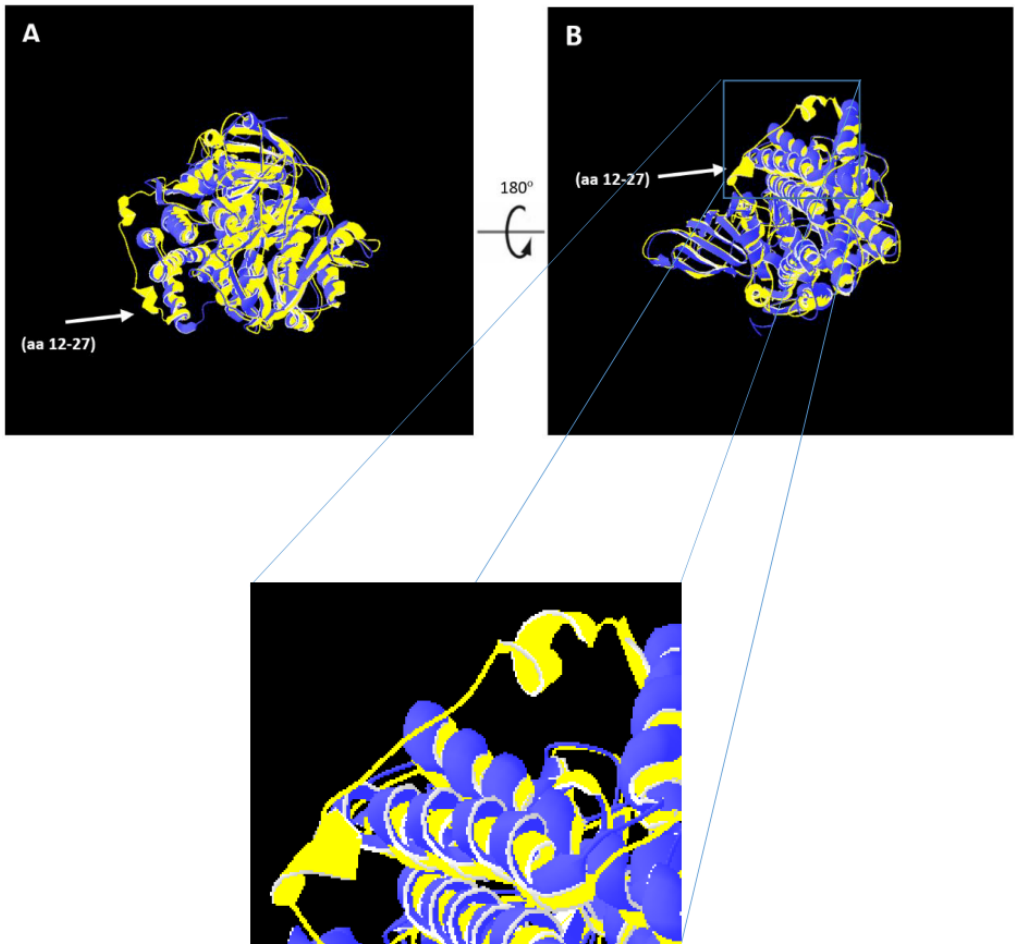

Figure 3.18: (Part 1) Superimposed models of the wild type BcsA and the mutated BcsA A449V proteins. A-B) Superimposed models of mutated BcsA A449V protein (purple) on BcsA wild type protein (yellow) are given given with 180° rotations. A mismatched structure in the region of amino acids 12 to 27 is indicated by the arrow and the circle indicates the alanine residue at position 449.

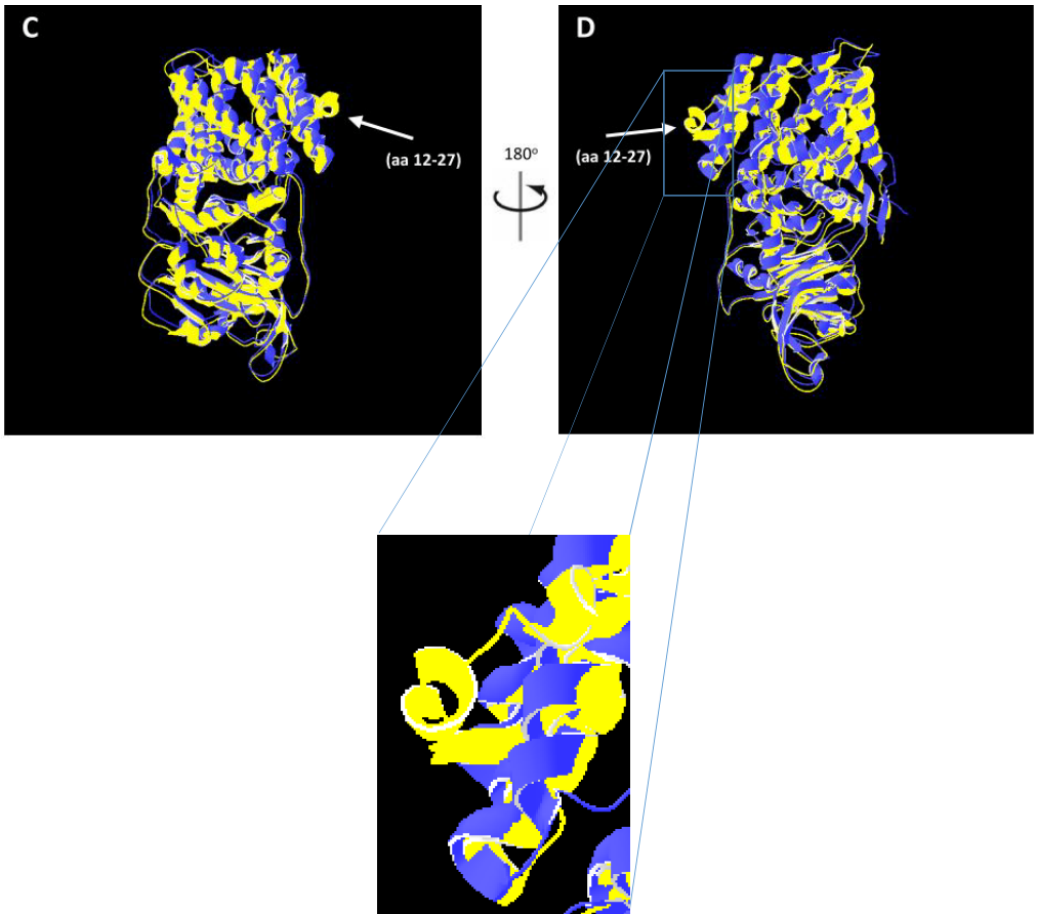

Figure 3.18: (Part 2) Superimposed models of the wild type BcsA and the mutated BcsA A449V proteins. C-D) Superimposed models of mutated BcsA A449V protein (purple) on BcsA wild type protein (yellow) are given given with 180° rotations. A mismatched structure in the region of amino acids 12 to 27 is indicated by the arrow and the circle indicates the alanine residue at position 449.

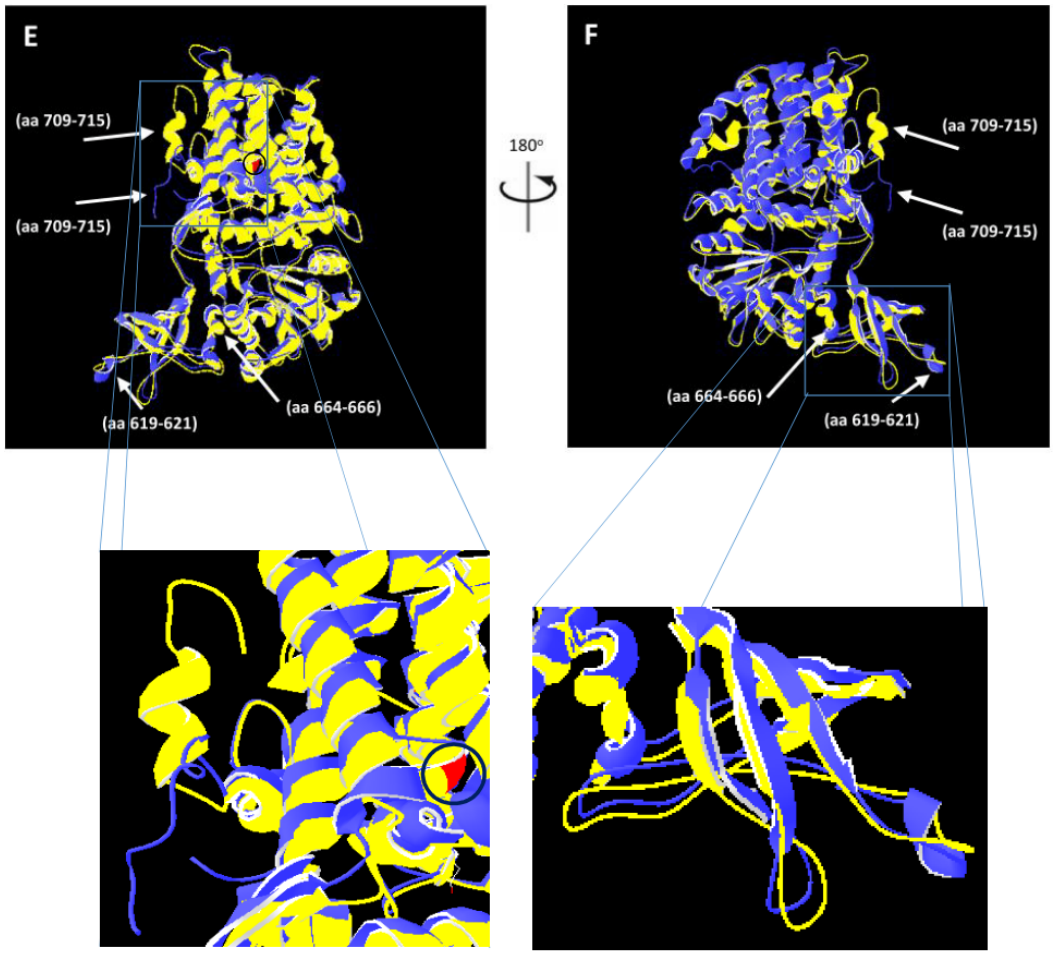

Figure 3.18: (Part 3) Superimposed models of the wild type BcsA and the mutated BcsA A449V proteins. E-F) Superimposed models of mutated BcsA A449V protein (purple) on BcsA wild type protein (yellow) are given given with 180° rotations. Mismatched structures in the region of amino acids 619-621, 664-666, and 709-715 are indicated by the arrows and the circle indicates the alanine residue at position 449.

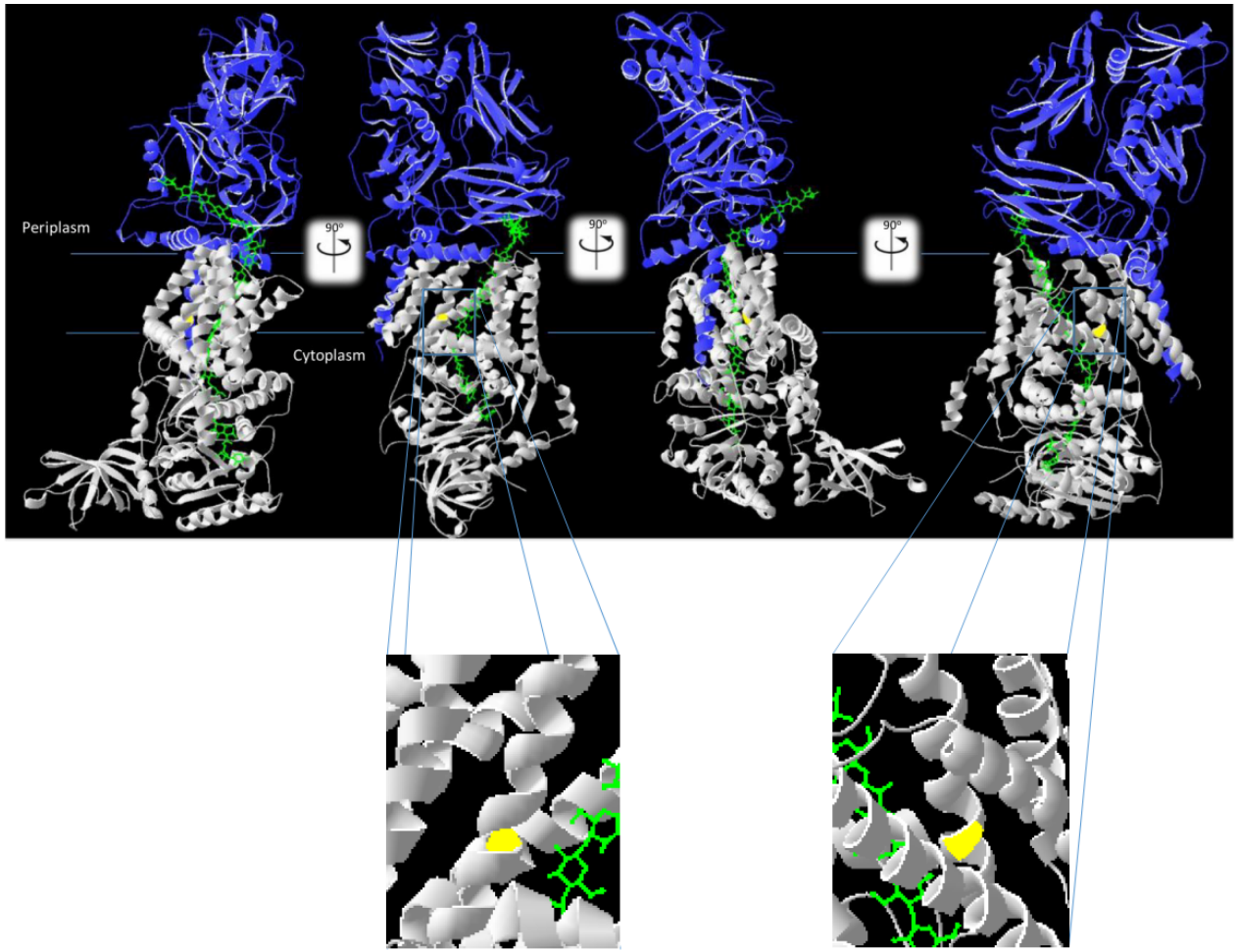

Figure 3.19: Structure of the BcsA-BcsB cellulose translocation intermediate showing the predicted location of the alanine residue at position 449 of BcsA with respect to the translocating glucan. The BcsA protein is coloured in light grey and the BcsB protein is coloured in purple. The predicted location of the alanine residue at position 449 is coloured in yellow and the translocating glucan is shown as a green chain. The model was built from the pdb structure 4HG6.

Chapter 4

Discussion and General Conclusions

The concluding chapter of this thesis provides an overview of the study, including a discussion of the results (Chapter 3) and of the major methods involved (Chapter 2). In addition, the strengths and the limitations of the project are contemplated at the end of this chapter, leading to various recommendations for further cellulose biosynthesis research.

In the present work, the idea that the *bcsA* gene in *G. xylinus* plays an indispensable role in cellulose crystallization has been addressed. To the best of the author's knowledge, there are no studies that explore the direct impact of the *bcsA* gene functionality in this context. The discussion of the results obtained revolves around two major aspects; namely, the phenotypic characterization of pellicin-resistant *G. xylinus* mutants, and the possible mechanisms by which pellicin inhibits the process of cellulose crystallization.

4.1 Phenotypic effects of mutations in *G. xylinus* mutants resistant to pellicin

A forward genetics analysis was performed to identify and manipulate candidate genes in *G. xylinus* involved in cellulose crystallization. *G. xylinus* mutants resistant to the novel cellulose I inhibitor known as pellicin, previously generated through ethyl methanesulfonate (EMS) mutagenesis, were employed for this purpose. Based

on phenotypic analysis of 15 of these mutants, 3 of them displayed high resistance to pellicin (Figure 3.1). Only these 3 mutants, referred hereafter as high pellicin-resistant *G. xylinus* (HPR*Gx*) mutants, were considered for carrying further analysis in this study.

The first part of the analysis consisted in quantifying the amount of crystalline cellulose present in the pellicles formed by the HPR*Gx* mutants. In medium lacking pellicin, comparable amounts of crystalline cellulose was found to be produced by both HPR*Gx* mutants and by the wild type (Figure 3.2). However, in the presence of the inhibitor, the amount of crystalline cellulose produced by the HPR*Gx* mutants significantly decreased by approximately 23% (Figure 3.3), while no crystalline cellulose was detected in the case of the wild type. These results suggest that a mutation in the HPR*Gx* mutants make them highly resistant to the inhibitor but not completely resistant. The reduced amount of crystalline cellulose produced by these mutants in the presence of pellicin may be due to alterations in their cellulose synthase activity. A possible factor leading to these changes in the cellulose synthase activity of these mutants is discussed in the next section of the discussion.

Additionally, a comparison of the colony morphology between the wild type and HPR*Gx* mutants was performed. Microscopic analysis of colony morphology revealed the formation of rough colonies with an external web of cellulose microfibrils in the case of pellicin-untreated wild type. These same characteristics were present in HPR*Gx* mutant colonies, regardless of the presence of pellicin. In contrast, pellicin-treated wild type colonies exhibited a smooth and flat morphology without an external web of cellulose microfibrils (Figure 3.4).

Furthermore, the impact of pellicin on growth on both the HPR*Gx* mutants and on the wild type was studied. In particular, only the growth of the wild type increased significantly upon the addition of pellicin to the medium. Contrary to the case HPR*Gx* mutants, which exhibited a growth comparable to that of the pellicin-untreated wild type regardless of the presence pellicin (Figure 3.5). On the other hand, the M13 mutant showed a particular lower growth rate than that of the remaining mutants, but no considerable difference was observed in terms of their final cell density. Although it is possible that this particular mutant has a mutation that affects growth, the underlying cause of this difference in growth has yet to be determined. In contrast to the cell growth rate, the final cell density did increase on the *G. xylinus* wild type upon addition of pellicin to the medium (Figure 3.5). This observation suggests that the inhibitor causes a positive effect on the overall growth in *G. xylinus*, as

previously observed (Strap et al., 2011). Since cellulose crystallization was inhibited by pellicin while increasing the growth only in the *G. xylinus* wild type, it is then possible that a connection between growth and cellulose biosynthesis exists in this organism. Expanding this idea, it has been shown that not only the growth, but the rate of glucan polymerization increases in *G. xylinus* in the presence of pellicin (Strap et al., 2011). In this regard, observations that the rate of cellulose production is proportional to the cell growth rate, and that the partial steps of crystallization and ribbon assembly do limit the overall biogenic cellulose process have been previously reported (Yang et al., 1998; Colvin and Witter, 1983; Hestrin and Schramm, 1954).

Overall, the aforementioned results collected from the phenotypic analysis suggest that mutations in the HPR*Gx* mutants are likely involved in the process of cellulose crystallization exclusively as no significant phenotypic alterations (other than pellicin resistance) were observed in these mutants in the presence of the inhibitor.

Cloning the causative mutations of pellicin-resistant mutants revealed that the A449T mutation in the BcsA protein of HPR*Gx* mutants was involved in pellicin resistance, as confirmed by site-directed mutagenesis. In addition, a BcsA A449V mutant was introduced, which resulted in equally resistant mutants. It is possible that this mutant was the result of a polymerase error during the PCR reaction step of site-directed mutagenesis. Although not originally planned, the generation of this mutant facilitated further exploration of the A449 residue of BcsA in the context of pellicin resistance. In this regard, the A449T mutation resulted in a non-polar to polar substitution and the A449V mutation in a non-polar to a non-polar one; therefore, it seems that the polarity aspects of the substitution at the A449 position of BcsA is not the determining factor to confer resistance to pellicin.

A recommended course of action in terms of phenotypic analysis follows. A more extended characterization of the BcsA A449T and A449V mutants is required to complement the morphological profile presented in this study. These mutants may form an altered cellulose product when compared to that of the wild type. In this respect, X-ray diffraction analysis of mercerized cells could be used to assess the crystallinity level of the cellulose produced by the BcsA mutants. Also scanning electron microscopy analysis of pellicles formed by these mutants in the presence and absence of pellicin could be employed to determine whether they are able to produce cellulose II or not. Finally, atomic microscopy could also be used to identify the ratio of cellulose Iα and Iβ allomorphs formed by the mutants.

4.2 Potential binding sites and modes of action of pellicin

4.2.1 Pellicin may affect glucan translocation in BcsA

In order to localize the alanine 449 residue in BcsA as well to identify critical structures that may be involved in pellicin binding and pellicin resistance, 3D models of the BcsA wild type and BcsA mutants were built and compared (as discussed in section 3.10). Alignment with the BcsA protein from *Rhodobacter sphaeroides* revealed that the alanine 449 residue of BcsA is located in the transmembrane domain 6 (TMH6) of the protein (Figures 3.16 and 3.17-A). Additionally, the position of the alanine 449 residue with respect to the translocating glucan in a BcsA-BcsB cellulose translocation intermediate was also modelled, showing that this residue is in close proximity to the translocating glucan (Figure 3.19). The TMH6 of BcsA forms part of the transmembrane pore which allows the translocation of a newly formed glucan chain from the plasma membrane into the periplasm (Morgan et al., 2013). To the best of the author's knowledge, it is not known how the cellulose translocation process across the BcsA protein may influence the final assembly of cellulose I.

Studies in *Arabidopsis thaliana* have showed the quinoxyphen-resistant CESA1 A903V mutant displays a reduced crystalline cellulose content as well as crystallite size (Harris et al., 2012). The CESA1 A903V mutant aligns with the tyrosine 455 residue of BcsA of *R. sphaeroides* which has been shown to create a hydrogen bond with the glucan (Morgan et al., 2013). The latter residue in turn aligns in *G. xylinus* within the TMH6 of the BcsA protein with the histidine 445 residue, which is positionally analogous to the aforementioned alanine 449 residue. Hence, one may contend that pellicin may affect the translocation process by altering hydrogen bonding of the glucan with amino acids in the TMH6 of BcsA. Therefore, more research on the translocation process and how this process influences crystallization is required. In this regard, site-directed mutagenesis could be used to create mutants in amino acids of the translocating channel which are known to interact with the glucan. The impact of these mutations on cellulose I assembly would allow to study the possible relationships between translocation and cellulose crystallization processes.

The above discussion does not indicate the means by which the translocation

process may influence cellulose crystallization. In this regard, and parallel to the analysis presented in (Li et al., 2014), the alteration of interactions between amino acids of TMH6 and the translocating glucan may result in configuration changes of the nascent chain before crystalline microfibril assembly in *G. xylinus*. These alterations may in turn cause collateral effects in crystalline cellulose production.

Another possible way in which alterations in the translocation process may disrupt cellulose crystallization revolves around geometrical considerations of the glucan chain extrusion from the BcsA-BcsB complex. In particular, it is worth noting that the exit of the glucan towards the periplasm occurs between loops 5/6 and 7/8 at the BcsA-BcsB interface, where the glucan particularly twists to protrude from the complex sideways (Morgan et al., 2013). These precise extrusion characteristics could be indispensable for the proper interaction between the nascent glucan and other proteins in the periplasm for the purpose of cellulose crystallization. Therefore, if pellicin were able to alter the TM region of the BcsA, it could also affect this precise extrusion of the glucan, and hence hinder the crystallization process overall.

4.2.2 Pellicin as an allosteric modulator

It has been shown that the effects of inhibitor-protein interactions are often propagated to remote locations with respect to the inhibitor binding site (Freire, 1999). Based on this observation, one might expect that pellicin could allosterically affect the BcsA protein, and that conformational changes on the BcsA A449T and BcsA A449T mutants are able to counteract this effect; thus, promoting normal functionality of the protein. Analysis of the superimposed models of BcsA proteins built in this study revealed potential sites of the BcsA protein that can be affected by pellicin by these means. In particular, both BcsA A449T and BcsA A449V mutant proteins revealed two structural changes localized in the PilZ domain within the cytosolic region of BcsA and two structural changes within the transmembrane region of the protein, as shown in Figures 3.17 (part 3) and 3.18 (part 3).

It has been suggested that inhibition of microfibril assembly is manifested by an increase on the overall rate at which glucose is incorporated into insoluble polyglucan chains (Haigler, 1985). Likewise, it is known that crystallization may limit the rate of polymerization in bacteria and plants (Ross et al., 1991). As a result, one may conjecture that pellicin modulates cellulose synthase activity in an allosterical manner. This modulation may take place through protein-protein

interactions, and could raise the polymerization rate, resulting in a disruption on the cellulose crystallization process. By binding to a component of the cellulose synthesizing complex, pellicin may induce conformational changes which further propagate through the complex, ultimately invigorating cellulose synthase activity. This hypothesis may explain the role of the two conformational changes in the PilZ domain observed in BcsA A449T and BcsA A449V mutant proteins, in the context of pellicin resistivity. In particular, such conformational changes may cause a slight reduction of cyclic-di-GMP affinity to its binding site in the PilZ domain, resulting in a reduced cellulose synthase activity. Contrary to the case of the *G. xylinus* wild type, these conformational changes in the BcsA A449T and BcsA A449V mutants may counteract the increase in cellulose synthase activity induced by the presence of pellicin, in such a way that cellulose crystallization is not inhibited entirely. This would explain the reduced, yet significant crystalline cellulose production observed in these mutants in the presence of pellicin (Figure 3.5). In order to validate these assumptions, the cellulose synthase activities of the *G. xylinus* wild type and of both the BcsA A449T and BcsA A449V mutants could be studied and compared using *in vitro* cellulose synthase assays with UDP [^{3}H] glucose as a substrate.

As previously mentioned, two additional conformational changes appeared in the transmembrane domain of the BcsA protein. On the one hand, the region of amino acids 709 to 715 within the C-terminus region of the BcsA appears to have been altered in two major ways. Firstly, an α-helical structure present in the wild type protein appears to have been replaced by a loop structure in both BcsA A449T and BcsA A449V. Additionally, the region of amino acids 709 to 715 of BcsA appears to have been twisted towards the cytosolic region in the mutated BcsA proteins when compared to that of the wild type (Figures 3.17 (part 3) and 3.18 (part 3)). Based on the crystal structure of BcsA elucidated from *Rhodobacter spharoides*, this particular region is not known to have a particular functionality (Morgan et al., 2013). However, due to its proximity to the cellulose conducting channel in BcsA, the author hypothesizes that it could play a determining role in the positioning and alignment of the latter (Figures 3.17 (part 3) and 3.18 (part 3)). As mention above in this section, alterations in the cellulose conducting channel of BcsA may alter the precise extrusion characteristics that may be important for the proper interaction between the nascent glucan and other proteins in the periplasm required for cellulose crystallization.

The second structural change in the transmembrane domain of the BcsA protein corresponds to the region of amino acids 12 to 27 at the N-terminus region (Figures

3.17 (parts 1 and 2) and 3.18 (parts 1 and 2)). In *R. sphaeroides*, BcsB has been shown to anchor the membrane via a single C-terminal TM helix that contacts the N-terminus of BcsA. This contact occurs specifically at the TM1 and the loop between TM1 and TM2 in BcsA (Morgan et al., 2013). Although the BcsB subunit has been shown to be essential for catalysis in cellulose biosynthesis by forming an association with BcsA, its precise function in this complex remains unclear (Omadjela et al., 2013). It has been suggested that BcsB may aid to stabilize the TM region of BcsA and direct the glucan across the periplasm toward the outer membrane via two carbohydrate-binding domains (CBDs) (Morgan et al., 2013). This possible role of BcsB might also facilitate glucan chain coalescence or crystallization *in vivo* as it has been suggested (Morgan et al., 2013). Based on this information, the author suggests another potential way in which pellicin may inhibit cellulose I formation; namely, by allosterically altering the protein-protein interactions between BcsA and BcsB proteins. More precisely, possible alterations in the BcsA-BcsB interactions induced by pellicin, and manifesting in the TM region of BcsA or in the regulation of glucan movement across the periplasm, could explain the detrimental effects of pellicin on cellulose crystallization.

It is possible that several protein-protein interactions may be required for the process of cellulose crystallization. In this regard, protein-protein interactions have not been established for all the proteins coded by the genes of the *bcs* operon. Nevertheless, based on the principle of "guilt-by-association" (Oliver, 2000), these proteins could interact with each other, given that they are all known to be involved in cellulose biosynthesis (Saxena et al., 1994). The existence of protein-protein interactions between the proteins in the cellulose synthase complex is also supported by: the BcsA-BcsB complex formation (Morgan et al., 2013); the presence of tetratricopeptide (TPR) repeats in the BcsC protein (Keiski et al., 2010); and the periplasmic localization and the characteristic octameric-protein structure of BcsD (Hu et al., 2010; Iyer et al., 2011). In addition, protein-protein interactions have been suggested with other proteins unrelated to the *bcs* operon. For instance, it has been suggested that the CCPax protein interacts with the BcsD gene and may also play a critical role in ensuring proper structural conformation of terminal complexes (TCs) on the cell membrane (Deng et al., 2013; Sunagawa et al., 2013). Considering this information, the protein-protein interactions which may be altered by pellicin may not only include those in the BcsA-BcsB complex mentioned above, but also any interaction which may be involved in cellulose crystallization.

Following this idea, it is recommended to conduct a protein-protein interaction analysis involving the proteins encoded by the genes *cmcax, ccpax, bcsA, bcsB, bcsC, bcsD*, and *bglAx*, both in the presence and in the absence of pellicin. These genes have been suggested as a complete cellulose synthase complex in *G. xylinus* (Zhao et al., 2015). In this regard, among the protein products encoded by these genes, only the BcsC, CMCax and BglAx proteins have been shown to be exposed to the extracellular environment (Kawano et al., 2008; Morgan et al., 2014; Keiski et al., 2010; Iyer et al., 2011; Deng et al., 2013; Tonouchi et al., 1997). Under the hypothesis that pellicin exerts its effects solely on extracellular components, only these proteins could be targeted by pellicin for binding. In terms of the two glucanases CMCax and BglAx, studies have proposed that their function consist in cleaving tangle glucan chains when there is an improper arrangement of the glucans, thus aiding in the process of crystalline cellulose assembly (Deng et al., 2013; Nakai et al., 2013). Based on this, and assuming that pellicin inhibits cellulose crystallization by acting on any of these two proteins, it is unlikely that conformational changes of the BcsA would re-establish their proper functionality. The author therefore suggests that in the context of protein-protein interactions, these two proteins are not targets for pellicin binding. On the other hand, and as previously mentioned in this section, BcsC contains TPR repeats which may be involved in protein-protein interactions. Based on these assumptions, a hypothetical organization of the cellulose synthase complex and a possible mode of action of pellicin, whereby pellicin binds to the BcsC protein, is depicted in Figure 4.1.

Thus, the author hypothesizes that the inhibitor could allosterically alter protein-protein interactions in the cellulose synthase complex. This disruption, which may have adverse effects in cellulose crystallization, may be counteracted (e.g., as a result of the strengthening of such interactions) by the structural conformations induced by the A449T or A449V mutations in the BcsA protein of *G. xylinus*. To confirm these hypotheses, it is recommended to perform protein-protein interaction studies involving cellulose biosynthesis related proteins (both in the presence and absence of pellicin). A protein complex co-immunoprecipitation (Co-IP) approach using specific antibodies to target cellulose biosynthesis related proteins might be appropriate in this regard. Alternatively, allosteric inhibition of protein-protein interactions induced by pellicin could also be studied using electrospray ionization mass spectrophotometry (EMI/MS), which has been shown to be useful in this context (Davidson et al., 2003).

Finally, it is also possible that alterations of protein-protein interactions of

cellulose biosynthesis related proteins of *G. xylinus* can cause a disorganization of TCs in the membrane. In *G. xylinus*, a characteristic TC linear orientation along the longitudinal axis of the cell surface has been shown to be essential for the association of tactoidal aggregates into crystalline microfibrils and further ribbon assembly (Haigler et al., 1982). Therefore, it would be of particular interest to examine the arrangement of TCs in the presence of pellicin on the BcsA A449T and BcsA A449V mutants and on the wild type. In this case, freeze fracture analysis of the membranes could be performed to determine the alignment of the TCs on the cell surface.

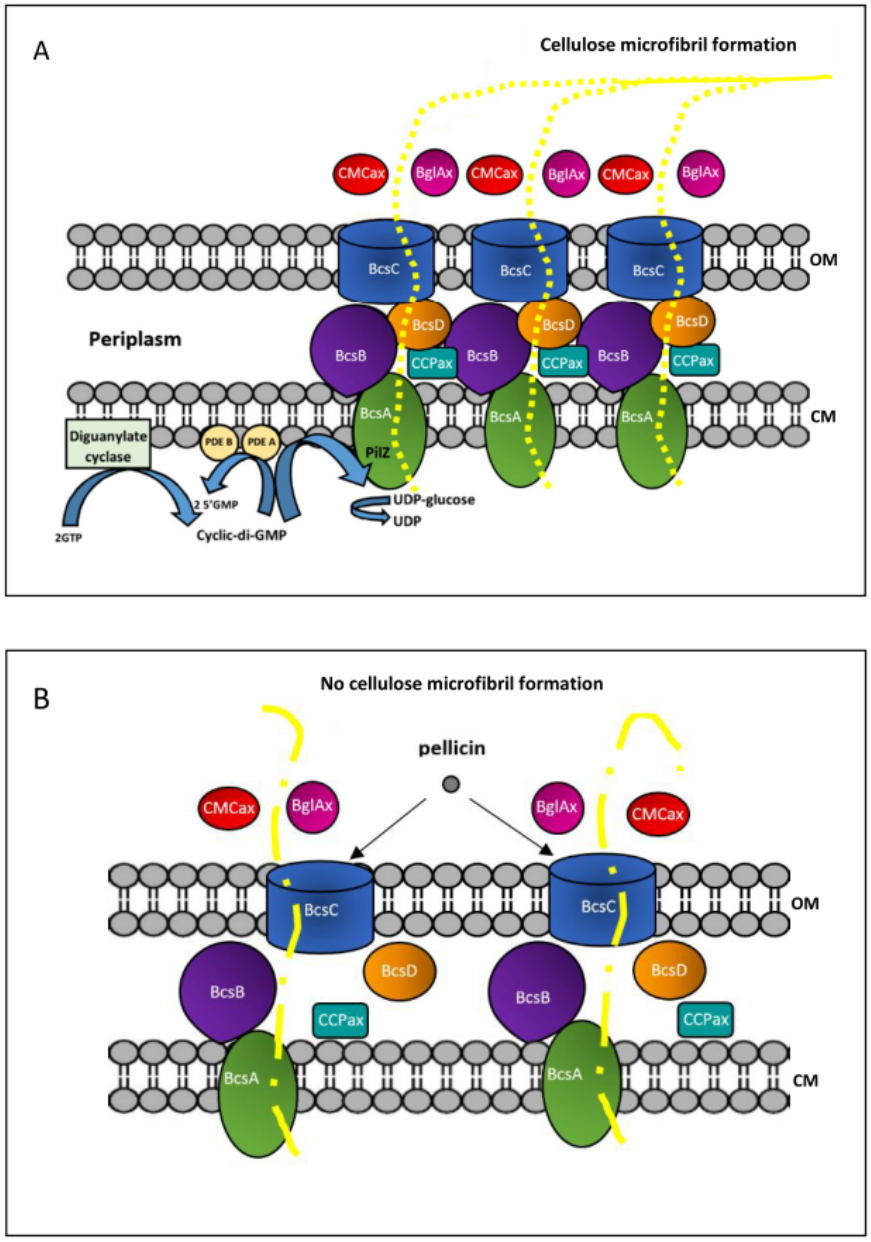

Figure 4.1: Proposed organization of proteins in the cellulose synthase complex of *G. xylinus* and hypothetical mode of action of pellicin. A) Hypothetical pattern interaction of proteins involved in cellulose biosynthesis in *G. xylinus*. The figure also shows a possible arrangement of multiple cellulose synthase complexes within a terminal complex in the cell membrane and the regulation of the intracellular second messenger cyclic-di-GMP. B) A hypothetical mode of inhibition of pellicin. Pellicin may inhibit cellulose crystallization by binding to the BcsC protein causing conformational changes of the protein and other proteins in the complex leading to alterations of protein-protein interactions required for proper cellulose crystallization. OM: outer membrane; CM: cytoplasmic membrane; PDE A: phosphodiesterase A; and PDE B: phosphodiesterase B.

4.3 Conclusions

In this study it was shown that the cellulose synthase gene *(bcsA)* not only plays a role in the catalytic polymerization process, but also in the process of cellulose I formation. The mutations A449T and A449V in the BcsA protein were found to confer high resistance to the cellulose I inhibitor pellicin. To best of the author's knowledge, this is the first study that shows that mutations on BcsA are exclusively involved in cellulose crystallization. Based on morphological analysis of *G. xylinus* mutants resistant to pellicin, it was observed that the mutations A449T and A449V in BcsA only cause pellicin resistance without affecting other phenotypic characteristics of *G. xylinus* cells. On the other hand, 3D protein modelling analysis of BcsA revealed that the A449 amino acid residue is located in the transmembrane spanning domain 6 of the protein being part of the glucan translocating channel.

Superimposed protein models revealed that the mutations in A449T and A449V cause morphological changes in the BcsA protein. From this analysis, two possible modes of actions of pellicin were inferred. One possible way by which pellicin inhibits cellulose I formation is by altering proper cellulose translocation of the glucan within the polysaccharide channel of the BcsA protein.

In addition, it is suggested by the present study that pellicin may act as an allosteric modulator with the potential to alter the functionality of BcsA or the interactions of the protein with other proteins likely involved in cellulose crystallization. As such, it is possible that conformational changes of BcsA as a result of A449T or A449V mutations could counterbalance this effect by conferring proper functionality to the BcsA protein or by strengthening protein-protein interactions.

Overall, the results presented in this study suggest that BcsA plays an important role in cellulose crystallization probably through an unknown mechanism involving glucan translocation or protein-protein interactions. In this respect, research based on the translocation process and protein-protein interactions in the context of cellulose crystallization is necessary to support these assumptions.

As a final remark, some recommendations from an experimental perspective can be made to improve further analysis on cellulose crystallization in *G. xylinus*. In terms of genetic analysis, a *G. xylinus* strain other than the ATCC 53582 would be recommended to use since DNA transfer either by electroporation or conjugation has been shown particularly difficult to accomplish with this strain (Saxena et al.,

1994). This could explain the intensive screening and multiple strategies required in this study to successfully transform *G. xylinus* cells. In addition, sub-cloning of the *bcsA* gene into the pKNG101 suicide vector could only be achieved by insertion of the ColE1 origin of replication from the pZErO-2 plasmid. Attempts to replicate the final construct without the ColE1 origin of replication was not possible as the R6K origin of replication from pKNG101 only allows the replication of the plasmid in specific *E. coli* strains supplying a π protein. Therefore, for future experiments using the pKNG101 plasmid vector, the use of *E. coli* strains such as SM10λ *pir* is recommended for amplification of the plasmid or for cloning purposes.

References

Åkerholm, M., Hinterstoisser, B., and Salmén, L. (2004). Characterization of the crystalline structure of cellulose using static and dynamic FT-IR spectroscopy. *Carbohydrate research*, 339(3):569–578.

Amikam, D. and Galperin, M. Y. (2006). PilZ domain is part of the bacterial c-di-GMP binding protein. *Bioinformatics*, 22(1):3–6.

Ausmees, N., Mayer, R., Weinhouse, H., Volman, G., Amikam, D., Benziman, M., and Lindberg, M. (2001). Genetic data indicate that proteins containing the GGDEF domain possess diguanylate cyclase activity. *FEMS Microbiology Letters*, 204(1):163–167.

Baldan, B., Andolfo, P., Navazio, L., Tolomio, C., and Mariani, P. (2001). Cellulose in algal cell wall: an "*in situ*" localization. *European Journal of Histochemistry*, 45(1):51–56.

Benziman, M. (1969). Factors affecting the activity of pyruvate kinase of *Acetobacter xylinum*. *Biochemistry Journal*, 112:631–636.

Benziman, M. and Eizen, N. (1971). Pyruvate-phosphate dikinase and the control of gluconeogenesis in *Acetobacter xylinum*. *Journal of Biological Chemistry*, 246(1):57–61.

Benziman, M., Russo, A., Hochman, S., and Weinhouse, H. (1978). Purification and regulatory properties of the oxaloacetate decarboxylase of *Acetobacter xylinum*. *Journal of Bacteriology*, 134(1):1–9.

Blanton, R. L., Fuller, D., Iranfar, N., Grimson, M. J., and Loomis, W. F. (2000). The cellulose synthase gene of *Dictyostelium*. *Proceedings of the National Academy of Sciences*, 97(5):2391–2396.

Brown, A. J. (1886). XLIII.on an acetic ferment which forms cellulose. *J. Chem. Soc., Trans.*, 49:432–439.

Brown, R. M., Willison, J., and Richardson, C. L. (1976). Cellulose biosynthesis in *Acetobacter xylinum*: visualization of the site of synthesis and direct measurement of the *in vivo* process. *Proceedings of the National Academy of Sciences*, 73(12):4565–4569.

Brown, Jr, R. M. (1992). Emerging technologies and future prospects for industrialization of microbially derived cellulose. *Harnessing Biotechnology for the 21st Century*, page 76.

Brown, Jr, R. M. (1996). The biosynthesis of cellulose. *Journal of Macromolecular Science, Part A: Pure and Applied Chemistry*, 33(10):1345–1373.

Bureau, T. E. and Brown, R. M. (1987). *In vitro* synthesis of cellulose II from a cytoplasmic membrane fraction of *Acetobacter xylinum*. *Proceedings of the National Academy of Sciences*, 84(20):6985–6989.

Cannon, R. E. and Anderson, S. M. (1991). Biogenesis of bacterial cellulose. *Critical Reviews in Microbiology*, 17(6):435–447.

Charnock, S. J., Henrissat, B., and Davies, G. J. (2001). Three-dimensional structures of UDP-sugar glycosyltransferases illuminate the biosynthesis of plant polysaccharides. *Plant Physiology*, 125(2):527–531.

Cifuentes, C., Bulone, V., and Emons, A. M. C. (2010). Biosynthesis of callose and cellulose by detergent extracts of tobacco cell membranes and quantification of the polymers synthesized *in vitro*. *Journal of Integrative Plant Biology*, 52(2):221–233.

Çoban, E. P. and Biyik, H. (2013). Effect of various carbon and nitrogen sources on cellulose synthesis by *Acetobacter lovaniensis* HBB5. *African Journal of Biotechnology*, 10(27):5346–5354.

Colvin, J. R. and Witter, D. (1983). Congo red and calcofluor white inhibition of *Acetobacter xylinum* cell growth and of bacterial cellulose microfibril formation: Isolation and properties of a transient, extracellular glucan related to cellulose. *Protoplasma*, 116(1):34–40.

Coucheron, D. (1991). An *Acetobacter xylinum* insertion sequence element associated with inactivation of cellulose production. *Journal of bacteriology*, 173(18):5723–5731.

Czaja, W., Krystynowicz, A., Bielecki, S., and Brown, R. M. (2006). Microbial cellulosethe natural power to heal wounds. *Biomaterials*, 27(2):145–151.

Davidson, W., Hopkins, J. L., Jeanfavre, D. D., Barney, K. L., Kelly, T. A., and Grygon, C. A. (2003). Characterization of the allosteric inhibition of a protein–protein interaction by mass spectrometry. *Journal of the American Society for Mass Spectrometry*, 14(1):8–13.

Delmer, D. P. and Amor, Y. (1995). Cellulose biosynthesis. *The Plant Cell*, 7(7):987.

Deng, Y., Nagachar, N., Xiao, C., Tien, M., and Kao, T.-h. (2013). Identification and characterization of non-cellulose-producing mutants of *Gluconacetobacter hansenii* generated by Tn5 transposon mutagenesis. *Journal of Bacteriology*, 195(22):5072–5083.

Dobre, T., Stoica, A., Parvulescu, O. C., Stroescu, M., and Iavorschi, G. (2008). Factors influence on bacterial cellulose growth in static reactors. *Revista de Chimie-Bucharest-original edition*, 59(5):591.

Dudman, W. (1960). Cellulose production by *Acetobacter* strains in submerged culture. *Journal of General Microbiology*, 22(1):25–39.

Endler, A., Sánchez-Rodríguez, C., and Persson, S. (2010). Glycobiology: Cellulose squeezes through. *Nature Chemical Biology*, 6(12):883–884.

Freire, E. (1999). The propagation of binding interactions to remote sites in proteins: analysis of the binding of the monoclonal antibody D1. 3 to lysozyme. *Proceedings of the National Academy of Sciences*, 96(18):10118–10122.

Galperin, M. Y. (2005). A census of membrane-bound and intracellular signal transduction proteins in bacteria: bacterial IQ, extroverts and introverts. *BMC Microbiology*, 5(1):35.

Gayathry, G. and Gopalaswamy, G. (2014). Production and characterization of microbial cellulosic fibre from *Acetobacter xylinum*. *Indian Journal of Fibre and Textile Research*, 39:93–96.

Geyer, U., Klemm, D., and Schmauder, H.-P. (1994). Kinetics of the utilization of different C sources and the cellulose formation by *Acetobacter xylinum*. *Acta Biotechnologica*, 14(3):261–266.

Glaser, L. (1958). The synthesis of cellulose in cell-free extracts of *Acetobacter xylinum*. *Journal of Biological Chemistry*, 232(2):627–636.

Goelzer, F., Faria-Tischer, P., Vitorino, J., Sierakowski, M.-R., and Tischer, C. (2009). Production and characterization of nanospheres of bacterial cellulose from *Acetobacter xylinum* from processed rice bark. *Materials Science and Engineering: C*, 29(2):546–551.

Gromet, Z., Schramm, M., and Hestrin, S. (1957). Synthesis of cellulose by *Acetobacter xylinum*. 4. Enzyme systems present in a crude extract of glucose-grown cells. *Biochemical Journal*, 67(4):679.

Haigler, C. H. (1985). The functions and biogenesis of native cellulose. In *Cellulose chemistry and its applications*, pages 31–83. Ellis Horwood Limited.

Haigler, C. H., White, A. R., Brown, R. M., and Cooper, K. M. (1982). Alteration of in vivo cellulose ribbon assembly by carboxymethylcellulose and other cellulose derivatives. *The Journal of Cell Biology*, 94(1):64–69.

Hall, M., Bansal, P., Lee, J. H., Realff, M. J., and Bommarius, A. S. (2010). Cellulose crystallinity - a key predictor of the enzymatic hydrolysis rate. *FEBS journal*, 277(6):1571–1582.

Harris, D. M., Corbin, K., Wang, T., Gutierrez, R., Bertolo, A. L., Petti, C., Smilgies, D.-M., Estevez, J. M., Bonetta, D., Urbanowicz, B. R., et al. (2012). Cellulose microfibril crystallinity is reduced by mutating c-terminal transmembrane region residues CESA1A903V and CESA3T942I of cellulose synthase. *Proceedings of the National Academy of Sciences*, 109(11):4098–4103.

Hestrin, S. and Schramm, M. (1954). Synthesis of cellulose by *Acetobacter xylinum*. 2. preparation of freeze-dried cells capable of polymerizing glucose to cellulose. *Biochemical Journal*, 58(2):345.

Himmel, M. E., Ding, S.-Y., Johnson, D. K., Adney, W. S., Nimlos, M. R., Brady, J. W., and Foust, T. D. (2007). Biomass recalcitrance: engineering plants and enzymes for biofuels production. *Science*, 315(5813):804–807.

Hornung, M., Ludwig, M., Gerrard, A., and Schmauder, H.-P. (2006). Optimizing the production of bacterial cellulose in surface culture: Evaluation of substrate mass transfer influences on the bioreaction (Part 1). *Engineering in Life Sciences*, 6(6):537–545.

Hu, S.-Q., Gao, Y.-G., Tajima, K., Sunagawa, N., Zhou, Y., Kawano, S., Fujiwara, T., Yoda, T., Shimura, D., Satoh, Y., et al. (2010). Structure of bacterial cellulose synthase subunit D octamer with four inner passageways. *Proceedings of the National Academy of Sciences*, 107(42):17957–17961.

Hundle, B. S., O'Brien, D. A., Alberti, M., Beyer, P., and Hearst, J. E. (1992). Functional expression of zeaxanthin glucosyltransferase from *Erwinia herbicola* and a proposed uridine diphosphate binding site. *Proceedings of the National Academy of Sciences*, 89(19):9321–9325.

Irick, T., West, K., Brownell, H., Schwald, W., and Saddler, J. (1988). Comparison of colorimetric and HPLC techniques for quantitating the carbohydrate components of steam-treated wood. *Applied Biochemistry and Biotechnology*, 17(1):137–149.

Iyer, P. R., Catchmark, J., Brown, N. R., and Tien, M. (2011). Biochemical localization of a protein involved in synthesis of *Gluconacetobacter hansenii* cellulose. *Cellulose*, 18(3):739–747.

Jonas, R. and Farah, L. F. (1998). Production and application of microbial cellulose. *Polymer Degradation and Stability*, 59(1):101–106.

Kaniga, K., Delor, I., and Cornelis, G. R. (1991). A wide-host-range suicide vector for improving reverse genetics in gram-negative bacteria: inactivation of the *blaA* gene of *Yersinia enterocolitica*. *Gene*, 109(1):137–141.

Kawano, S., Tajima, K., Kono, H., Numata, Y., Yamashita, H., Satoh, Y., and Munekata, M. (2008). Regulation of endoglucanase gene (*cmcax*) expression in *Acetobacter xylinum*. *Journal of Bioscience and Bioengineering*, 106(1):88–94.

Kawano, S., Tajima, K., Uemori, Y., Yamashita, H., Erata, T., Munekata, M., and Takai, M. (2002). Cloning of cellulose synthesis related genes from *Acetobacter xylinum* ATCC23769 and ATCC53582: Comparison of cellulose synthetic ability between strains. *DNA Research*, 9(5):149–156.

Keiski, C.-L., Harwich, M., Jain, S., Neculai, A. M., Yip, P., Robinson, H., Whitney, J. C., Riley, L., Burrows, L. L., Ohman, D. E., et al. (2010). AlgK is a TPR-containing protein and the periplasmic component of a novel exopolysaccharide secretin. *Structure*, 18(2):265–273.

Kelley, L. A., Mezulis, S., Yates, C. M., Wass, M. N., and Sternberg, M. J. E. (2015). The Phyre2 web portal for protein modeling, prediction and analysis. *Nat Protoc*, 10(6):845–858.

Keshk, S. (2014). Bacterial cellulose production and its industrial applications. *Bioproces Biotechnique*, 4:2.

Kimura, S. and Itoh, T. (1995). Evidence for the role of the glomerulocyte in cellulose synthesis in the tunicate, metandrocarpa uedai. *Protoplasma*, 186(1-2):24–33.

Klemm, D., Schumann, D., Udhardt, U., and Marsch, S. (2001). Bacterial synthesized cellulose artificial blood vessels for microsurgery. *Progress in Polymer Science*, 26(9):1561–1603.

Koizumi, S., Yue, Z., Tomita, Y., Kondo, T., Iwase, H., Yamaguchi, D., and Hashimoto, T. (2008). Bacterium organizes hierarchical amorphous structure in microbial cellulose. *The European Physical Journal E*, 26(1-2):137–142.

Krystynowicz, A., Czaja, W., Wiktorowska-Jezierska, A., Gonçalves-Miśkiewicz, M., Turkiewicz, M., and Bielecki, S. (2002). Factors affecting the yield and properties of bacterial cellulose. *Journal of Industrial Microbiology and Biotechnology*, 29(4):189–195.

Krystynowicz, A., Koziolkiewicz, M., Wiktorowska-Jezierska, A., Bielecki, S., Klemenska, E., Masny, A., and Pluciennicza k, A. (2005). Molecular basis of cellulose biosynthesis disappearance in submerged culture of *Acetobacter xylinum*. *Acta Biochimica Polonica-English Edition-*, 52(3):691.

Li, S., Logan Bashline, L. L., and Gu, Y. (2014). Cellulose synthesis and its regulation. *The Arabidopsis book/American Society of Plant Biologists*, 12.

Lin, F. C., Brown, R. M., Cooper, J. B., and Delmer, D. P. (1985). Synthesis of fibrils *in vitro* by a solubilized cellulose synthase from *Acetobacter xylinum*. *Science*, 230(4727):822–825.

Lynd, L. R., Weimer, P. J., Van Zyl, W. H., and Pretorius, I. S. (2002). Microbial cellulose utilization: fundamentals and biotechnology. *Microbiology and Molecular Biology Reviews*, 66(3):506–577.

Marchessault, R. and Howsmon, J. (1957). Experimental evaluation of the lateral-order distribution in cellulose. *Textile Research Journal*, 27(1):30–41.

Matsuoka, M., Tsuchida, T., Matsushita, K., Adachi, O., and Yoshinaga, F. (1996). A synthetic medium for bacterial cellulose production by *Acetobacter xylinum* subsp. *sucrofermentans*. *Bioscience, Biotechnology, and Biochemistry*, 60(4):575–579.

Matthysse, A. G., White, S., and Lightfoot, R. (1995). Genes required for cellulose synthesis in *Agrobacterium tumefaciens*. *Journal of Bacteriology*, 177(4):1069–1075.

Mehta, K., Pfeffer, S., and Brown Jr, R. M. (2015). Characterization of an *acsD* disruption mutant provides additional evidence for the hierarchical cell-directed self-assembly of cellulose in *Gluconacetobacter xylinus*. *Cellulose*, 22(1):119–137.

Mittal, A., Katahira, R., Himmel, M. E., Johnson, D. K., et al. (2011). Effects of alkaline or liquid-ammonia treatment on crystalline cellulose: changes in crystalline structure and effects on enzymatic digestibility. *Biotechnol Biofuels*, 4(1):41.

Morgan, J. L., McNamara, J. T., and Zimmer, J. (2014). Mechanism of activation of bacterial cellulose synthase by cyclic di-GMP. *Nature Structural and Molecular Biology*, 21(5):489–496.

Morgan, J. L., Strumillo, J., and Zimmer, J. (2013). Crystallographic snapshot of cellulose synthesis and membrane translocation. *Nature*, 493(7431):181–186.

Murray, M. and Thompson, W. F. (1980). Rapid isolation of high molecular weight plant DNA. *Nucleic Acids Research*, 8(19):4321–4326.

Nakai, T., Nishiyama, Y., Kuga, S., Sugano, Y., and Shoda, M. (2002). ORF2 gene involves in the construction of high-order structure of bacterial cellulose. *Biochemical and Biophysical Research Communications*, 295(2):458–462.

Nakai, T., Sugano, Y., Shoda, M., Sakakibara, H., Oiwa, K., Tuzi, S., Imai, T., Sugiyama, J., Takeuchi, M., Yamauchi, D., et al. (2013). Formation of highly twisted ribbons in a carboxymethylcellulase gene-disrupted strain of a cellulose-producing bacterium. *Journal of Bacteriology*, 195(5):958–964.

Napoli, C., Dazzo, F., and Hubbell, D. (1975). Production of cellulose microfibrils by *Rhizobium*. *Applied Microbiology*, 30(1):123–131.

Nishiyama, Y., Langan, P., and Chanzy, H. (2002). Crystal structure and hydrogen-bonding system in cellulose Iβ from synchrotron x-ray and neutron fiber diffraction. *Journal of the American Chemical Society*, 124(31):9074–9082.

Nobles, D. R., Romanovicz, D. K., and Brown, R. M. (2001). Cellulose in *Cyanobacteria*. origin of vascular plant cellulose synthase? *Plant Physiology*, 127(2):529–542.

Nobles, Jr, D. R. and Brown, Jr, R. M. (2007). Many paths up the mountain: tracking the evolution of cellulose biosynthesis. In *Cellulose: Molecular and Structural Biology*, pages 1–15. Springer.

Nunes, M. A., Dias, M. A., Correia, M. M., and Oliveira, M. M. (1984). Further studies on growth and osmoregulation of sugar beet leaves under low salinity conditions. *Journal of Experimental Botany*, 35(3):322–331.

Oehme, D. P., Downton, M. T., Doblin, M. S., Wagner, J., Gidley, M. J., and Bacic, A. (2015). Unique aspects of the structure and dynamics of elementary Iβ cellulose microfibrils revealed by computational simulations. *Plant Physiology*, 168(1):3–17.

Oglesby, L. L., Jain, S., and Ohman, D. E. (2008). Membrane topology and roles of *Pseudomonas aeruginosa Alg8* and *Alg44* in alginate polymerization. *Microbiology*, 154(6):1605–1615.

Oikawa, T., Ohtori, T., and Ameyama, M. (1995). Production of cellulose from D-mannitol by *Acetobacter xylinum*KU-1. *Bioscience, Biotechnology, and Biochemistry*, 59(2):331–332.

Oliver, S. (2000). Proteomics: guilt-by-association goes global. *Nature*, 403(6770):601–603.

Omadjela, O., Narahari, A., Strumillo, J., Mélida, H., Mazur, O., Bulone, V., and Zimmer, J. (2013). BcsA and BcsB form the catalytically active core of bacterial cellulose synthase sufficient for in vitro cellulose synthesis. *Proceedings of the National Academy of Sciences*, 110(44):17856–17861.

Park, J. K., Park, Y. H., and Jung, J. Y. (2003). Production of bacterial cellulose by *Gluconacetobacter hansenii* PJK isolated from rotten apple. *Biotechnology and Bioprocess Engineering*, 8(2):83–88.

Park, S., Baker, J. O., Himmel, M. E., Parilla, P. A., and Johnson, D. K. (2010). Cellulose crystallinity index: measurement techniques and their impact on interpreting cellulase performance. *Biotechnol Biofuels*, 3(10).

Peng, L., Xiang, F., Roberts, E., Kawagoe, Y., Greve, L. C., Kreuz, K., and Delmer, D. P. (2001). The experimental herbicide CGA 325 615 inhibits synthesis of crystalline cellulose and causes accumulation of non-crystalline β-1, 4-glucan associated with CesA protein. *Plant Physiology*, 126(3):981–992.

Pircher, N., Veigel, S., Aigner, N., Nedelec, J., Rosenau, T., and Liebner, F. (2014). Reinforcement of bacterial cellulose aerogels with biocompatible polymers. *Carbohydrate Polymers*, 111:505–513.

Pu, Y., Hu, F., Huang, F., Davison, B. H., Ragauskas, A. J., et al. (2013). Assessing the molecular structure basis for biomass recalcitrance during dilute acid and hydrothermal pretreatments. *Biotechnol Biofuels*, 6(1):1–13.

Rehm, B. (2009). *Microbial production of biopolymers and polymer precursors: applications and perspectives*. Horizon Scientific Press.

Robledo, M., Rivera, L., Jiménez-Zurdo, J. I., Rivas, R., Dazzo, F., Velázquez, E., Martínez-Molina, E., Hirsch, A. M., Mateos, P. F., et al. (2012). Role of *Rhizobium* endoglucanase *CelC2* in cellulose biosynthesis and biofilm formation on plant roots and abiotic surfaces. *Microb. Cell Fact*, 11:125.

Römling, U. (2002). Molecular biology of cellulose production in bacteria. *Research in microbiology*, 153(4):205–212.

Ross, P., Mayer, R., and Benziman, M. (1991). Cellulose biosynthesis and function in bacteria. *Microbiological Reviews*, 55(1):35–58.

Ross, P., Weinhouse, H., Aloni, Y., Michaeli, D., Weinberger-Ohana, P., Mayer, R., Braun, S., De Vroom, E., Van der Marel, G., Van Boom, J., et al. (1987). Regulation of cellulose synthesis in *Acetobacter xylinum* by cyclic diguanylic acid. *Nature*.

Sakurai, N. (1991). Cell wall functions in growth and developmentA physical and chemical point of view. *The Botanical Magazine-Shokubutsu-gaku-zasshi*, 104(3):235–251.

Sambrook, J. and Russell, D. W. (2001). Molecular cloning: a laboratory manual, 3rd eds. *New York: Cold Spring Harbor Laboratory Press*, 6:4–6.

Saxena, I. and Brown, Jr, R. (1989). Cellulose biosynthesis in *Acetobacter xylinum*: a genetic approach.

Saxena, I. M. and Brown, R. M. (2005). Cellulose biosynthesis: current views and evolving concepts. *Annals of Botany*, 96(1):9–21.

Saxena, I. M., Brown, Jr, R. M., Fevre, M., Geremia, R. A., and Henrissat, B. (1995). Multidomain architecture of beta-glycosyl transferases: implications for mechanism of action. *Journal of Bacteriology*, 177(6):1419.

Saxena, I. M., Kudlicka, K., Okuda, K., and Brown, Jr, R. M. (1994). Characterization of genes in the cellulose-synthesizing operon (*acs* operon) of *Acetobacter xylinum*: implications for cellulose crystallization. *Journal of Bacteriology*, 176(18):5735.

Saxena, M., Dandekar, T., and Brown, R. (2000). Mechanisms in cellulose biosynthesis. *University of Texas at Austin, Austin*, 78712.

Sega, G. A. (1984). A review of the genetic effects of ethyl methanesulfonate. *Mutation Research/Reviews in Genetic Toxicology*, 134(2):113–142.

Shah, J. and Brown, Jr, R. M. (2005). Towards electronic paper displays made from microbial cellulose. *Applied Microbiology and Biotechnology*, 66(4):352–355.

Shi, Z., Zhang, Y., Phillips, G. O., and Yang, G. (2014). Utilization of bacterial cellulose in food. *Food Hydrocolloids*, 35:539–545.

Simm, R., Morr, M., Kader, A., Nimtz, M., and Römling, U. (2004). GGDEF and EAL domains inversely regulate cyclic di-GMP levels and transition from sessility to motility. *Molecular Microbiology*, 53(4):1123–1134.

Slabaugh, E., Davis, J. K., Haigler, C. H., Yingling, Y. G., and Zimmer, J. (2014). Cellulose synthases: new insights from crystallography and modeling. *Trends Plant Sci*, 19(2):99–106.

Somerville, C. (2006). Cellulose synthesis in higher plants. *Annu. Rev. Cell Dev. Biol.*, 22:53–78.

Stöckmann, V. E. (1972). Developing a hypothesis: native cellulose elementary fibrils are formed with metastable structure. *Biopolymers*, 11(1):251–270.

Strap, J. L., Latos, A., Shim, I., and Bonetta, D. T. (2011). Characterization of pellicle inhibition in *Gluconacetobacter xylinus* 53582 by a small molecule, pellicin, identified by a chemical genetics screen. *PloS one*, 6(12):e28015.

Sunagawa, N., Fujiwara, T., Yoda, T., Kawano, S., Satoh, Y., Yao, M., Tajima, K., and Dairi, T. (2013). Cellulose complementing factor (Ccp) is a new member of the cellulose synthase complex (terminal complex) in *Acetobacter xylinum*. *Journal of Bioscience and Bioengineering*, 115(6):607–612.

Szymańska-Chargot, M., Cybulska, J., and Zdunek, A. (2011). Sensing the structural differences in cellulose from apple and bacterial cell wall materials by Raman and FT-IR spectroscopy. *Sensors*, 11(6):5543–5560.

Tonouchi, N., Sugiyama, M., and Yokozeki, K. (2003). Coenzyme specificity of enzymes in the oxidative pentose phosphate pathway of *Gluconobacter oxydans*. *Bioscience, Biotechnology, and Biochemistry*, 67(12):2648–2651.

Tonouchi, N., Tahara, N., Kojima, Y., Nakai, T., Sakai, F., Hayashi, T., Tsuchida, T., and Yoshinaga, F. (1997). A beta-glucosidase gene downstream of the cellulose synthase operon in cellulose-producing *Acetobacter*. *Bioscience, Biotechnology, and Biochemistry*, 61(10):1789–1790.

Updegraff, D. M. (1969). Semimicro determination of cellulose inbiological materials. *Analytical Biochemistry*, 32(3):420–424.

Valla, S., Coucheron, D. H., Fjærvik, E., Kjosbakken, J., Weinhouse, H., Ross, P., Amikam, D., and Benziman, M. (1989). Cloning of a gene involved in cellulose biosynthesis in *Acetobacter xylinum*: complementation of cellulose-negative mutants by the UDPG pyrophosphorylase structural gene. *Molecular and General Genetics MGG*, 217(1):26–30.

Vandamme, E., De Baets, S., Vanbaelen, A., Joris, K., and De Wulf, P. (1998). Improved production of bacterial cellulose and its application potential. *Polymer Degradation and Stability*, 59(1):93–99.

Vazquez, A., Foresti, M. L., Cerrutti, P., and Galvagno, M. (2013). Bacterial cellulose from simple and low cost production media by *Gluconacetobacter xylinus*. *Journal of Polymers and the Environment*, 21(2):545–554.

Weinhouse, H. and Benziman, M. (1972). Regulation of gluconeogenesis in *Acetobacter xylinum*. *European Journal of Biochemistry*, 28(1):83–88.

Weinhouse, H. and Benziman, M. (1976). Phosphorylation of glycerol and dihydroxyacetone in *Acetobacter xylinum* and its possible regulatory role. *Journal of Bacteriology*, 127(2):747–754.

Whitney, J. and Howell, P. (2013). Synthase-dependent exopolysaccharide secretion in Gram-negative bacteria. *Trends in Microbiology*, 21(2):63–72.

Whitney, S. E., Gothard, M. G., Mitchell, J. T., and Gidley, M. J. (1999). Roles of cellulose and xyloglucan in determining the mechanical properties of primary plant cell walls. *Plant Physiology*, 121(2):657–664.

Williams, W. S. and Cannon, R. E. (1989). Alternative environmental roles for cellulose produced by *Acetobacter xylinum*. *Applied and Environmental Microbiology*, 55(10):2448–2452.

Yamada, Y., Yukphan, P., Vu, H. T. L., Muramatsu, Y., Ochaikul, D., and Nakagawa, Y. (2012). Subdivision of the genus *Gluconacetobacter* Yamada, Hoshino and Ishikawa 1998: the proposal of *Komagatabacter* gen. nov., for strains accommodated to the *Gluconacetobacter xylinus* group in the *α-Proteobacteria*. *Annals of Microbiology*, 62(2):849–859.

Yamanaka, S., Watanabe, K., Kitamura, N., Iguchi, M., Mitsuhashi, S., Nishi, Y., and Uryu, M. (1989). The structure and mechanical properties of sheets prepared from bacterial cellulose. *Journal of Materials Science*, 24(9):3141–3145.

Yang, Y. K., Park, S. H., Hwang, J. W., Pyun, Y. R., and Kim, Y. S. (1998). Cellulose production by *Acetobacter xylinum* BRC5 under agitated condition. *Journal of Fermentation and Bioengineering*, 85(3):312–317.

Yao, M., Hu, S., Gao, Y., Tajima, K., Yoda, T., Shimura, D., Satoh, Y., Kawano, S., Tanaka, I., and Munekata, M. (2008). Purification, crystallization and preliminary x-ray studies of AxCesD required for efficient cellulose biosynthesis in *Acetobacter xylinum*. *Protein and Peptide Letters*, 15(1):115–117.

Yoshinaga, F. and Tonouchi, N. (1997). Watanabe., k.(1997). research progress in production of bacteria cellulose by aeration and agitation culture and its application as a new industrial material. *Bioscience, Biotechnology and Biochemistry*, 61:219–224.

Zaar, K. (1979). Visualization of pores (export sites) correlated with cellulose production in the envelope of the gram-negative bacterium *Acetobacter xylinum*. *The Journal of Cell Biology*, 80(3):773–777.

Zhao, C., Li, Z., Li, T., Zhang, Y., Bryant, D. A., and Zhao, J. (2015). High-yield production of extracellular type-I cellulose by the cyanobacterium *Synechococcus* sp. PCC 7002. *Cell Discovery*, 1.

Zogaj, X., Nimtz, M., Rohde, M., Bokranz, W., and Römling, U. (2001). The multicellular morphotypes of *Salmonella typhimurium* and *Escherichia coli* produce cellulose as the second component of the extracellular matrix. *Molecular Microbiology*, 39(6):1452–1463.